NASA/TM-2003-212236/Vol.9

Topography Experiment (TOPEX) Software Document Series

Volume 9

TOPEX Radar Altimeter Engineering Assessment Report Update - Launch to January 1, 1996

May 1996

D.W. Hancock III
G.S. Hayne
C.L. Purdy
J.E. Lee
D.W. Lockwood

TOPEX Contact:

David W. Hancock III
NASA/GSFC Wallops Flight Facility
Wallops Island, Virginia 23337

About the Series

The TOPEX Radar Altimeter Technical Memorandum Series is a collection of performance assessment documents produced by the NASA Goddard Space Flight Wallops Flight Facility over a period starting before the TOPEX launch in 1992 and continuing over greater than 10 year TOPEX lifetime. Because of the mission's success over this long period and because the data are being used internationally to redefine many aspects of ocean knowledge, it is important to make a permanent record of the TOPEX radar altimeter performance assessments which were originally provided to the TOPEX project in a series of internal reports over the life of the mission. The original reports are being printed in this series without change in order to make the information more publicly available as the original investigators become less available to explain the altimeter operation and details of the various data anomalies that have been resolved.

Foreword

The Engineering Assessment of the TOPEX Radar Altimeter is performed on a continuing basis by the TOPEX Altimeter Team at NASA / GSFC Wallops Flight Facility. The Assessment Team members are:

David W. Hancock III / NASA: TOPEX Altimeter Verification Manager / Team Leader
George S. Hayne / NASA: TOPEX Altimeter Verification Manager
Craig L. Purdy / NASA: TOPEX Altimeter Development Manager
Laurence C. Rossi / NASA: TOPEX Altimeter Manager
Ronald G. Forsythe / NASA: TOPEX WFF Software Development Manager
J. Barton Bull / NASA: TOPEX Altimeter System Engineer
Ronald L. Brooks / CSC
Hayden H. Gordon / CSC
Jeffrey E. Lee / CSC
Dennis W. Lockwood / CSC
Carol T. Purdy / CSC

For additional information on this topic, please contact the Team Leader, David W. Hancock III. He may be reached at 804-824-1238 (Voice), 804-824-1036 (FAX), or by e-mail at hancock@osb.wff.nasa.gov.

Table of Contents

Foreword iii
Table of Contents v
List of Figures vii
List of Tables ix

Section 1 Introduction

1.1 Identification of Document 1-1

Section 2 On-Orbit Instrument Performance

2.1 Launch-to-Date Internal Calibrations 2-1
2.2 Launch-to-Date Cycle Summaries 2-7
2.3 Launch-to-Date Key Events 2-28

Section 3 Assessment of Instrument Performance

3.1 Range 3-1
3.2 AGC/Sigma Naught 3-6
3.3 Sea Surface Height Residuals as Indicators of Global Sea Level Change 3-14
3.4 Over-Land Losses of Lock: Seasonal Variations 3-16
3.5 Range Corrections for the Effects of Waveform Leakage 3-22

Section 4 Engineering Assessment Synopsis

4.1 Performance Overview 4-1

Section 5 References

5.1 Supporting Documentation 5-1

Attachment A - Waveform Leakage Range Correction

List of Figures

Figure 2-1 Ku-Band Range CAL-1 Results 2-3

Figure 2-2 C-Band Range CAL-1 Results 2-4

Figure 2-3 Ku-Band AGC CAL-1 and CAL-2 Results 2-5

Figure 2-4 C-Band AGC CAL-1 and CAL-2 Results 2-6

Figure 2-5 Cycle-Average Sea Surface Heights, in Meters, from the WFF TOPEX GDR Data Base 2-10

Figure 2-6 Cycle-Average Ku-Band Sigma-naught, in dB, from the WFF TOPEX GDR Data Base 2-11

Figure 2-7 Cycle-Average C-Band Sigma-naught, in dB, from the WFF TOPEX GDR Data Base 2-12

Figure 2-8 Cycle-Average Ku-Band Significant Wave Height, in Meters, from the WFF TOPEX GDR Data Base. 2-13

Figure 2-9 Cycle-Average Ku-Band Range RMS, in Millimeters, from the WFF TOPEX GDR Data Base 2-14

Figure 2-10 Ku-Band CAL-2 Waveform Sample History 2-15

Figure 2-11 Ku-Band STANDBY Waveform Sample History 2-16

Figure 2-12 C-Band CAL-2 Waveform Sample History 2-17

Figure 2-13 C-Band STANDBY Waveform Sample History. 2-18

Figure 2-14 Engineering Monitor Histories 2-20

Figure 2-15 Locations of SEU Occurrences 2-27

Figure 3-1 Results of the Ku-Band AGC/Sigma Naught Trend Analysis. 3-7

Figure 3-2 Results of the C-Band AGC/Sigma Naught Trend Analysis. 3-8

Figure 3-3 TOPEX Cycles 17-92 SSHres Fitted by Linear Plus Sinusoidal Annual and Semiannual Terms (AFTER correction for range bias drift) 3-17

Figure 3-4 Number of Occurrences per Day of Coarse Acquisition Mode, for Cycle 17 through Cycle 92 3-19

Figure 3-5 Histograms of Seasonal Occurrences of Coarse Acquisition Mode, per One-Degree Latitude Band, for: Northern Hemisphere Fall (Cycle 43), Winter (Cycle 52), Spring (Cycle 61) and Summer (Cycle 70).. 3-21

List of Tables

Table 2-1 Data Assessment for Cycles 1-8 2-8

Table 2-2 Telemetry Channels Affected by RIU-6B Anomaly on January 17, 1995. 2-19

Table 2-3 Anomalous Single Event Upsets 2-26

Table 2-4 NASA Altimeter - Key Events 2-28

Table 3-1 TOPEX Altimeter Range Bias Changes Based on Calibration Mode 1 Step 5. 3-2

Table 3-2 Summary of TOPEX AGC Cal Table Values 3-9

Section 1

Introduction

1.1 Identification of Document

The initial February 1994 TOPEX Mission Radar Altimeter Engineering Assessment Report presented performance results for the NASA Radar Altimeter on the TOPEX/POSEIDON spacecraft, from launch in August 1992 to February 1994. An addendum in March 1995 updated the performance results through the end of calendar year 1994. This report describes significant events that occurred in calendar year 1995.

As the performance data base has expanded, and as analysis tools and techniques continue to evolve, the longer-term trends of the altimeter data have become more apparent. The recent findings are presented here.

Section 2

On-Orbit Instrument Performance

From the time of initial turn-on after launch to the beginning of calendar year 1996, the NASA Radar Altimeter has been in TRACK mode for a total of approximately 25,900 hours. The altimeter has been in IDLE mode for an additional 3,200 hours since launch, generally due to the French Altimeter being turned-on. The altimeter has been in OFF mode for a total of 302 hours, due primarily to a 230-hour spacecraft-level Safehold which began on November 26, 1995.

Altimeter Side A continues to function well; Side B has not been turned-on since before launch, and will not be turned-on unless there is a failure of Side A. The C-Band frequency has remained at 320 MHz since launch except for a very brief period shortly after launch when the bandwidth was switched to 100 MHz, to affirm its operability.

The parameter file C35028SL, described in Table 5.8.4 of the February 1994 Engineering Assessment Report, was in use until day 40 of 1995. On that day, at 1920 UTC, a new parameter set, C3502840, was implemented. The only difference between the two parameter sets is that the initial AGC acquisition value prior to the first cal mode is 40 dB instead of the previous 60 dB. The rationale for this change is discussed in Section 2.2.8 (page 27) of last year's Engineering Assessment Addendum.

The succeeding sections discuss:

- launch-to-date internal calibration results
- launch-to-date cycle summary results
- assessment of instrument performance, based on both the internal calibrations and cycle summary databases

2.1 Launch-to-Date Internal Calibrations

Internal altimeter calibrations are scheduled twice-per-day, over land areas, at approximately 0000 UTC and 1200 UTC. Internal calibrations are also performed whenever the NASA altimeter is commanded from TRACK to IDLE for a period of tracking by the French altimeter, or from IDLE back to TRACK when tracking resumes for the NASA altimeter. The WFF data base presently contains more than 2200 internal calibration sets. The calibrations prior to and after the French altimeter operations are not constrained to land areas, and usually occur over open-ocean.

2.1.1 Range Calibrations

Our processing of the calibration mode data was modified in 1994; the revised method is discussed in Section 2.1.1 (page 2) of last year's Addendum. All the calibration data since launch have been reprocessed using the revised method. The change in Ku-Band range, from day 239 of 1992 to the beginning of 1996, is plotted in Figure 2-1 "Ku-Band Range CAL-1 Results". CAL-1 steps 4 through 7 are shown in the Fig-

ure. Step 5 best represents typical AGC levels for normal ocean fine-track operation, and has been used for the range trend analysis presented in Section 3.1.

The delta range shown in Figure 2-1 (and in the succeeding calibration plots) is calculated based on the measurement minus a reference. This calibration range plot suggests that the Ku-Band range rate of change decreased during 1995. In the figure, the year 1995 begins on elapsed day 857.

The change in C-Band calibration range is depicted in Figure 2-2 "C-Band Range CAL-1 Results". This plot indicates that, earlier in the mission, the C-Band range was changing at the rate of several millimeters per year. Beginning in the latter part of 1994, however, the C-Band range has generally stabilized, although there is more frequent toggling of the 7.3 mm quantization step.

Range calibrations and their correction values are discussed in more detail in Section 3.1.

2.1.2 AGC Calibrations

2.1.2.1 CAL-1 and CAL-2

The change in Ku-Band AGC since launch is shown in Figure 2-3 "Ku-Band AGC CAL-1 and CAL-2 Results". CAL-1 steps 4 through 6, plus CAL-2, are depicted in the Figure. As for the earlier range calibration, Step 5 of the CAL-1 AGC steps is considered to be the most typical for normal ocean operations. Based on these plots, there is an approximate 0.8 dB linear decrease in CAL-1 AGC since launch, and a decrease of about 0.3 dB in CAL-2 AGC.

The change in C-Band AGC since launch is shown in Figure 2-4 "C-Band AGC CAL-1 and CAL-2 Results". There is an apparent 0.6 dB linear decrease in CAL-1 AGC since launch, and no obvious change in CAL-2 AGC.

A more thorough analysis of the AGC calibration is presented in Section 3.2.

2.1.2.2 CAL2 Differences over Water and Land

In the CAL-2 plots, for both Ku- and C-Band, there are occasional AGC decreases of approximately 0.9 dB. These decreases are more prevalent earlier in the mission.

An examination of the CAL-2 calibrations which have decreased signal levels uncovered the fact that they generally occurred during the switchover to the French altimeter and during the switch back to the NASA altimeter. The signal level drops occurred more often early in the mission because there were more frequent altimeter switchovers then. Further, it is noted these particular calibrations all occurred over open ocean. Whenever the calibrations were over land areas, the AGC levels were normal.

The conclusion is that the decreases in power during CAL-2 are directly attributable to the type of surface directly below the altimeter. In CAL-2, the receive path is through the antenna, and higher passive emissions occur over land areas. Based on standard radiometric equations, the nominal emission difference between land and

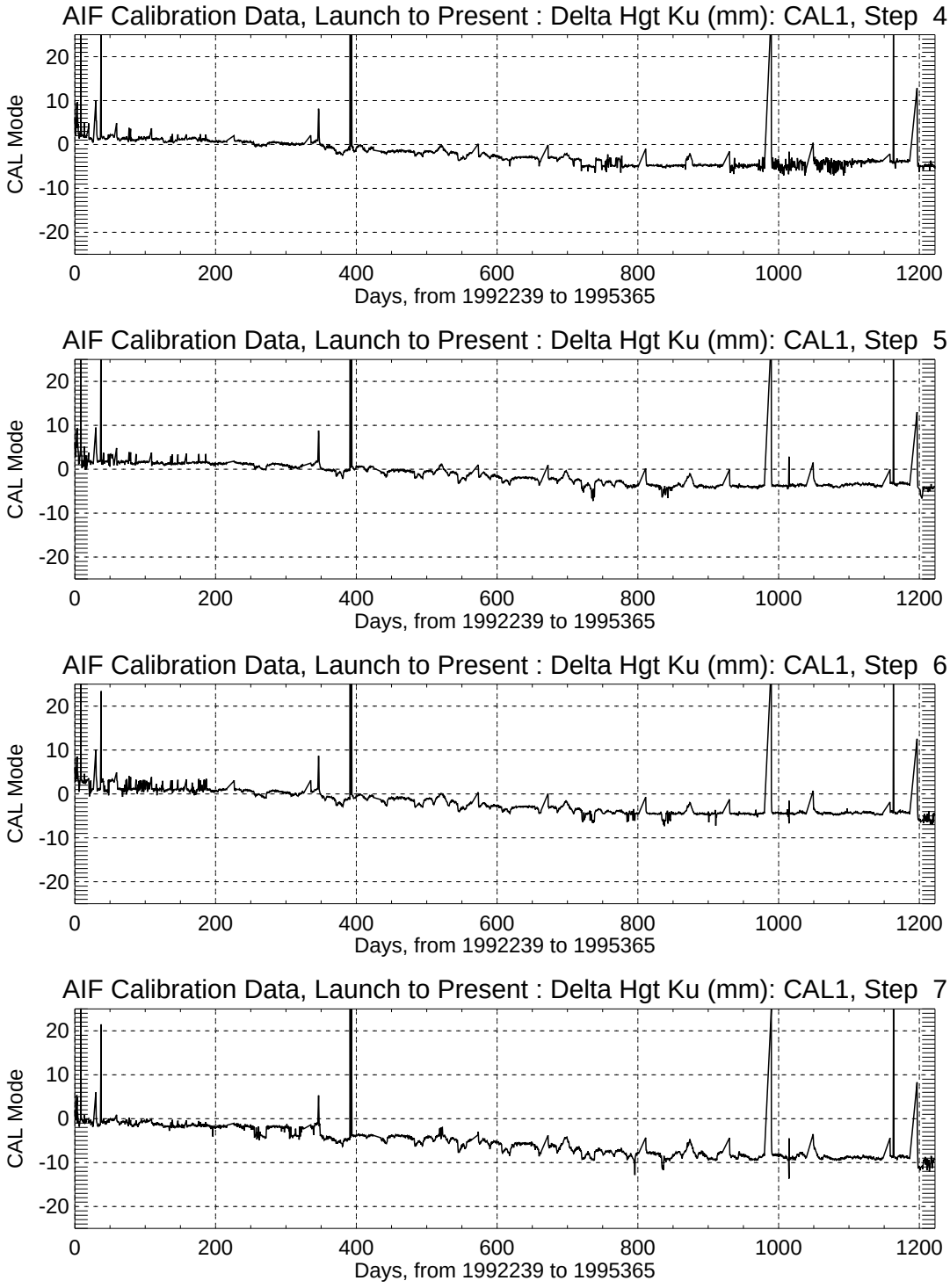

Figure 2-1 Ku-Band Range CAL-1 Results

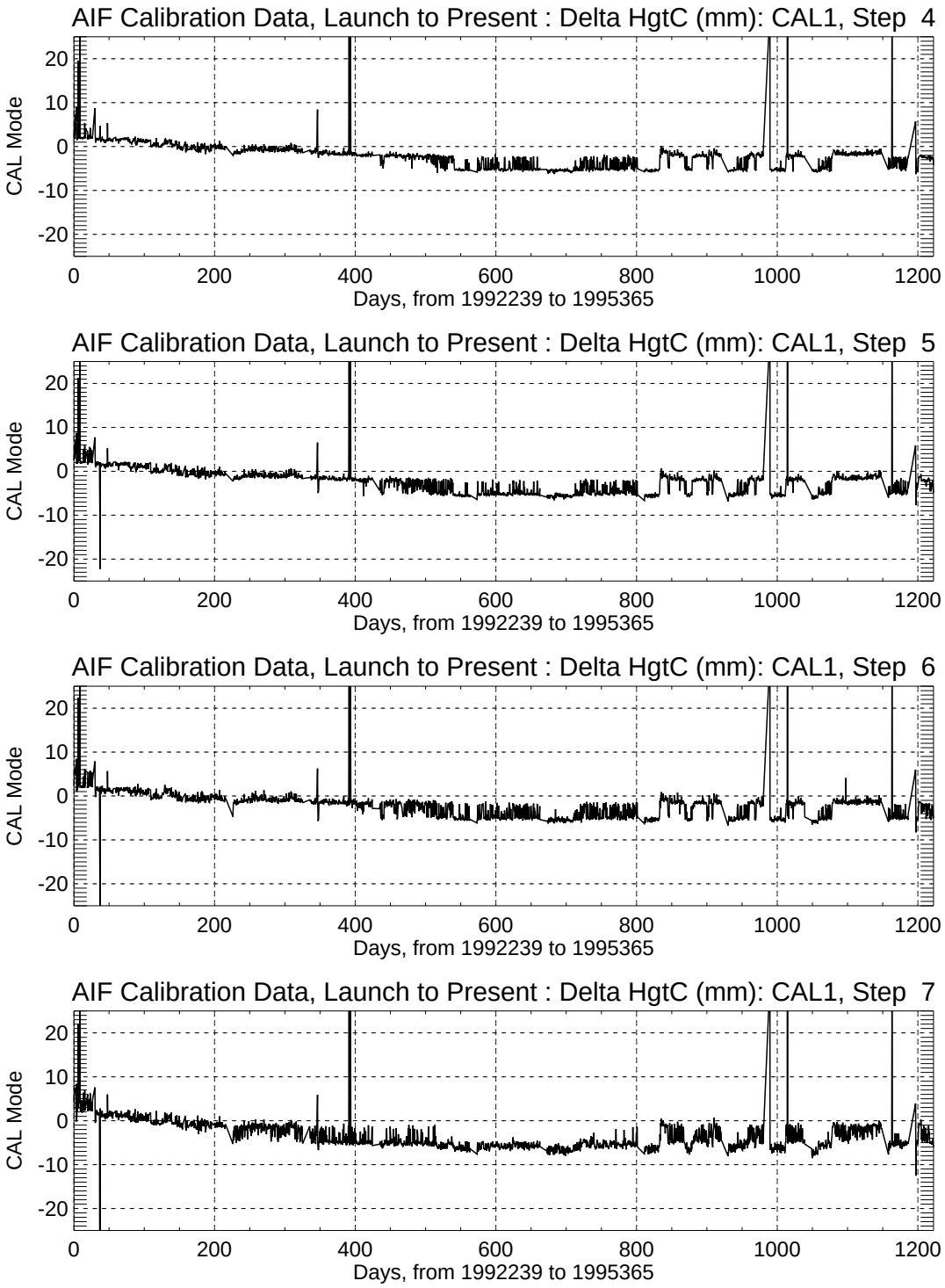

Figure 2-2 C-Band Range CAL-1 Results

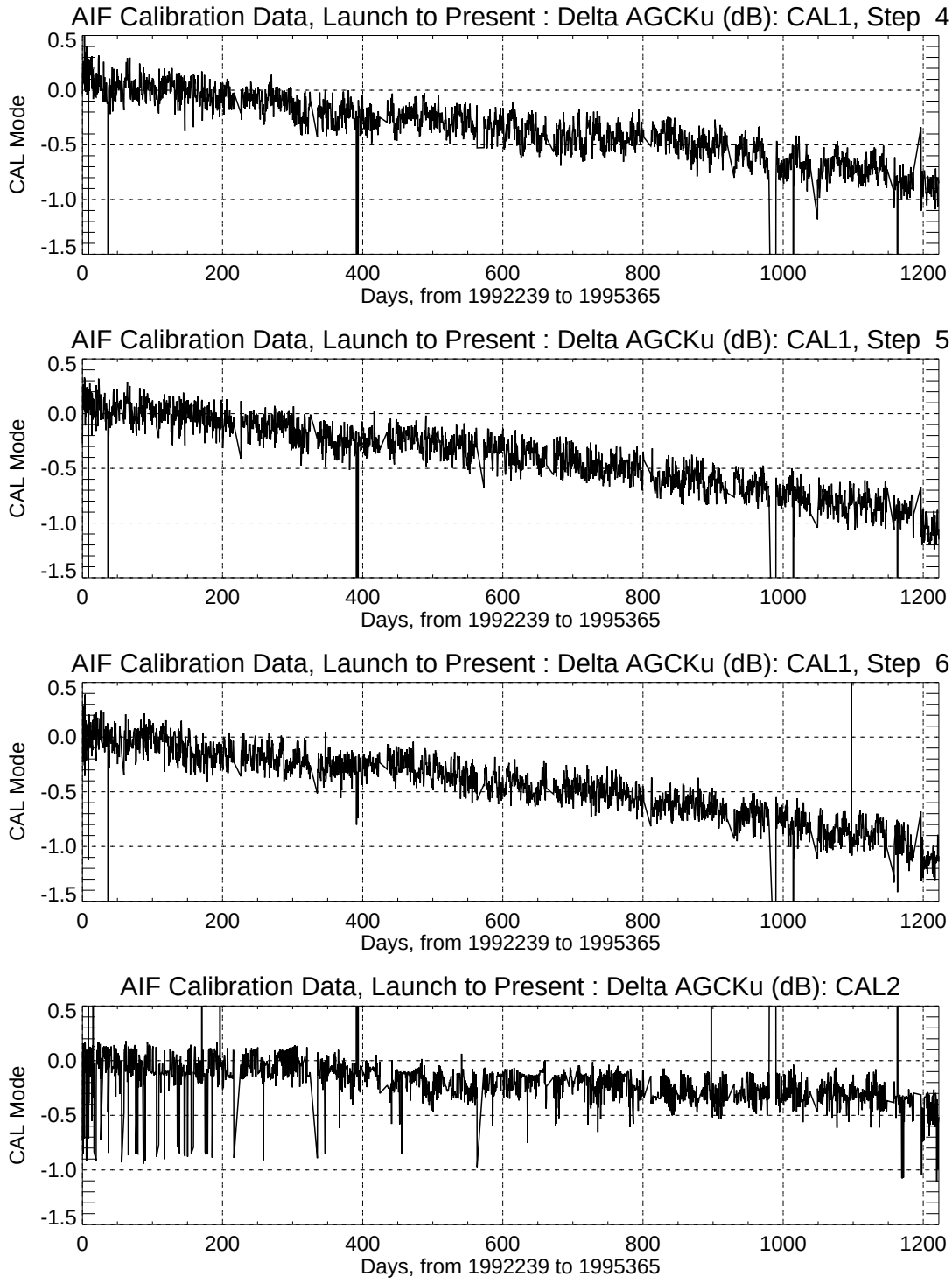

Figure 2-3 Ku-Band AGC CAL-1 and CAL-2 Results

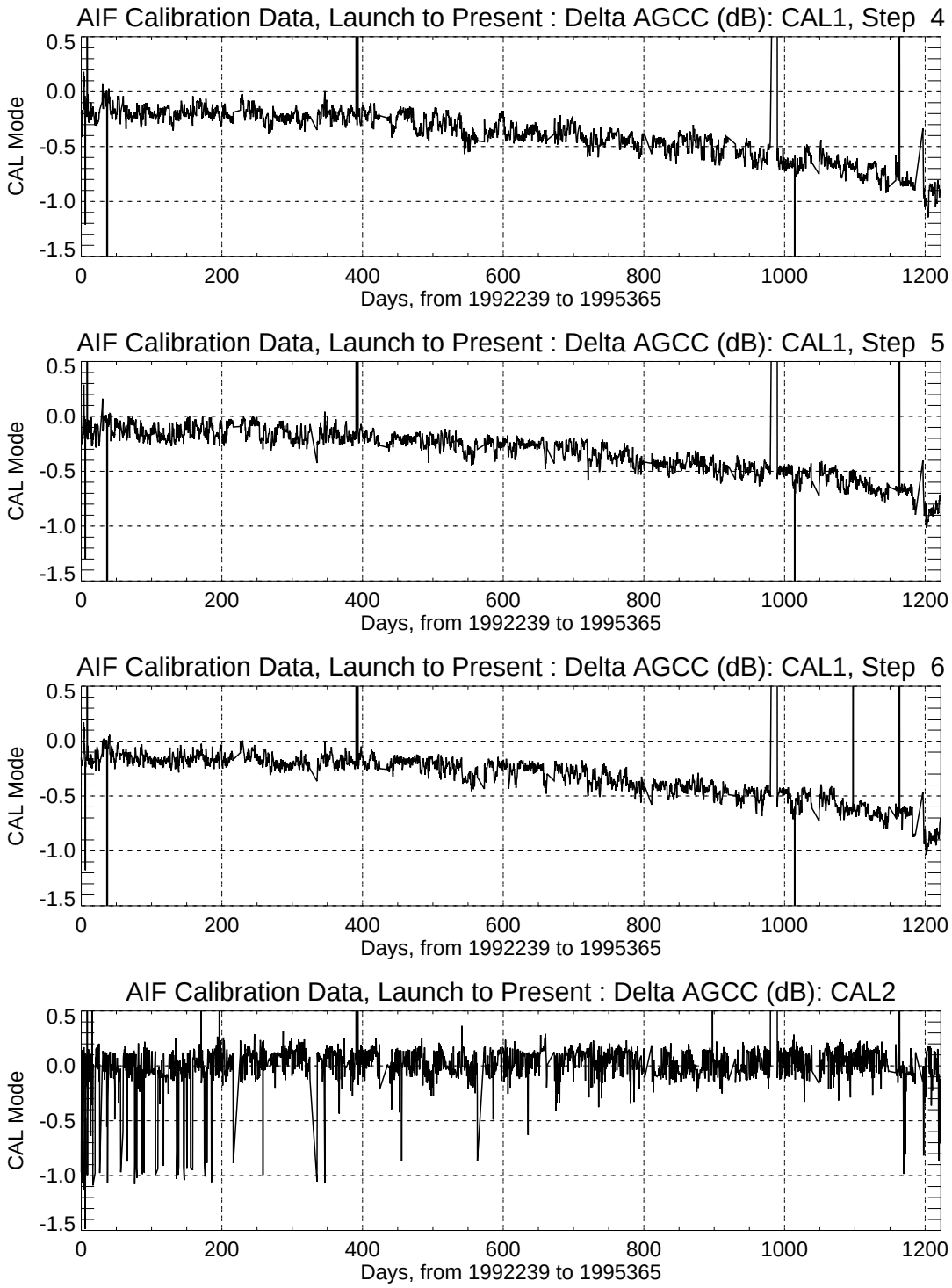

Figure 2-4 C-Band AGC CAL-1 and CAL-2 Results

water is 0.83 dB, very close to the observed power difference. This CAL-2 study is documented in the TOPEX/Poseidon Research News (Hancock, et al, 1995)

2.2 Launch-to-Date Cycle Summaries

The data in the launch-to-date cycle summary plots which follow are extracted from the Geophysical Data Record (GDR) data base at WFF. The criteria for TOPEX GDR measurements to be accepted for the WFF data base are: the data are classified as Deep Water, the data are in normal Track Mode, and selected data quality flags are not set.

For each measurement type, the plots contain one average measurement per cycle. The cycle average value is itself the mean of one-minute along-track boxcar averages, after editing. Data are excluded from the averaging process whenever the one-minute-averaged off-nadir angle exceeds 0.12 degree or the averaged Ku-Band sigma-naught exceeds 16 dB or whenever the number of non-flagged frames within the one-minute interval is fewer than 45. As a result of this edit, approximately 15% of the data base measurements are excluded from the averaging process. This tight editing is part of our effort to ensure that anomalous data are excluded from the performance assessment process.

Investigators should use the NASA radar altimeter (ALT) data products for data cycles 1-8 with great care. There are a number of reasons for this statement. These early cycles had numerous switches between ALT and SSALT, had several spacecraft (s/c) safeholds, and a series of attitude calibration maneuvers. The amount of ALT data available for these early cycles varies, but each of the cycles 1-8 has significantly less data than the normal later cycles. There were a number of operations related to the s/c that had not yet been fully stabilized; foremost among these was the control of the s/c attitude. There are a number of data effects dependent on the s/c attitude such as altimeter instrument correction, s/c center of gravity (c.g.) range correction, and orbit-related c.g. corrections. The s/c attitude control system had its last major adjustment and correction early in cycle 9; prior to that adjustment, the off-nadir angle occasionally exceeded 0.3 degrees. We believe the ALT instrument corrections for attitude are good out to about 0.3 degrees, but may be unreliable beyond that angle. Phil Callahan (ALT Measurement System Engineer) stated in his GDR data release notes that, at the time of processing, the s/c attitude was not determined well enough to provide a good range correction for the effect of the s/c c.g. change. We believe that similar effects may be in the precision orbit computations. Callahan has also noted that the tropospheric corrections do not compare as well with other tropospheric data sources during these earlier cycles. We have carefully examined the TOPEX ALT performance during these cycles. During "normal operations" times (specifically, when the off-nadir angle was 0.3 degrees or less), we have found no difference from the later cycles in the altimeter performance. We do fully believe that the first eight cycles should not be used unquestioningly and, if used at all, should be selectively used with care. For those wishing to selectively use the ALT data from the first eight 8 cycles, Table 2-1 "Data Assessment for Cycles 1-8" provides a listing of times for which we believe the data would be normal and acceptable.

Table 2-1 Data Assessment for Cycles 1-8

Cycle	Start Date YYYYDDD	Time HHMMSS	Stop Date YYYYDDD	Time HHMMSS	No. of Seconds Remaining After >0.3 ^{o} Edit	Percent Data Normal	WF Att Est. Degrees	Reason for Stop/ Comments
1	1992270	000000	1992275	162335	84,886	19.7	0.25 - 0.30	SSALT on/ This is good ALT data but the corrections are not. Attitude generally above 0.3^{o}. The s/c was switched to geoid ref at 275t205500 and bias entered at 223000. Data probably not useful.
2	1992277	013636	1992286	224535	292,188	68.0	0.25 - 0.30	ALT to idle. New parameter set loaded. ALT data good but corrections probably bad. Attitude about 0.3^{o}. Also check the cg correction
3	1992287 1992287	013000 230000	1992287 1992295	223000 120000	290,274	67.5	0.10 - 0.20	Attitude Bias changed at 287t223000. Moved att from above 0.3^{o} to near 0.2^{o}. Before this good ALT data, but corrections may not be. ALT to idle
4	1992298	200000	1992306	193211	327,402	76.1	0.08 - 0.20	End cycle 4/New parameter set loaded at 304t195000. Att swings.
5	1992306	193211	1992315	075500	341,053	79.3	0.10 - 0.30	ALT to idle/attitude swings above 0.3^{o}. Note that GDR and AttEstWF do not agree.
6	1992316 1992318 1992324	173042 204600 052400	1992317 1992324 1992325	093000 014400 063000	309,279	71.9	0.10	ALT to idle/ Att swings / attitude bias change. Att test/att is more stable. First real good data. SSALT on/ave att is 0.1^{o}

Table 2-1 Data Assessment for Cycles 1-8 (Continued)

Cycle	Start Date YYYYDDD	Time HHMMSS	Stop Date YYYYDDD	Time HHMMSS	No. of Seconds Remaining After >0.3 ^{o} Edit	Percent Data Normal	WF Att Est. Degrees	Reason for Stop/ Comments
7	1992326	152914	1992336	132745	350,459	81.5	0.10 - 0.30	End cycle/Att swings to above 0.3^{o} (attitude bias #s were wrong). Memory patch at 328t191300-202700
8	1992336	132745	1992345	014900	270,970	63.0	0.05 - 0.30	SSALTon/ Att swings to above 0.3^{o}

2.2.1 Sea Surface Height

The sea surface heights (ssh) contained in the GDR files are based on combined heights. Cycle-average ssh are shown in Figure 2-5 "Cycle-Average Sea Surface Heights, in Meters, from the WFF TOPEX GDR Data Base". It is not possible to discern range drifts at the millimeter level from these data, but annual variations of sea level are observable.

Beginning with cycle 17, ssh has a 37-cycle periodicity. For example, lower ssh levels during cycles 25 through 35 are echoed during cycles 62 through 72, and again during cycles 99 through 109. Higher ssh levels are observed during cycles 37 through 43, and again during cycles 74 through 80. A 37-cycle repeatability is anticipated because, with each cycle lasting 9.916 days, there are approximately 37 cycles per annum. Repeatability is not expected before cycle 17 because, prior to this, the NASA altimeter was not in TRACK mode for full cycles. This expected periodicity lends credence that the altimeter data remains internally consistent.

The only calibration correction applied to date to range is the +100 mm added to C-Band range shortly after launch. This correction was described in Section 5.1.2 of the February 1994 Engineering Assessment Report.

2.2.2 Sigma-Naught

The sigma-naught cycle-averages, subsequent to the application of the WFF-provided calibration corrections, are plotted in Figure 2-6 "Cycle-Average Ku-Band Sigma-naught, in dB, from the WFF TOPEX GDR Data Base" and Figure 2-7 "Cycle-Average C-Band Sigma-naught, in dB, from the WFF TOPEX GDR Data Base", for Ku-Band and C-Band, respectively.

From cycle 17 to the present, Ku-Band sigma-naughts, after correction, have remained within a window of 11.20$\pm$0.20 dB and C-Band sigma-naughts have remained at 14.70$\pm$0.15 dB. There are apparent annual cycles in the sigma-naught averages, particularly in the Ku-Band (low values occur at cycles 22, 59, and 96). Even

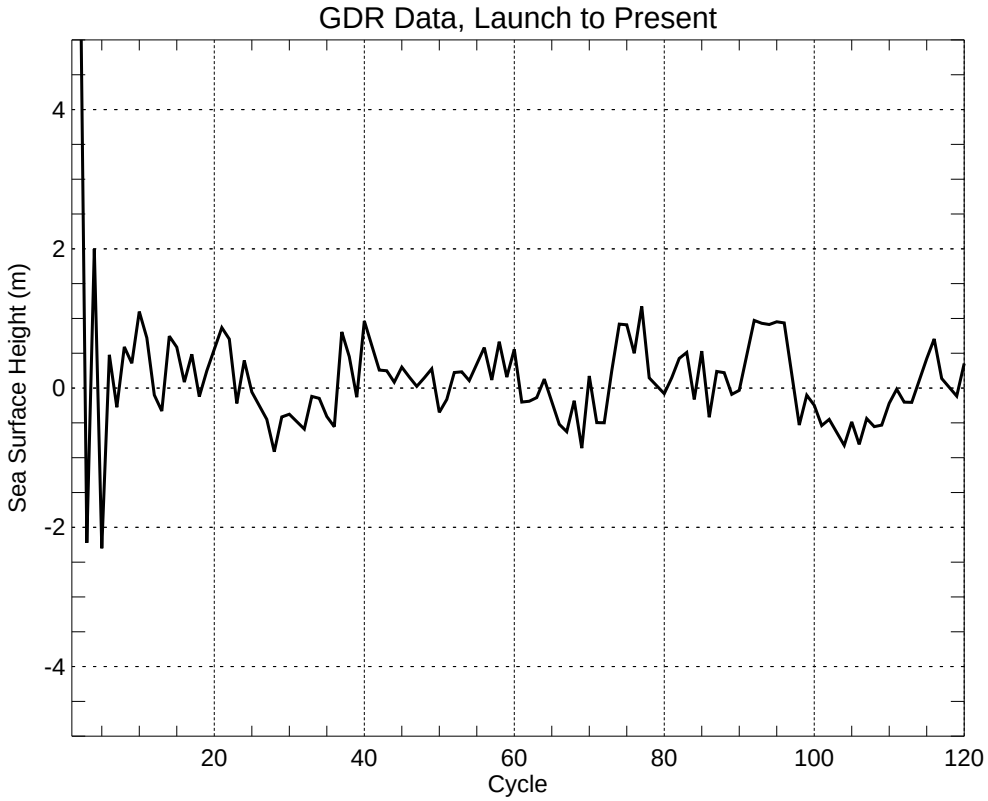

Figure 2-5 Cycle-Average Sea Surface Heights, in Meters, from the WFF TOPEX GDR Data Base

with the annual effects, the sigma-naughts have remained within the pre-launch design goal for sigma-naught accuracy of $\pm$0.25 dB

2.2.3 Significant Wave Height

Ku-Band cycle-averages for significant wave height (swh) are shown in Figure 2-8 "Cycle-Average Ku-Band Significant Wave Height, in Meters, from the WFF TOPEX GDR Data Base". Subsequent to cycle 8, the cycle-average swh's have remained in the range of 2.8+0.3 m, with no apparent long-term drift. As anticipated, the Ku-Band swh values are inversely correlated with the Ku-Band sigma-naughts shown in Figure 2-6 "Cycle-Average Ku-Band Sigma-naught, in dB, from the WFF TOPEX GDR Data Base".

There appears to be an annual cycle in the data, with particularly low swh's centered around cycles 11, 48, and 85 (2.5-2.6 m), gradually building up to 3.0-3.1 m swh centered around cycles 23, 60, and 97. Cycles 11, 48, and 85 occurred in early January 1993, January 1994, and January 1995, corresponding to summer in the southern hemisphere. Cycles 23, 60, and 97 were in early May 1993, May 1994, and May 1995, corresponding with early fall in the southern hemisphere. The southern hemisphere is referred to here because there is a considerably higher percentage of the total ocean area south of the equator.

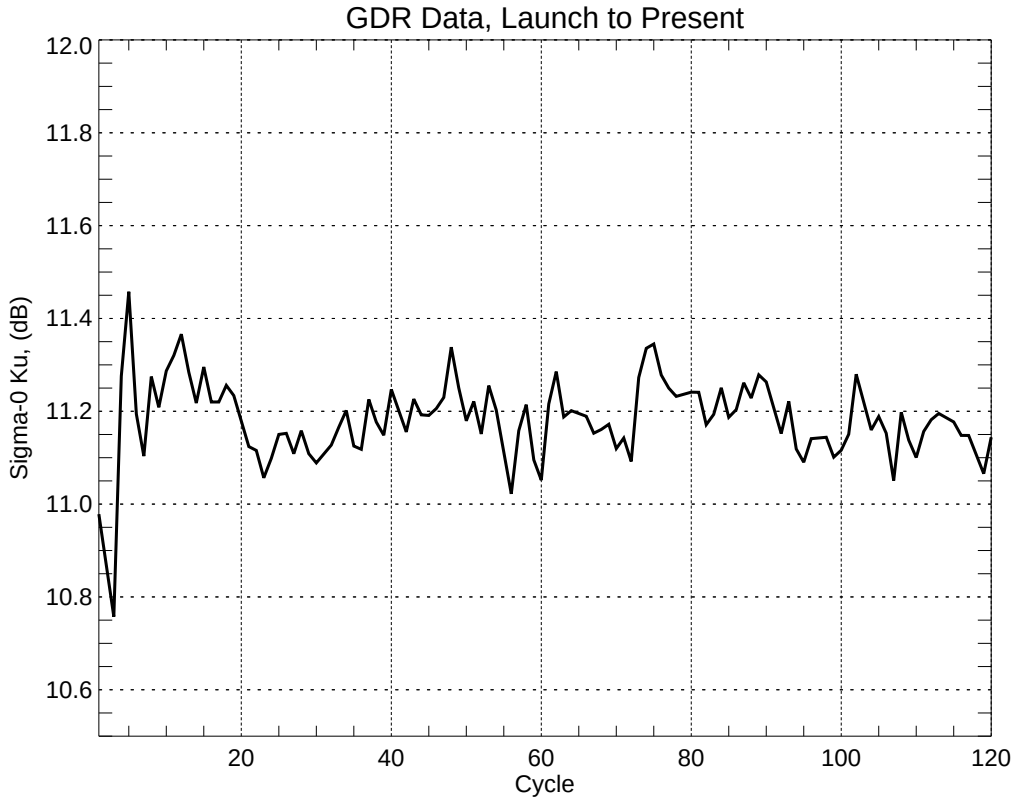

Figure 2-6 Cycle-Average Ku-Band Sigma-naught, in dB, from the WFF TOPEX GDR Data Base

2.2.4 Range RMS

The calculated Ku-Band range rms values depicted in Figure 2-9 "Cycle-Average Ku-Band Range RMS, in Millimeters, from the WFF TOPEX GDR Data Base" are based on the rms derivation described in Section 5.1.1 of the February 1994 Engineering Assessment Report. Subsequent to cycle 17, the rms values have remained in a narrow band of 18.4$\pm$0.8 mm, and are observed to be directly correlated with the swh's in Figure 2-8; the higher the SWH, the higher the rms. There has been no apparent change in range RMS since launch.

2.2.5 Waveform Monitoring

Selected telemetered waveform gates during CAL-2 and STANDBY modes are monitored daily, to discern waveform changes throughout the mission. CAL-2 waveform sets are generally available twice per day, during calibrations. STANDBY waveforms are generally available four times per day, since the altimeter passes through STANDBY mode just prior to and immediately after CALIBRATE mode. The relationship of telemetered waveform sample numbers to the onboard waveform sample numbers is listed in Table 6.2.1 of the February 1994 Engineering Assessment Report.

For both Ku-Band and C-Band, the monitored waveform samples are as follows: CAL-2 gates 23, 29, 48, and 93; and STANDBY gates 38, 39, 68, and 69. The Ku-Band waveform sample history is shown in Figure 2-10 "Ku-Band CAL-2 Waveform Sam-

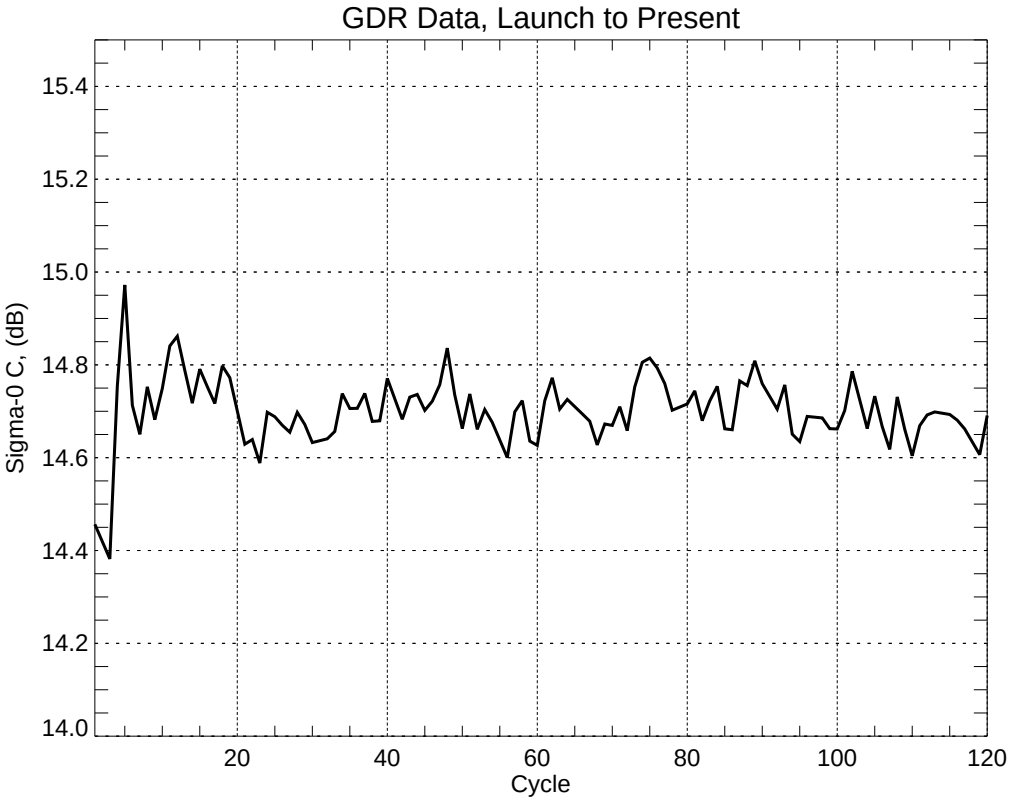

Figure 2-7 Cycle-Average C-Band Sigma-naught, in dB, from the WFF TOPEX GDR Data Base

ple History" and Figure 2-11 "Ku-Band STANDBY Waveform Sample History" for CAL-2 and STANDBY, respectively. The C-Band waveform history is depicted in Figure 2-12 "C-Band CAL-2 Waveform Sample History" and Figure 2-13 "C-Band STANDBY Waveform Sample History", respectively, for CAL-2 and STANDBY.

The monitored Ku-Band CAL-2 waveform samples in Figure 2-10 have each varied less than 1% throughout the mission, and exhibit little or no temperature dependence.

The Ku-Band STANDBY waveform samples in Figure 2-11, however, have fluctuated during the mission. The power in gate 38 has a very noticeable inverse dependence on temperature (selected launch-to-date temperatures are shown in Figure 2-14, on the same horizontal time scale as the waveform samples). Gate 39 is observed to have an inverse temperature dependence, and has had about a 40% reduction in power since launch. Gate 68 has a slight inverse dependence on temperature, and has had a small (4%) decrease in power. Gate 69 also has a modest temperature dependence, and its power level has decreased a total of about 20% during the mission.

The C-Band CAL-2 waveforms samples, shown in Figure 2-12, are similar to the Ku-Band CAL-2 waveforms in that they have varied less than about 1%, and exhibit no apparent temperature dependence.

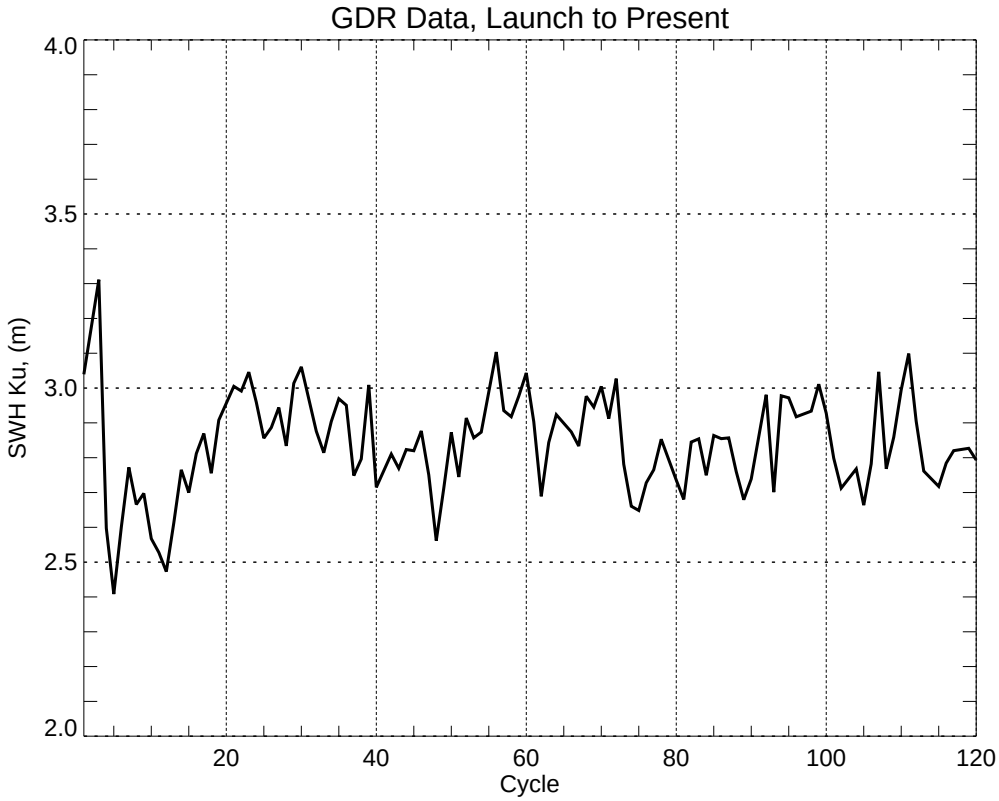

Figure 2-8 Cycle-Average Ku-Band Significant Wave Height, in Meters, from the WFF TOPEX GDR Data Base

The C-Band STANDBY waveform samples, shown in Figure 2-13, are also similar to their counterpart Ku-Band STANDBY waveforms. Gates 38, 39, 68, and 69 have an inverse dependence on temperature. Gate 39 has experienced about a 35% decrease in power since launch, gate 68 has decreased in power about 8%, and gate 69 has decreased approximately 22%. The rate of decrease for each of these three gates was smaller during 1995 than during the prior years.

2.2.6 Engineering Monitors

Altimeter temperatures, voltages, powers and currents continue to be monitored. The system is very stable, with no significant changes since launch.

2.2.6.1 Temperatures

The temperatures of all 26 internal thermistors continue to be within the design temperature range and are within the ranges used during the pre-launch Hot and Cold Balance Tests. The minimum / maximum values for each of the thermistors during TRACK mode remain within the bounds listed in Table 7.1 of the February 1994 Engineering Assessment Report.

Four sample launch-to-date temperature histories (C MTU IF Preamp, C MTU Power Monitor, CSSA GaAs FETS, and CSSA Power Converter) compose Figure 2-14 "Engi-

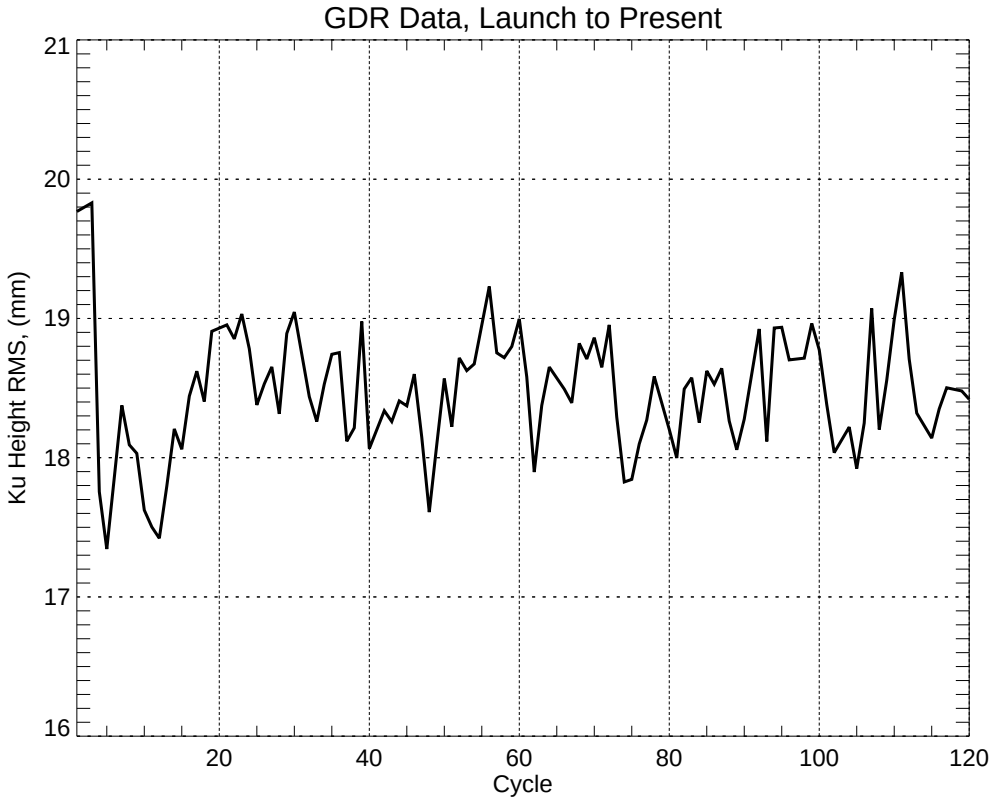

Figure 2-9 Cycle-Average Ku-Band Range RMS, in Millimeters, from the WFF TOPEX GDR Data Base

neering Monitor Histories". All the other thermistors follow the same temperature pattern.

Although not used during our routine monitoring, several of the altimeter-related baseplate temperature monitors serviced by Remote Interface Unit (RIU) 6B became uncalibrated on day 17 of 1995. The affected temperature monitors are listed in Table 2-2 "Telemetry Channels Affected by RIU-6B Anomaly on January 17, 1995". An abrupt change in the values occurred on that date, apparently due to a change in the current which is applied to the thermistor circuits.

2.2.6.2 Voltages, Powers and Currents

The altimeter's 17 monitors for voltages, powers and currents remain at consistent levels, with little deviations. Their launch-to-date histories are also shown in Figure 2-14 "Engineering Monitor Histories".

The eight voltages [LVPS +12V, LVPS +28V, LVPS +15V, LVPS -15V, LVPS +5V(5%), LVPS +5V(1%), LVPS -5.2V and LVPS -6V], have changed very little from the minimum / maximum values listed in Table 7.2 of the February 1994 report. Three of the voltages (LVPS +28V, LVPS +15V and LVPS -5.2V) exhibit more bit toggling than previously, while the LVPS +5V(5%) is toggling less. LVPS -5V has had a slight (0.03V) decrease.

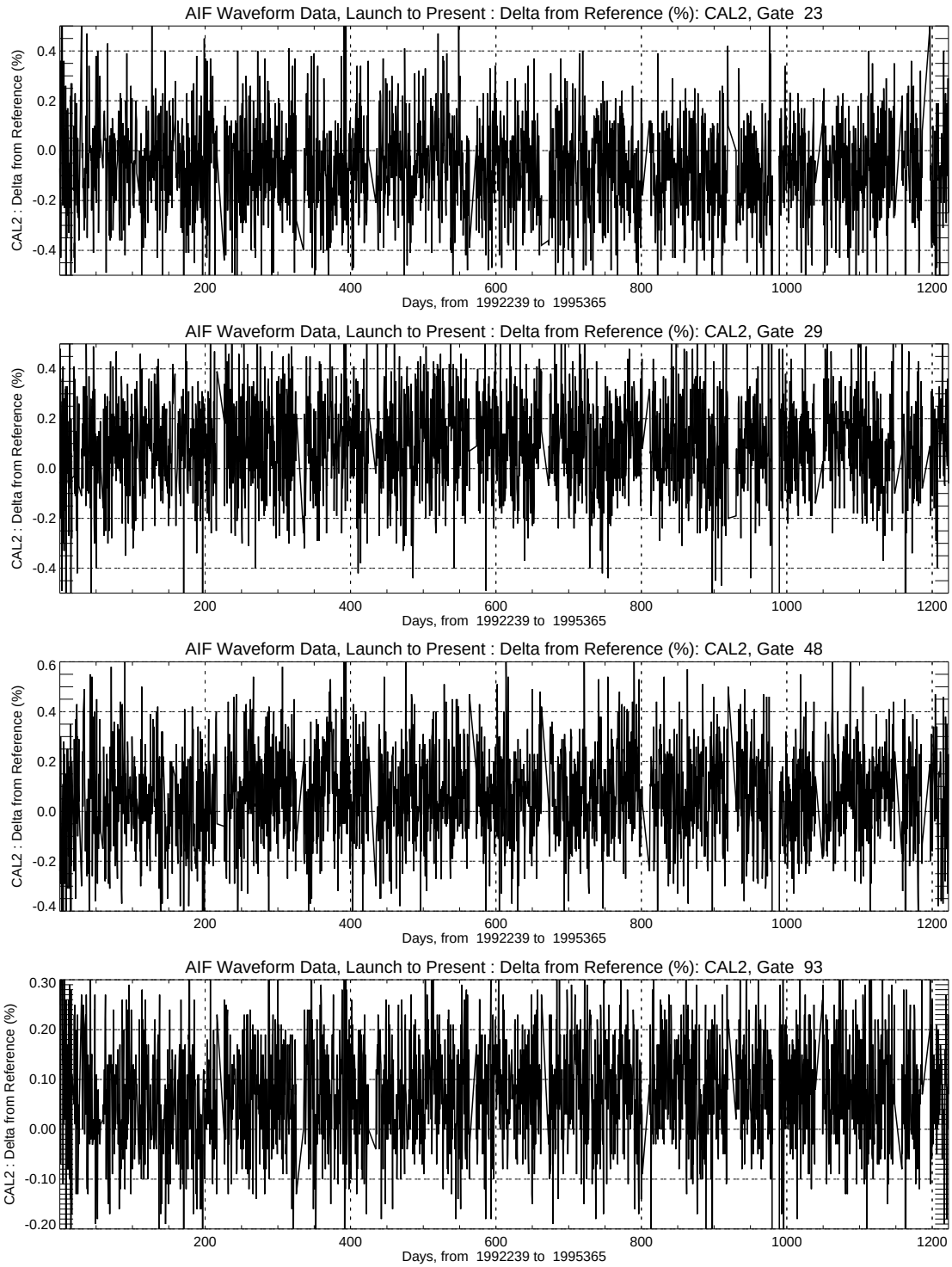

Figure 2-10 Ku-Band CAL-2 Waveform Sample History

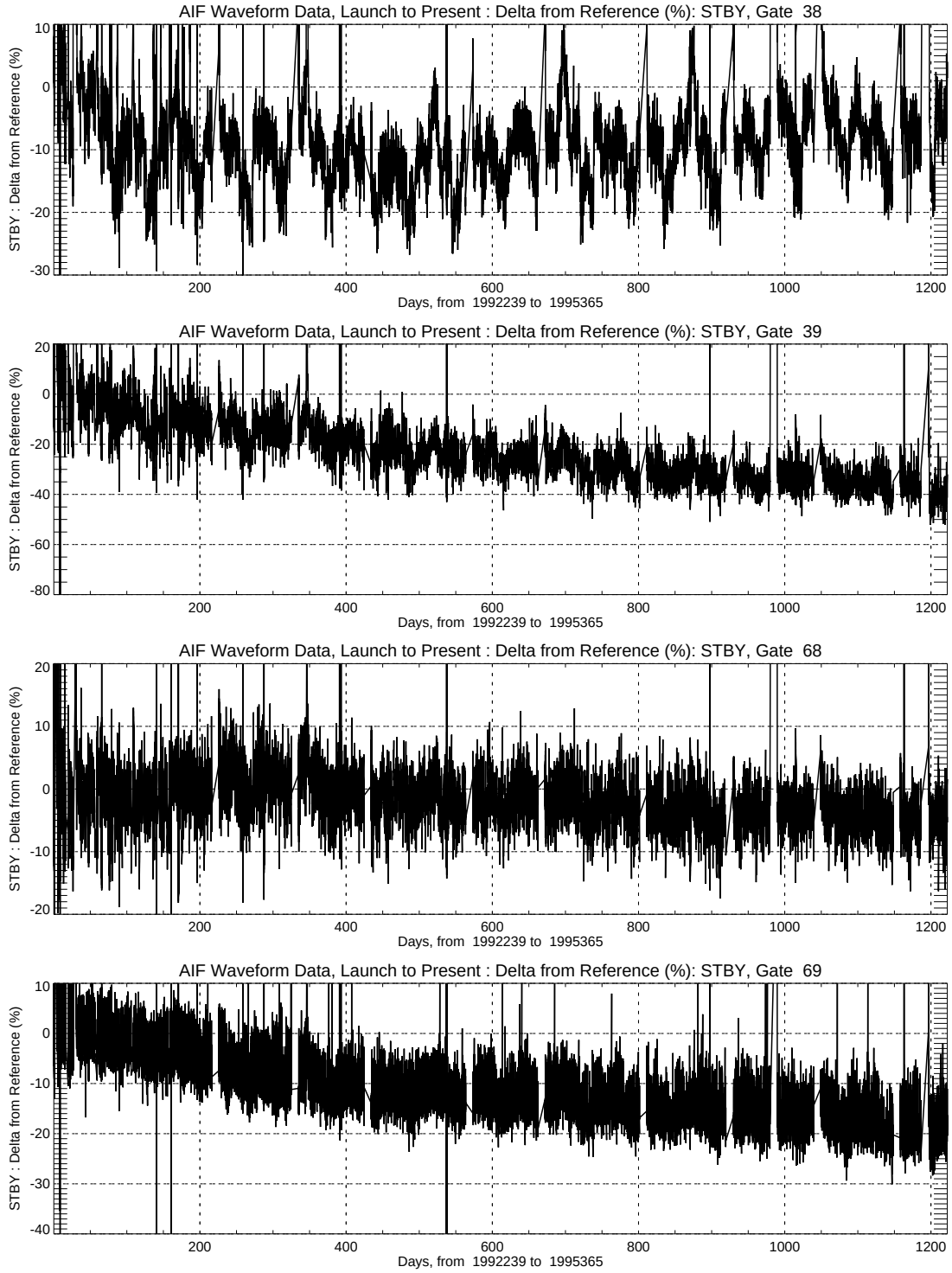

Figure 2-11 Ku-Band STANDBY Waveform Sample History

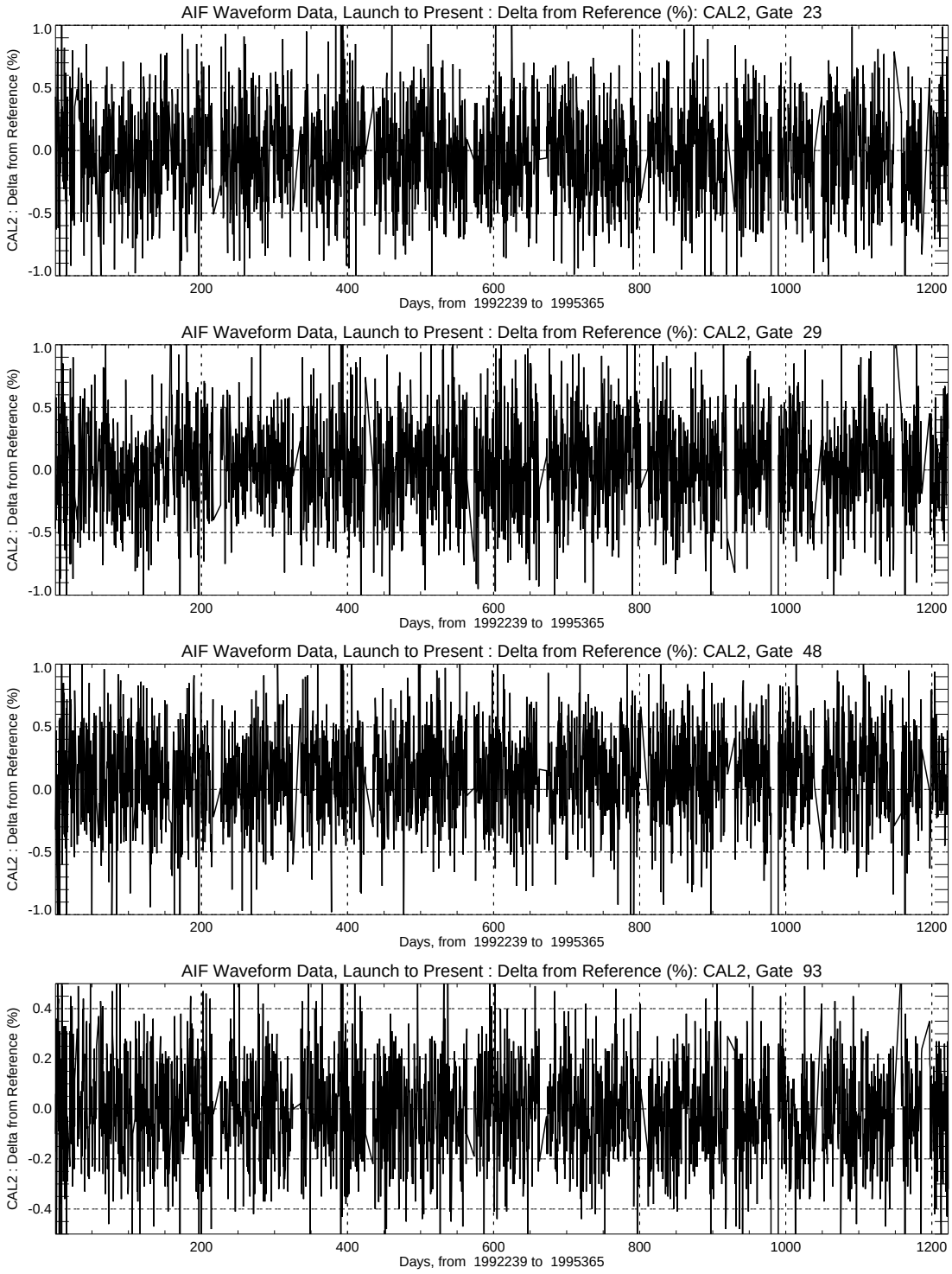

Figure 2-12 C-Band CAL-2 Waveform Sample History

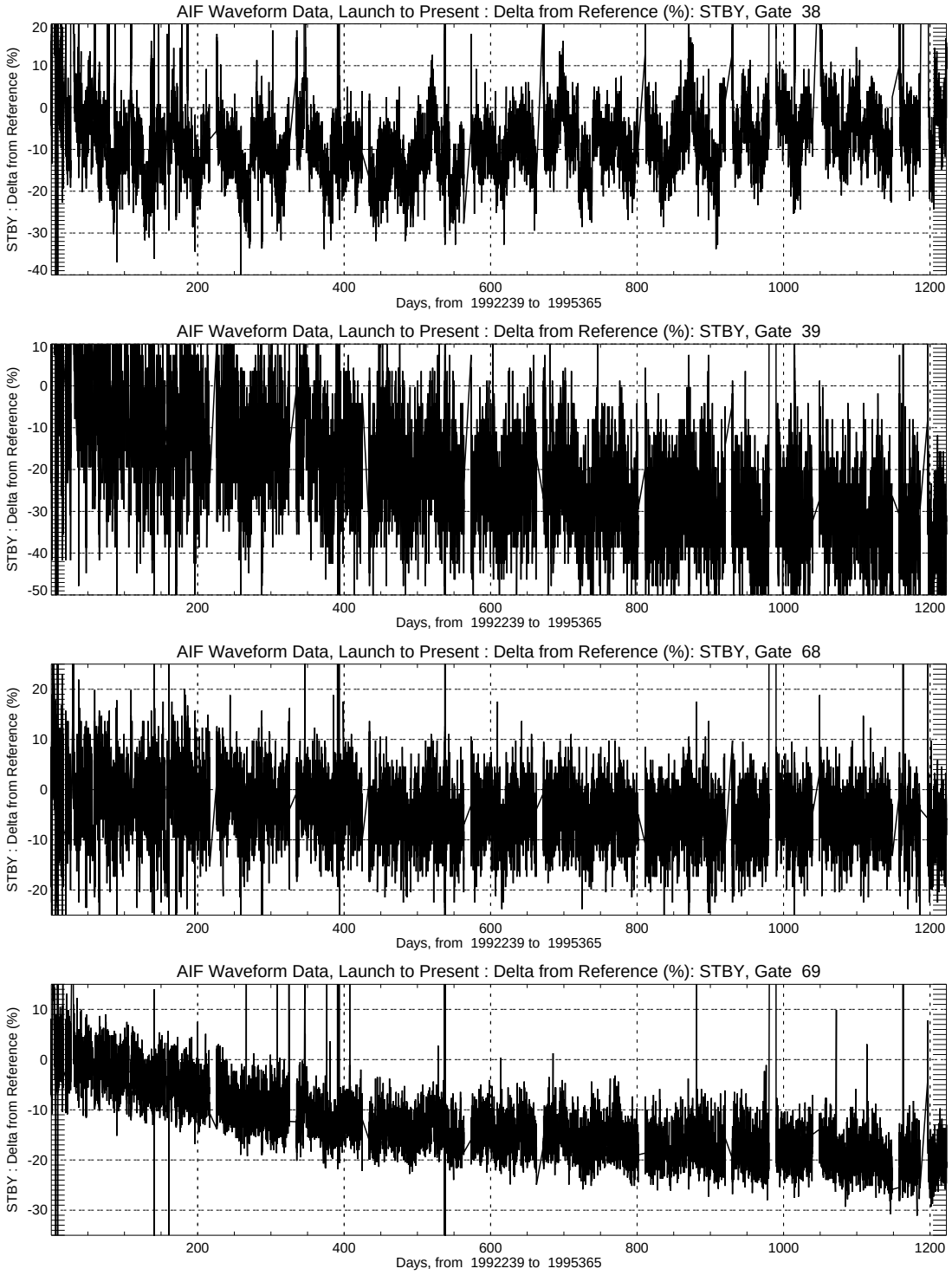

Figure 2-13 C-Band STANDBY Waveform Sample History

The Ku-Band Transmit Power has decreased about 0.3 watt during the past year, while the C-Band Transmit Power has remained at about the same level.

Table 2-2 Telemetry Channels Affected by RIU-6B Anomaly on January 17, 1995

TELEMETRY CHANNEL	SUBSYSTEM	TELEMETRY SIGNAL
16	FRU-A	FRU-A Oscillator Flask Temperature
17	FRU-A	FRU-A Oscillator Baseplate Temperature
18	FRU-B	FRU-B Oscillator Flask Temperature
19	FRU-B	FRU-B Oscillator Baseplate Temperature
20	IM	FRU Mounting Plate Temperature
24	IM	ALT Ant-IM Near Fitting Temperature
25	IM	ALT Ant-On Fitting Temperature
29	IM	ALT C Band Power AMP +Z Deck Temperature
30	IM	ALT Down Converter +Z Cntr PNL Temperature
31	IM	ALT C Band MTU +Z Deck Temperature

There are no observed changes in the operating levels of the TWTA Cathode voltage, TWTA Helix current, or CSSA Input RF power. There continues to be gradual decrease in the CSSA Bus current level; the level has now decreased 0.04 amp since launch. There have been gradual increases in the maximum levels of both the TWTA Bus current and the LVPS Bus current; the increases have been 0.05 amps and 0.2 amps, respectively, since launch.

2.2.7 Single Event Upsets

There have been a total of 154 Single Event Upsets (SEUs) from launch to the beginning of 1996. The vast majority of them have occurred in the South Atlantic Anomaly, as shown in Figure 2-15 "Locations of SEU Occurrences". The altimeter processor automatically recovered from 130 of the SEUs, with only a few seconds of data lost per SEU. The other 24 SEUs were of longer duration, and the majority of these required manual ground intervention to reset the processor. Table 2-3 "Anomalous Single Event Upsets" lists the dates of these 24 SEUs, along with the type of reset.

The dots in Figure 2-15 denote the locations of normal SEU occurrences, while the diamonds indicate that the SEU was abnormal.

The three diamonds at latitude -90 degrees were placed there because their occurrence times (and corresponding geographic locations) could not be pin-pointed due to the altimeter being in IDLE mode.

This past year has been typical, in that there was approximately one SEU per eight days. This ratio has been consistent throughout the on-orbit mission.

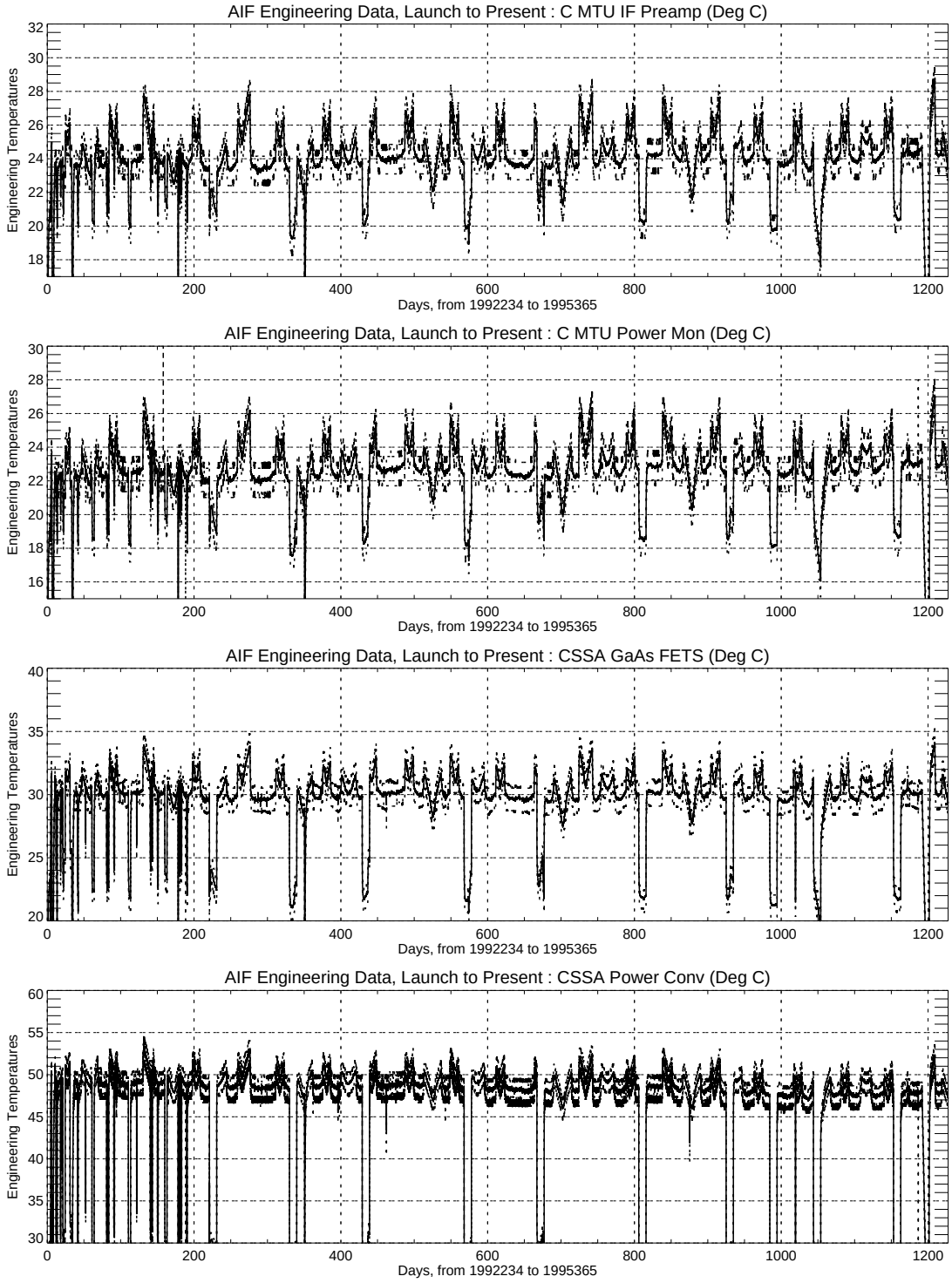

Figure 2-14 Engineering Monitor Histories

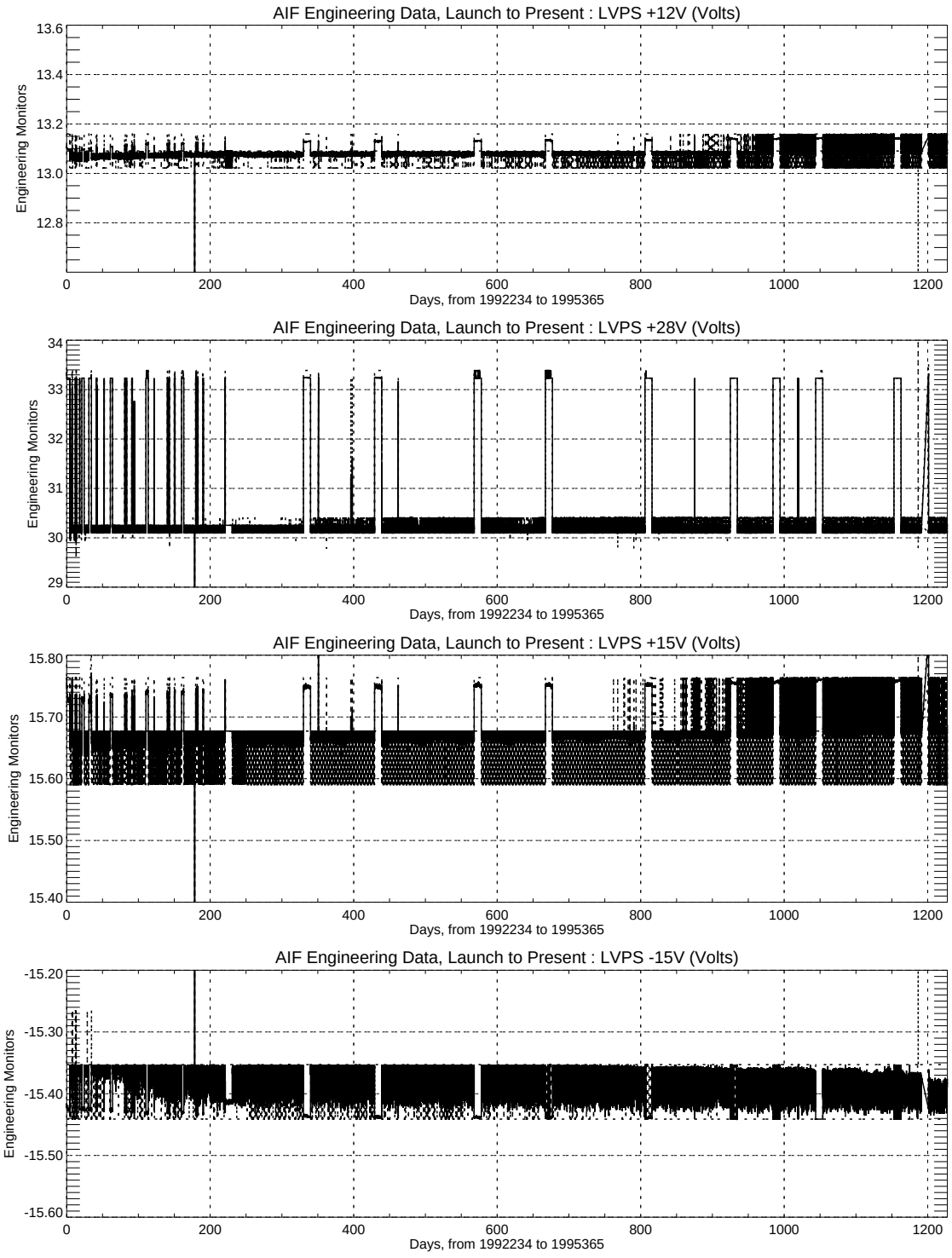

Figure 2-14 Engineering Monitor Histories (Continued)

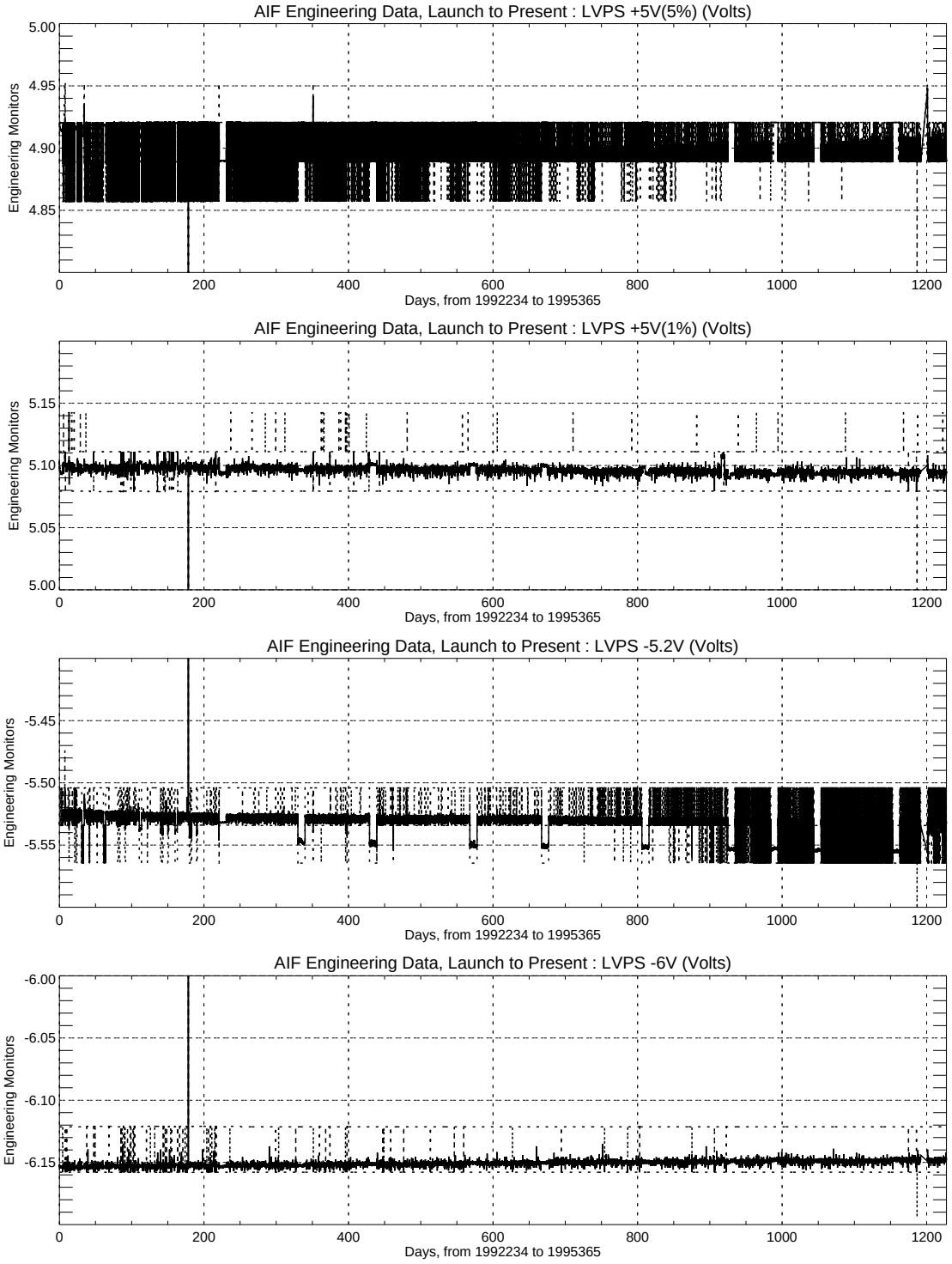

Figure 2-14 Engineering Monitor Histories (Continued)

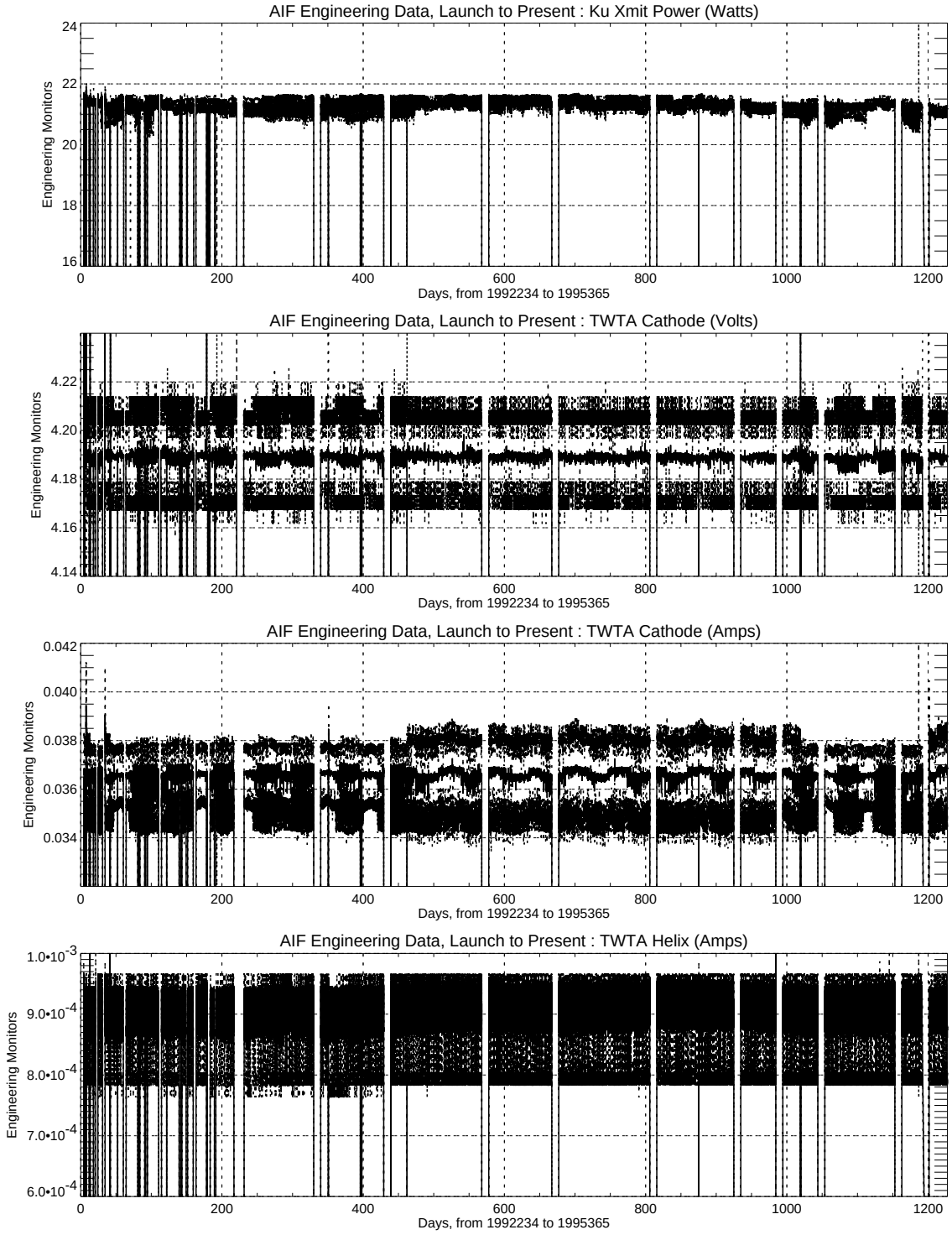

Figure 2-14 Engineering Monitor Histories (Continued)

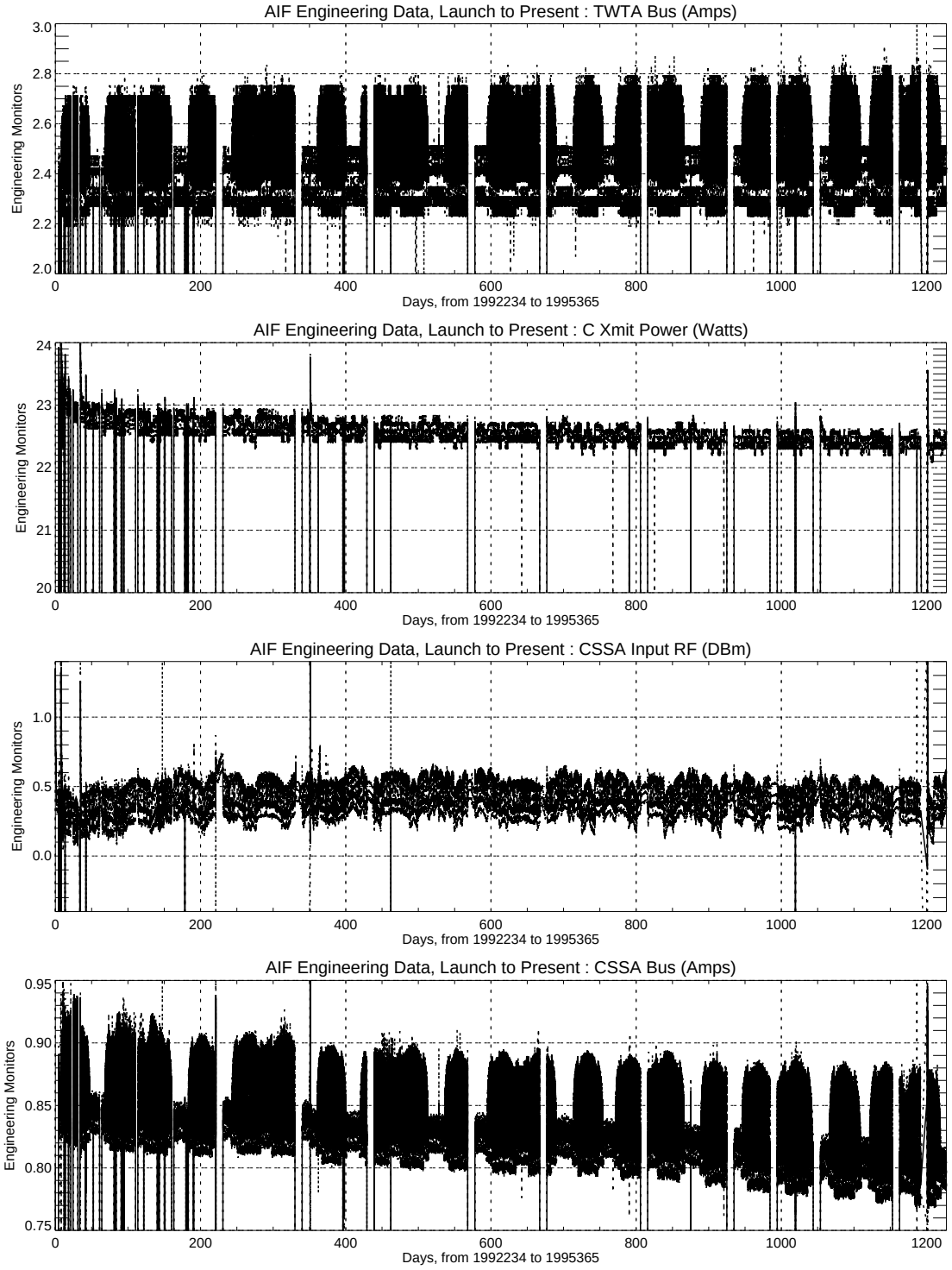

Figure 2-14 Engineering Monitor Histories (Continued)

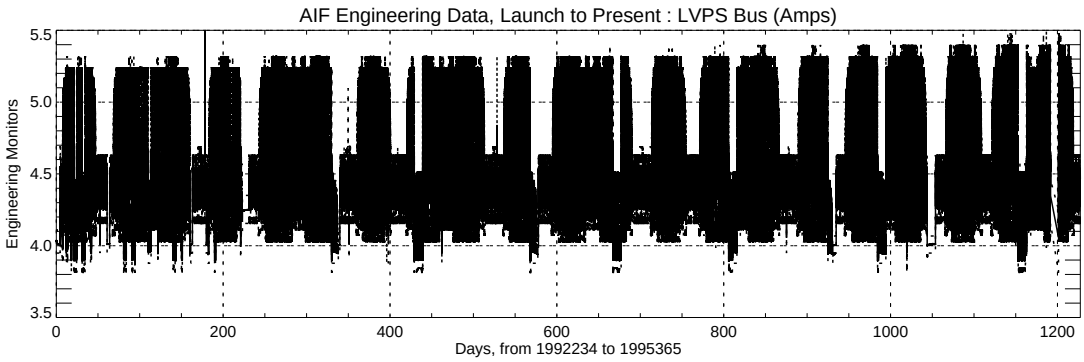

Figure 2-14 Engineering Monitor Histories (Continued)

Table 2-3 Anomalous Single Event Upsets

Year	Day	Duration (Hr)	Reset Type
1992	247	11.0	Automatic
1992	354	16.8	Manua
1993	012	0.5	Automatic
1993	230	1.3	Automatic
1993	264	14.5	Manual
1993	266	7.5	Manual
1993	307	2.3	Manua
1993	330	8.3	Manua
1994	001	3.8	Manua
1994	112	1.1	Manua
1994	256	4.3	Manual
1994	271	0.1	Automatic
1994	288	2.5	Manual
1994	294	1.3	Automatic
1994	324	3.1	Manual
1995	012	0.7	Automatic
1995	083	1.6	Manual
1995	132	0.2	Manual
1995	157	8.4	Manual
1995	251	3.9	Manual
1995	306	3.4	Manua
1995	325	1.8	Manua
1995	327	3.5	Manual
1995	361	3.3	Manual
		Total = 105.2 Hours	

The year 1995 was not typical in that there were a few more anomalous SEUs than in prior years; two of them required more than a ground-commanded reset. Those two events were:

a. Day 012 - The SEU caused a change in most RAM memory values, although the ALT was performing normally; this raised a concern that the altimeter

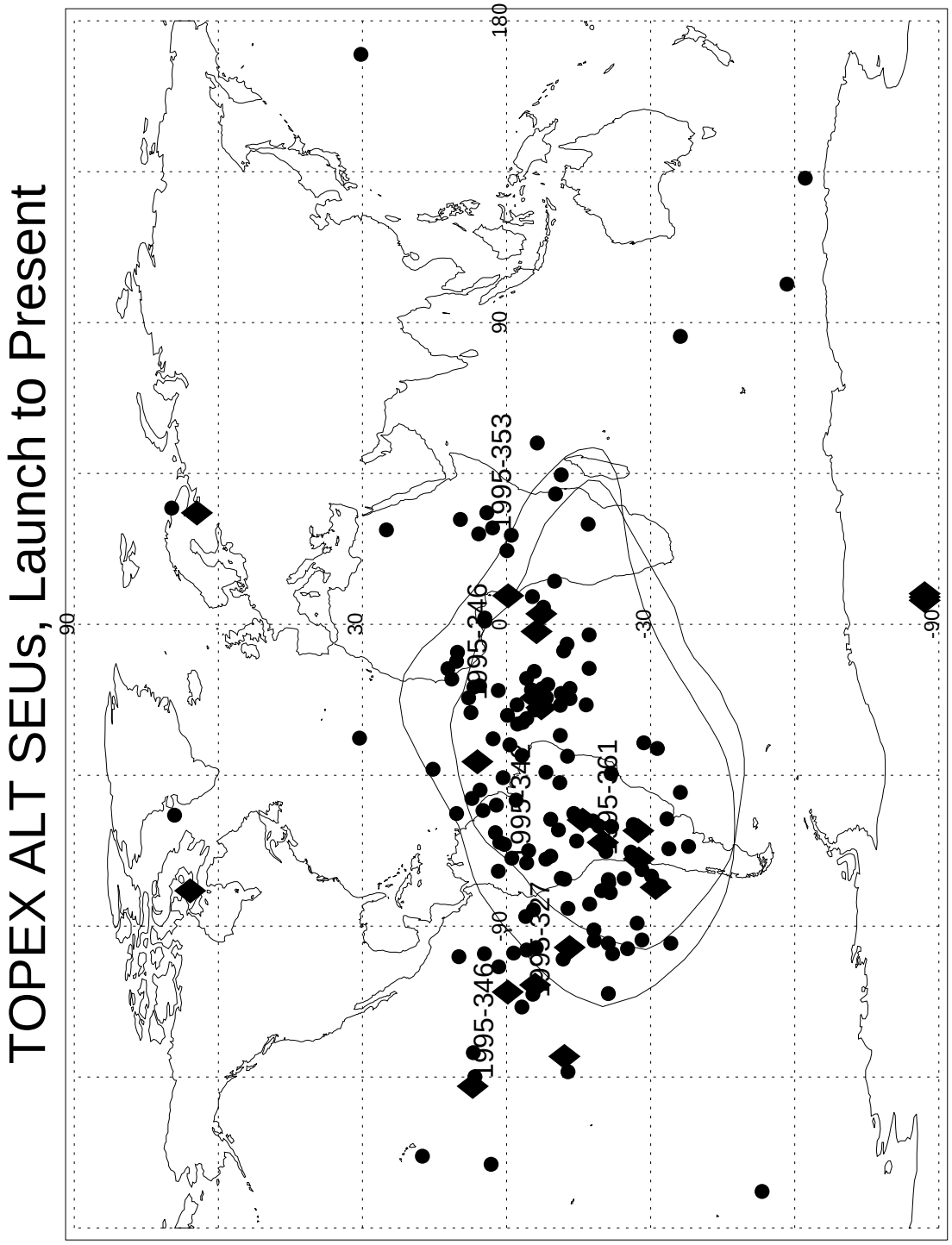

Figure 2-15 Locations of SEU Occurrences

may not perform certain operations properly. Commands were sent to the altimeter on day 013 to reload the memory patches and the parameter file. These commands restored all memory to normal values.

b. Day 157 - The Ku MTU Receive Side switched from Side A to Side B. The Ku signal was mostly lost with the system trying to track a signal at about 13 dB AGC. The return waveforms appeared to be a combination of noise and a leakage of the real return through the switch. Commands were sent to bring the altimeter to Safe Idle. Command Block 27, which contains a ground reset and an A/B MTU toggle switch, was subsequently sent to the altimeter. These commands rectified the problem. There was no harm to the altimeter.

2.3 Launch-to-Date Key Events

The launch-to-date key events for the TOPEX Radar Altimeter are summarized in Table 2-4 "NASA Altimeter - Key Events".

Table 2-4 NASA Altimeter - Key Events

Day	Event
92/234	Altimeter Turned On to IDLE Mode
92/238	First TRACK
92/240	Safehold During Inclination Maneuver
92/242	Returned to TRACK Mode
92/242	Turned Off by TMON at Start of Eclipse
92/242	Returned to TRACK Mode
92/247	Improper SEU Recovery due to Corruption of Pulse Count Variable
92/268	Safehold
92/269	Returned to TRACK Mode
92/304	50ms Acquisition Parameter Set Upload
92/328	Software Patch to Refresh Pulse Count (see Day 247 above)
92/354	Loss of Science Data and Clock Between SEUs (lost 16 hours of data)
93/012	Improper SEU Recovery (lost 12 min. of data)
93/089	Turned Off by TMON
93/089	Returned to TRACK Mode
93/089	Changed to IDLE Mode for SSALT
93/099	Returned to TRACK Mode
93/198	Changed to IDLE Mode for SSALT
93/208	Returned to TRACK Mode
93/218	Turned Off by TMON
93/219	Returned to TRACK Mode

Table 2-4 NASA Altimeter - Key Events (Continued)

Day	Event
93/230	Improper SEU Recovery (lost 1.5 hours of data)
93/264	Improper SEU Recovery (lost 14.5 hours of data)
93/266	Improper SEU Recovery (lost 7.5 hours of data)
93/297	Changed to IDLE Mode for SSALT
93/307	Returned to TRACK Mode
93/307	Improper SEU Recovery (lost 2.3 hours of data)
93/330	Improper SEU Recovery (lost 8.2 hours of data)
94/001	Improper SEU Recovery (lost 3.7 hours of data)
94/071	Changed to IDLE Mode for SSALT
94/081	Returned to TRACK Mode
94/112	Improper SEU Recovery (lost 1.1 hours of data)
94/170	Changed to IDLE Mode for SSALT
94/180	Returned to TRACK Mode
94/256	Improper SEU Recovery (lost 4.3 hours of data)
94/288	Improper SEU Recovery (lost 2.5 hours of data)
94/294	Improper SEU Recovery (lost 1.3 hours of data)
94/309	Changed to IDLE Mode for SSALT
94/319	Returned to TRACK Mode
94/324	Improper SEU Recovery (lost 3.1 hours of data)
95/012	Improper SEU Recovery (lost 0.7 hours of data)
95/040	Changed Operating Parameter Set for Faster Acquisition after a Reset
95/063	Changed to IDLE Mode for SSALT
95/073	Returned to TRACK Mode
95/083	Improper SEU Recovery (lost 1.6 hours of data)
95/123	Changed to IDLE Mode for SSALT
95/133	Returned to TRACK Mode
95/157	Improper SEU Recovery (lost 8.4 hours of data)
95/182	Changed to IDLE Mode for SSALT
95/192	Returned to TRACK Mode
95/251	Improper SEU Recovery (lost 3.9 hours of data)

Table 2-4 NASA Altimeter - Key Events (Continued)

Day	Event
95/291	Changed to IDLE Mode for SSALT
95/301	Returned to TRACK Mode
95/306	Improper SEU Recovery (lost 3.4 hours of data)
95/325	Improper SEU Recovery (lost 1.8 hours of data)
95/327	Improper SEU Recovery (lost 3.5 hours of data)
95/330	Spacecraft Safehold (lost 230 hours of data)
95/340	Returned to TRACK Mode
95/361	Improper SEU Recovery (lost 3.3 hours of data)

Section 3

Assessment of Instrument Performance

3.1 Range

The CAL-1 Step-5 Ku-Band and C-Band delta ranges have been processed to form a set of delta combined range values. There are about twenty delta combined ranges for each TOPEX data cycle, corresponding to the two calibrations per 10-day cycle.

Range bias changes for the NASA radar altimeter of the TOPEX / POSEIDON mission are described by Hayne, et al (1994). Reported here are the additional bias change results to date. Table 3-1 "TOPEX Altimeter Range Bias Changes Based on Calibration Mode 1 Step 5" lists values for the combined (Ku&C) delta range, in millimeters, with the same sign convention used in the October 1994 article. We have made one change in Table 3-1 as of February 1996: the Table 3-1 now contains bias change results both with and without temperature correction. Before February 1996, the versions of Table 3-1 contained only the temperature corrected results; we are now also providing results with no temperature correction. For the TOPEX GDR data end user who does not have easy access to the T_u data, it would be more appropriate to use the combined delta range results NOT corrected for temperature.

Temperatures are measured at about two dozen different positions within the TOPEX altimeter. Because all these temperatures move up and down together, it is not possible to determine which of these temperatures is the most important to range bias, and for our analyses we use the UCFM temperature of the upconverter / frequency multiplier (UCFM) unit; this will be designated T_u below. There is a correlation of the individual delta range measurement with T_u, and we have found a simple quadratic correction of the delta range for T_u variation. Using the individual delta range estimates from calibration mode 1 step 5 together with the T_u data for cycles 10-87, we have used simple least-squares fitting to find that an additive delta range adjustment Da in millimeters is approximately

$$Da = -1.817*(T_u - 25.5) - 0.073*(T_u - 25.5)**2,$$

where T_u is in degrees C and Da is in millimeters.

The temperature correction Da both smooths out the trend of cycle averages of combined delta range and reduces the standard deviations of the cycle averages. From our instrument science interests, it is appropriate to examine and to report the combined range bias changes after correction for the T_u.

For the results reported in Table 3-1, very slightly different edit criteria were used on the calibration mode data than in the October 1994 article, and the data fit for temperature effects now includes 13 more data cycles than the October 1994 results. The result of the different fit is that the combined delta range values here may differ from those in the October 1994 article, typically by 0.05 mm. The delta range results

reported here may be valid at levels approaching a millimeter, but we think it is unrealistic to worry about differences at the level of tenths of a millimeter

The first column in Table 3-1 "TOPEX Altimeter Range Bias Changes Based on Calibration Mode 1 Step 5" is the TOPEX data cycle and the second column indicates the number of individual calibrations in each cycle average. The dRc_av_N is the cycle average of the combined delta range in millimeters, with NO correction for temperature, and the standard deviation estimate of the individual combined delta range (with no temperature correction) is dRc_sd_N. For the temperature-corrected combined delta range, the corresponding cycle averages and standard deviations are designated dRc_av_T and dRc_sd_T. The cycle average for UCFM temperature in degrees centigrade is T_u_av, and the individual calibration standard deviation for this temperature is T_u_sd. Notice that the third and fourth columns of Table 3-1, the dRc_av_N and dRc_sd_N, have not been reported in earlier versions of this update work such as the October 1994 article.

Table 3-1 TOPEX Altimeter Range Bias Changes Based on Calibration Mode 1 Step 5

Cyc	Count	dR_av_N	dR_sd_N	dRc_av_T	dRc_sd_T	T_u_av	T_u_sd
001	15	+2.795	1.691	+2.003	0.645	25.086	0.834
002	18	+1.867	0.644	+1.747	0.725	25.488	0.166
003	18	+2.527	1.191	+1.792	1.085	25.143	0.239
004	18	+1.811	0.929	+1.731	0.827	25.507	0.335
005	20	+1.947	0.808	+1.611	0.680	25.368	0.207
006	20	+1.792	0.975	+2.305	0.578	25.826	0.433
007	14	+1.602	0.178	+2.104	0.625	25.823	0.331
008	18	+1.799	0.194	+1.534	0.411	25.408	0.149
009	17	+1.751	0.661	+1.437	0.524	25.378	0.282
010	20	+1.594	0.253	+1.780	0.618	25.651	0.376
011	20	+1.342	0.500	+2.350	0.481	26.092	0.316
012	19	+1.645	0.757	+1.978	0.614	25.732	0.332
013	15	+1.622	0.236	+1.475	0.285	25.473	0.113
014	17	+1.941	0.532	+1.181	0.592	25.129	0.227
015	19	+1.985	0.474	+1.288	0.702	25.163	0.328
016	20	+2.060	0.461	+1.772	0.511	25.393	0.266
017	21	+1.723	0.319	+2.023	0.393	25.715	0.299
018	18	+1.484	0.223	+1.867	0.394	25.761	0.202

Table 3-1 TOPEX Altimeter Range Bias Changes Based on Calibration Mode 1 Step 5

Cyc	Count	dR_av_N	dR_sd_N	dRc_av_T	dRc_sd_T	T_u_av	T_u_sd
019	16	+1.615	0.151	+1.039	0.359	25.234	0.163
021	20	+2.047	0.149	+1.713	0.336	25.368	0.236
022	20	+1.672	0.205	+1.657	0.562	25.544	0.278
023	19	+1.354	0.355	+1.505	0.341	25.635	0.246
024	21	+0.624	0.289	+1.229	0.349	25.881	0.191
025	20	+0.553	0.545	+1.454	0.439	26.031	0.462
026	19	+1.517	0.155	+1.080	0.260	25.313	0.153
028	20	+1.131	0.217	+1.074	0.307	25.523	0.201
029	20	+0.614	0.255	+1.040	0.486	25.784	0.241
030	18	+0.924	0.372	+0.726	0.337	25.443	0.267
032	18	+1.727	0.397	+0.882	0.209	25.079	0.291
033	17	+0.805	0.869	+0.561	0.337	25.409	0.540
034	20	+0.023	0.152	-0.126	0.491	25.471	0.242
035	18	-0.490	0.606	-0.061	0.431	25.784	0.295
036	20	-0.777	0.667	-0.181	0.461	25.876	0.189
037	18	+0.283	0.482	+0.049	0.526	25.426	0.129
038	19	+0.734	0.322	+0.622	0.250	25.491	0.268
039	20	+0.834	0.406	+0.629	0.315	25.440	0.260
040	21	+0.690	0.419	+0.607	0.242	25.507	0.246
042	20	-0.609	0.536	+0.224	0.422	26.002	0.185
043	19	-0.081	0.240	+0.043	0.344	25.621	0.216
044	17	+0.152	0.227	-0.027	0.370	25.455	0.169
045	20	+0.170	0.223	+0.156	0.267	25.547	0.099
046	19	-0.316	0.655	+0.208	0.514	25.837	0.212
047	19	-1.348	0.334	-0.496	0.422	26.012	0.168
048	19	-0.148	0.588	+0.136	0.375	25.707	0.268
049	18	-0.165	0.421	-0.318	0.434	25.468	0.266
050	19	+1.349	0.603	-0.001	0.309	24.789	0.255
051	20	-0.076	0.723	-0.183	0.427	25.493	0.294
052	20	-0.183	0.270	-0.398	0.344	25.436	0.122

Table 3-1 TOPEX Altimeter Range Bias Changes Based on Calibration Mode 1 Step 5

Cyc	Count	dR_av_N	dR_sd_N	dRc_av_T	dRc_sd_T	T_u_av	T_u_sd
053	20	-1.823	0.666	-1.079	0.389	25.954	0.254
054	21	-0.810	0.702	-0.609	0.310	25.661	0.269
056	20	-0.435	0.715	-0.561	0.697	25.483	0.269
057	20	-1.059	0.418	-0.691	0.448	25.752	0.285
058	20	-0.957	0.323	-1.188	0.293	25.427	0.167
059	20	-2.053	0.580	-1.487	0.450	25.860	0.194
060	20	-2.299	0.543	-1.664	0.346	25.895	0.288
061	19	-1.569	0.236	-1.709	0.307	25.477	0.155
062	20	-1.455	0.157	-1.837	0.282	25.344	0.128
063	20	-1.392	0.158	-1.864	0.294	25.293	0.124
064	21	-2.245	0.554	-1.866	0.469	25.758	0.274
066	20	-1.488	0.154	-1.910	0.221	25.321	0.131
067	19	-1.843	0.400	-2.031	0.349	25.449	0.245
068	20	-0.302	0.639	-1.938	0.390	24.621	0.261
069	20	-2.039	0.472	-1.956	0.324	25.598	0.260
070	20	-2.554	1.102	-2.351	0.458	25.657	0.479
071	20	-3.780	0.575	-3.011	0.456	25.968	0.197
072	20	-4.598	1.804	-3.667	1.111	26.046	0.491
073	19	-2.411	0.518	-2.456	0.281	25.528	0.236
074	20	-2.742	0.410	-2.917	0.276	25.458	0.138
075	20	-3.112	0.595	-2.958	0.292	25.637	0.239
076	19	-2.598	0.483	-2.794	0.390	25.446	0.157
077	19	-3.883	0.374	-3.314	0.407	25.862	0.192
078	20	-3.715	0.444	-3.132	0.632	25.867	0.299
080	19	-3.059	0.350	-2.809	0.308	25.690	0.157
081	20	-3.526	0.300	-3.114	0.340	25.778	0.125
082	20	-5.491	1.251	-4.348	0.960	26.163	0.283
083	20	-4.814	0.724	-3.974	0.844	26.006	0.198
084	20	-3.976	0.258	-4.118	0.322	25.476	0.137
085	20	-3.276	1.038	-3.712	0.418	25.304	0.512

Table 3-1 TOPEX Altimeter Range Bias Changes Based on Calibration Mode 1 Step 5

Cyc	Count	dR_av_N	dR_sd_N	dRc_av_T	dRc_sd_T	T_u_av	T_u_sd
086	20	-1.596	1.172	-2.628	0.637	24.970	0.384
087	20	-4.199	0.212	-3.843	0.433	25.746	0.282
088	21	-4.296	0.252	-3.827	0.502	25.808	0.216
089	20	-4.434	0.327	-3.561	0.493	26.023	0.194
090	20	-4.181	0.262	-3.921	0.625	25.691	0.393
092	20	-3.337	0.855	-2.838	0.681	25.824	0.202
093	20	-3.732	0.244	-3.631	0.540	25.608	0.236
094	20	-3.918	0.273	-3.481	0.422	25.791	0.205
095	20	-4.374	0.294	-3.650	0.486	25.945	0.143
096	19	-4.268	0.248	-4.079	0.502	25.656	0.240
098	19	-3.373	0.152	-3.689	0.297	25.379	0.142
099	20	-3.528	0.161	-3.660	0.408	25.481	0.176
100	19	-3.759	1.072	-3.452	0.572	25.714	0.468
101	20	-4.003	0.232	-3.706	0.551	25.714	0.265
102	20	-3.895	0.161	-4.137	0.408	25.420	0.217
104	20	-2.646	1.185	-3.306	0.504	25.177	0.545
105	20	-3.457	0.213	-3.126	0.497	25.732	0.276
106	20	-3.779	0.499	-3.170	0.592	25.882	0.229
107	20	-4.509	0.207	-3.579	0.481	26.053	0.244
108	19	-3.955	0.196	-3.961	0.352	25.551	0.177
109	19	-3.808	0.168	-3.531	0.415	25.704	0.240
110	20	-3.705	0.252	-3.311	0.296	25.769	0.152
111	20	-3.727	0.143	-3.807	0.260	25.511	0.149
112	20	-4.028	0.351	-3.418	0.255	25.884	0.173
113	20	-4.251	0.202	-3.275	0.277	26.078	0.174
115	17	-3.092	0.336	-2.734	0.321	25.748	0.167
116	20	-3.045	0.295	-2.779	0.391	25.699	0.127
117	16	-3.191	0.299	-2.586	0.430	25.881	0.194
119	17	-5.211	1.013	-3.527	0.925	26.438	0.482

Table 3-1 TOPEX Altimeter Range Bias Changes Based on Calibration Mode 1 Step 5

Cyc	Count	dR_av_N	dR_sd_N	dRc_av_T	dRc_sd_T	T_u_av	T_u_sd
120	20	-4.668	0.454	-4.420	0.593	25.689	0.207
121	19	-3.735	0.675	-4.940	0.315	24.869	0.430

3.2 AGC/Sigma Naught

The corrections to AGC and Sigma Naught have been derived from analyses of the calibration mode AGC and cycle-summary sigma naughts. Both data sets indicate that the AGC and sigma naught values have been decreasing since launch.

For this study, the cycle-summary sigma naughts were modified as follows:

- The sigma naught corrections that had been entered into the GDR processing by the TOPEX / POSEIDON Project were removed so that the long-term terms, sans corrections, could be plotted.
- The sigma naught values were then normalized to a standard swh of 2.85 m. This additive change to each cycle-summary sigma naught was calculated as: +0.4dB * (swhcycle - 2.85 m), based on empirical changes in sigma naught as a function of swh.
- Biases of 11.32 dB and 15.30 dB were subtracted from the Ku-Band and C-Band sigma naughts, respectively, so that the origins of their trend lines would very nearly coincide with the CAL-1 trend line origins.

Figure 3-1 "Results of the Ku-Band AGC / Sigma Naught Trend Analysis" provides the results of the Ku-Band AGC / sigma-naught analysis, and Figure 3-2 "Results of the C-Band AGC / Sigma Naught Trend Analysis"similarly presents the results of the C-Band analysis. Each figure contains the following: that frequency's CAL-1 Step-5 and CAL-2 trend plots, the cycle-summary sigma naughts after the three modification steps presented above, and a linear fit to the sigma naughts from cycle 10 onward. Cycles 1-9 were excluded from the linear fitting due to the spacecraft pointing problems discussed earlier in Section 2.2. These two figures also contain, as a reference, a plot of the relative change in that frequency's transmitter power converted to dB.

The linear fits to the cycle-summary sigma naughts are used as the basis for ascribing values for the AGC corrections (Table 3-2 "Summary of TOPEX AGC Cal Table Values") used by the TOPEX Project. The slope of the Ku-Band trend is -0.0075 dB per cycle, while for C-Band it is -0.0060 dB per cycle.

The TOPEX ground processing includes an automatic gain control (AGC) Calibration Table whose entries are additive corrections to the Ku- and C-band AGC values. This table is referred to as the AGC Cal Table. Since the altimeter's sigma-0 estimates vary directly as AGC, the AGC Cal Table can also be viewed as a correction table for the altimeter's sigma-0 estimates.

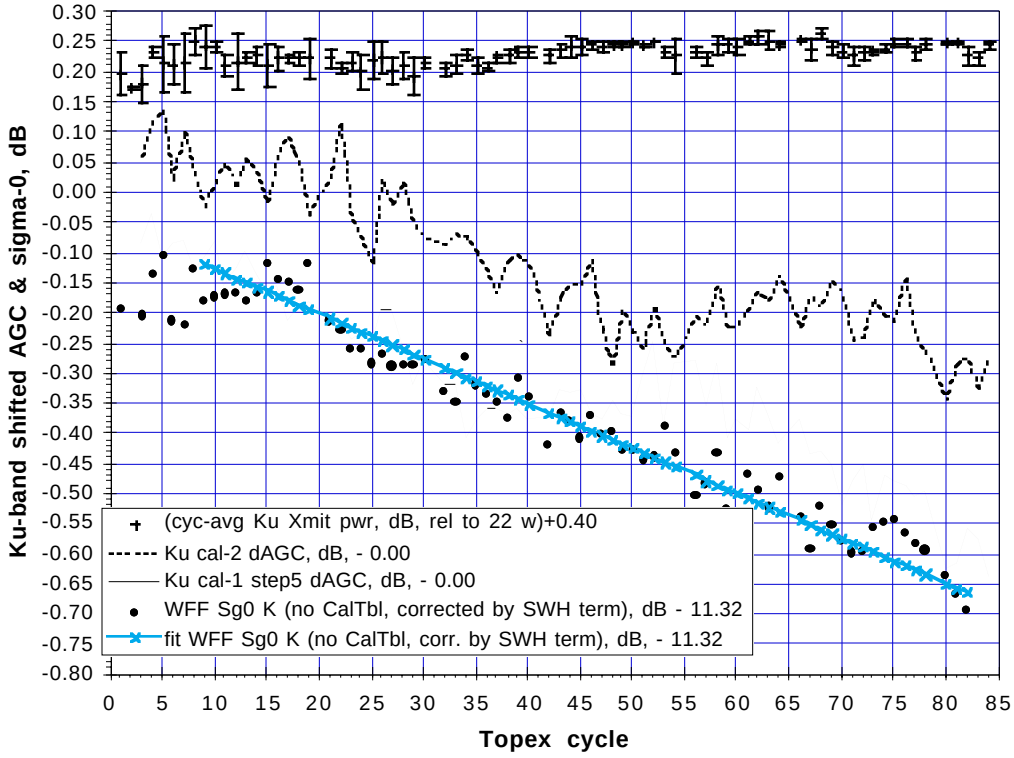

Figure 3-1 Results of the Ku-Band AGC/Sigma Naught Trend Analysis

Table 3-2 provides the current best estimates of the Ku- and C-band AGC Cal Table values. These corrections are in the rightmost two columns of Table 3-2, labeled as "Ku (or C) corr for'96 recomputation" because these corrections are to be used for the recomputation of the TOPEX geophysical data records (GDRs); the recomputation is to occur sometime in the first half of 1996. The TOPEX data cycle number is in the leftmost column of Table 3-2. Also in Table 3-2, the fourth and sixth columns give the AGC Cal Table values, for Ku- and C-band respectively, which were used in producing the GDRs which have been distributed to date.

For obtaining the best estimates of TOPEX sigma-0, the AGC Cal Table values used in producing the GDR should be removed (subtracted) from a sigma-0 estimate and be replaced (by addition) by the new AGC corrections given in the rightmost two columns of Table 3-2. For TOPEX cycles from 112 onwards, this removal/replacement is unnecessary since the current best estimate AGC Cal Table values (the "..'96 recomputation" values) are the ones used in the production of the TOPEX GDRs.

A brief summary and history of the contents of the AGC Cal Table follows.

- Initially this AGC Cal Table had zero entries for both Ku- and C-band.

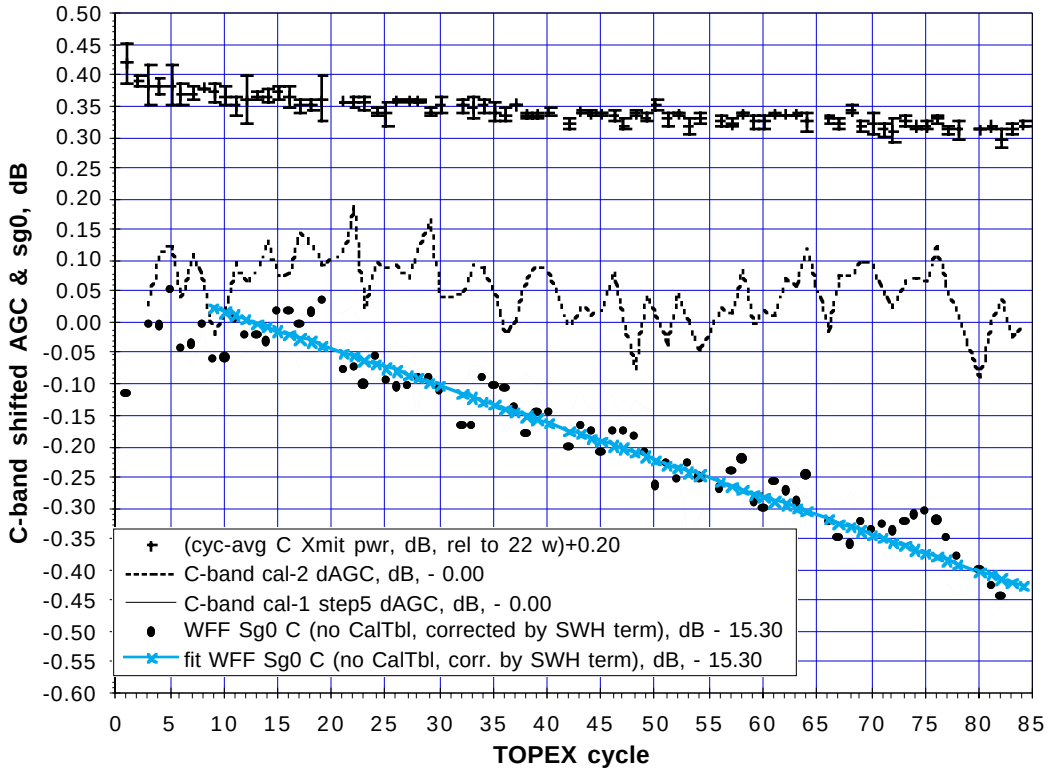

Figure 3-2 Results of the C-Band AGC/Sigma Naught Trend Analysis

- Starting with TOPEX cycle 048, several AGC Cal Table entries were introduced to try to hold the cycle-averaged sigma-0 values constant over the TOPEX history.
- In October 1994, we reassessed the GDR-based, cycle-average data from launch to that time, and decided that the AGC Cal Table entries should follow a linear trend, typically with 0.05 dB steps. We published in the October 1994 issue of *TOPEX/Poseidon Research News* (Callahan et al, 1994) a description of the linear trend, and provided values for that trend for cycles 001 forward; those values are listed in columns 3 and 5 in Table 3-2. Beginning with cycle 076, this linear trend (actually two trends, one each for Ku- and C-band) was used as a predictive entry for the AGC Cal Table.
- In September 1995, the data from launch to that time were reassessed. The cycle-average sigma-0 values were fitted by an empirical function which contained a linear function of time, an annual and a semiannual time variation, and a linear and a quadratic term in cycle- average SWH. We decided to use only the time-linear terms for the AGC Cal Table entries, but decided to make 0.03 dB increments from cycle 115 onward, for both the Ku- and C-band AGC

Cal Table entries. From cycles 115 onward, the AGC Cal Table values used for the distributed GDRs were based on this linear trend with its 0.03 dB increments.

- As of early January 1996, there is still no compelling evidence not to continue the September 1995 linear trends with the 0.03 dB steps. These two trends (Ku- and C-band) will be the basis for the AGC Cal Table sigma-0 values when the entire set of TOPEX GDRs is recomputed and reissued sometime in the first half of 1996.

The values in Table 3-2 are projected forward through cycle 149. The Ku- and C-band sigma-0 trends will be reassessed several times between now and the start of cycle 149, and we may have to retune the linear trends by then.

Table 3-2 Summary of TOPEX AGC Cal Table Values

Cycle	Altimeter	Oct.'94 Ku corr ("linear"), dB	Ku corr as distr. on GDRs, dB	Oct.'94 C corr ("linear"), dB	C corr as distr. on GDRs, dB	Ku corr for '96 recomp.	C corr for '96 recomp.
		P.Callahan new TOPEX Cal Table AGC entries (10/17/94 & subsequently)... see also Hayne memo 95/09/08				Recommended from Sept '95 Fit with 0.03 dB steps	
1	mixed	-0.15	0	0	0	-0.06	-0.06
2	mixed	-0.15	0	0	0	-0.06	-0.06
3	mixed	-0.15	0	0	0	-0.06	-0.03
4	mixed	-0.15	0	0	0	-0.03	-0.03
5	mixed	-0.15	0	0	0	-0.03	-0.03
6	mixed	-0.15	0	0	0	-0.03	-0.03
7	mixed	-0.15	0	0	0	-0.03	-0.03
8	mixed	-0.15	0	0	0	+0.00	+0.00
9	mixed	0	0	0	0	+0.00	+0.00
10	mixed	0	0	0	0	+0.00	+0.00
11	mixed	0	0	0	0	+0.00	+0.00
12	mixed	0	0	0	0	+0.00	+0.00
13	mixed	0	0	0	0	+0.03	+0.03
14	mixed	0	0	0	0	+0.03	+0.03
15	mixed	0	0	0	0	+0.03	+0.03
16	mixed	0	0	0	0	+0.03	+0.03
17	NRA	0	0	0	0	+0.06	+0.03

Table 3-2 Summary of TOPEX AGC Cal Table Values (Continued)

Cycle	Altimeter	Oct.'94 Ku corr ("linear"), dB	Ku corr as distr. on GDRs, dB	Oct.'94 C corr ("linear"), dB	C corr as distr. on GDRs, dB	Ku corr for '96 recomp.	C corr for '96 recomp.
18	NRA	0	0	0	0	+0.06	+0.06
19	NRA	0	0	0	0	+0.06	+0.06
20	SSALT						
21	NRA	+0.10	0	+0.10	0	+0.09	+0.06
22	NRA	+0.10	0	+0.10	0	+0.09	+0.06
23	NRA	+0.10	0	+0.10	0	+0.09	+0.06
24	NRA	+0.10	0	+0.10	0	+0.09	+0.09
25	NRA	+0.15	0	+0.10	0	+0.12	+0.09
26	NRA	+0.15	0	+0.10	0	+0.12	+0.09
27	NRA	+0.15	0	+0.10	0	+0.12	+0.09
28	NRA	+0.15	0	+0.10	0	+0.12	+0.09
29	NRA	+0.15	0	+0.10	0	+0.15	+0.12
30	NRA	+0.15	0	+0.10	0	+0.15	+0.12
31	SSALT						
32	NRA	+0.20	0	+0.15	0	+0.15	+0.12
33	NRA	+0.20	0	+0.15	0	+0.18	+0.12
34	NRA	+0.20	0	+0.15	0	+0.18	+0.15
35	NRA	+0.20	0	+0.15	0	+0.18	+0.15
36	NRA	+0.20	0	+0.15	0	+0.18	+0.15
37	NRA	+0.20	0	+0.15	0	+0.21	+0.15
38	NRA	+0.20	0	+0.15	0	+0.21	+0.15
39	NRA	+0.20	0	+0.15	0	+0.21	+0.18
40	NRA	+0.20	0	+0.15	0	+0.21	+0.18
41	SSALT						
42	NRA	+0.20	0	+0.15	0	+0.24	+0.18
43	NRA	+0.20	0	+0.15	0	+0.24	+0.18
44	NRA	+0.20	0	+0.15	0	+0.24	+0.21
45	NRA	+0.25	0	+0.20	0	+0.27	+0.21

Table 3-2 Summary of TOPEX AGC Cal Table Values (Continued)

Cycle	Altimeter	Oct.'94 Ku corr ("linear"), dB	Ku corr as distr. on GDRs, dB	Oct.'94 C corr ("linear"), dB	C corr as distr. on GDRs, dB	Ku corr for '96 recomp.	C corr for '96 recomp.
46	NRA	+0.25	0	+0.20	0	+0.27	+0.21
47	NRA	+0.25	0	+0.20	0	+0.27	+0.21
48	NRA	+0.25	+0.25	+0.20	+0.10	+0.27	+0.21
49	NRA	+0.25	+0.25	+0.20	+0.10	+0.30	+0.21
50	NRA	+0.30	+0.25	+0.25	+0.10	+0.30	+0.24
51	NRA	+0.30	+0.25	+0.25	+0.10	+0.30	+0.24
52	NRA	+0.30	+0.25	+0.25	+0.10	+0.30	+0.24
53	NRA	+0.30	+0.25	+0.25	+0.10	+0.33	+0.24
54	NRA	+0.30	+0.25	+0.25	+0.10	+0.33	+0.24
55	SSALT						
56	NRA	+0.35	+0.30	+0.25	+0.15	+0.33	+0.27
57	NRA	+0.35	+0.30	+0.25	+0.15	+0.36	+0.27
58	NRA	+0.35	+0.30	+0.25	+0.15	+0.36	+0.27
59	NRA	+0.35	+0.30	+0.30	+0.15	+0.36	+0.27
60	NRA	+0.35	+0.30	+0.30	+0.15	+0.36	+0.30
61	NRA	+0.35	+0.30	+0.30	+0.15	+0.39	+0.30
62	NRA	+0.35	+0.30	+0.30	+0.15	+0.39	+0.30
63	NRA	+0.35	+0.30	+0.30	+0.15	+0.39	+0.30
64	NRA	+0.35	+0.30	+0.30	+0.15	+0.39	+0.30
65	SSALT						
66	NRA	+0.40	+0.30	+0.35	+0.15	+0.42	+0.33
67	NRA	+0.40	+0.30	+0.35	+0.15	+0.42	+0.33
68	NRA	+0.40	+0.30	+0.35	+0.15	+0.42	+0.33
69	NRA	+0.40	+0.30	+0.35	+0.15	+0.45	+0.33
70	NRA	+0.45	+0.30	+0.35	+0.15	+0.45	+0.36
71	NRA	+0.45	+0.30	+0.35	+0.15	+0.45	+0.36
72	NRA	+0.45	+0.30	+0.35	+0.15	+0.45	+0.36
73	NRA	+0.45	+0.30	+0.35	+0.15	+0.48	+0.36

Table 3-2 Summary of TOPEX AGC Cal Table Values (Continued)

Cycle	Altimeter	Oct.'94 Ku corr ("linear"), dB	Ku corr as distr. on GDRs, dB	Oct.'94 C corr ("linear"), dB	C corr as distr. on GDRs, dB	Ku corr for '96 recomp.	C corr for '96 recomp.
74	NRA	+0.45	+0.30	+0.35	+0.15	+0.48	+0.36
75	NRA	+0.45	+0.30	+0.35	+0.15	+0.48	+0.36
76	NRA	+0.45	+0.45	+0.35	+0.35	+0.48	+0.39
77	NRA	+0.45	+0.45	+0.35	+0.35	+0.48	+0.39
78	NRA	+0.45	+0.45	+0.35	+0.35	+0.51	+0.39
79	SSALT						
80	NRA	+0.45	+0.45	+0.35	+0.35	+0.51	+0.39
81	NRA	+0.45	+0.45	+0.35	+0.35	+0.51	+0.42
82	NRA	+0.50	+0.50	+0.40	+0.40	+0.54	+0.42
83	NRA	+0.50	+0.50	+0.40	+0.40	+0.54	+0.42
84	NRA	+0.50	+0.50	+0.40	+0.40	+0.54	+0.42
85	NRA	+0.50	+0.50	+0.40	+0.40	+0.54	+0.42
86	NRA	+0.55	+0.55	+0.45	+0.45	+0.57	+0.45
87	NRA	+0.55	+0.55	+0.45	+0.45	+0.57	+0.45
88	NRA	+0.55	+0.55	+0.45	+0.45	+0.57	+0.45
89	NRA	+0.55	+0.55	+0.45	+0.45	+0.57	+0.45
90	NRA	+0.55	+0.55	+0.45	+0.45	+0.60	+0.45
91	SSALT						
92	NRA	+0.55	+0.55	+0.45	+0.45	+0.60	+0.48
93	NRA	+0.55	+0.55	+0.45	+0.45	+0.60	+0.48
94	NRA	+0.55	+0.55	+0.45	+0.45	+0.63	+0.48
95	NRA	+0.55	+0.55	+0.45	+0.45	+0.63	+0.48
96	NRA	+0.55	+0.55	+0.45	+0.45	+0.63	+0.48
97	SSALT						
98	NRA	+0.55	+0.55	+0.45	+0.45	+0.66	+0.51
99	NRA	+0.60	+0.60	+0.45	+0.45	+0.66	+0.51
100	NRA	+0.60	+0.60	+0.45	+0.45	+0.66	+0.51
101	NRA	+0.60	+0.60	+0.45	+0.45	+0.66	+0.51

Table 3-2 Summary of TOPEX AGC Cal Table Values (Continued)

Cycle	Altimeter	Oct.'94 Ku corr ("linear"), dB	Ku corr as distr. on GDRs, dB	Oct.'94 C corr ("linear"), dB	C corr as distr. on GDRs, dB	Ku corr for '96 recomp.	C corr for '96 recomp.
102	NRA	+0.60	+0.60	+0.45	+0.45	+0.69	+0.54
103	SSALT						
104	NRA	+0.65	+0.65	+0.50	+0.50	+0.69	+0.54
105	NRA	+0.65	+0.65	+0.50	+0.50	+0.69	+0.54
106	NRA	+0.65	+0.65	+0.50	+0.50	+0.72	+0.54
107	NRA	+0.70	+0.70	+0.55	+0.55	+0.72	+0.57
108	NRA	+0.70	+0.70	+0.55	+0.55	+0.72	+0.57
109	NRA	+0.70	+0.70	+0.55	+0.55	+0.72	+0.57
110	NRA	+0.75	+0.75	+0.55	+0.55	+0.75	+0.57
111	NRA	+0.75	+0.75	+0.55	+0.55	+0.75	+0.57
112	NRA	+0.75	+0.75	+0.60	+0.60	+0.75	+0.60
113	NRA	+0.75	+0.75	+0.60	+0.60	+0.75	+0.60
114	SSALT						
115	NRA	+0.78	+0.78	+0.60	+0.60	+0.78	+0.60
116	NRA	+0.78	+0.78	+0.60	+0.60	+0.78	+0.60
117	NRA	+0.78	+0.78	+0.63	+0.63	+0.78	+0.63
118	NRA	+0.81	+0.81	+0.63	+0.63	+0.81	+0.63
119	NRA	+0.81	+0.81	+0.63	+0.63	+0.81	+0.63
120	NRA	+0.81	+0.81	+0.63	+0.63	+0.81	+0.63
121	NRA	+0.81	+0.81	+0.63	+0.63	+0.81	+0.63
122	NRA	+0.84	+0.84	+0.63	+0.63	+0.84	+0.63
123	NRA	+0.84	+0.84	+0.66	+0.66	+0.84	+0.66
124	NRA	+0.84	+0.84	+0.66	+0.66	+0.84	+0.66
125	NRA	+0.84	+0.84	+0.66	+0.66	+0.84	+0.66
126	SSALT						
127	NRA	+0.87	+0.87	+0.66	+0.66	+0.87	+0.66
128	NRA	+0.87	+0.87	+0.69	+0.69	+0.87	+0.69
129	NRA	+0.87	+0.87	+0.69	+0.69	+0.87	+0.69

Table 3-2 Summary of TOPEX AGC Cal Table Values (Continued)

Cycle	Altimeter	Oct.'94 Ku corr ("linear"), dB	Ku corr as distr. on GDRs, dB	Oct.'94 C corr ("linear"), dB	C corr as distr. on GDRs, dB	Ku corr for '96 recomp.	C corr for '96 recomp.
130	NRA	+0.90	+0.90	+0.69	+0.69	+0.90	+0.69
131	NRA	+0.90	+0.90	+0.69	+0.69	+0.90	+0.69
132	NRA	+0.90	+0.90	+0.69	+0.69	+0.90	+0.69
133	NRA	+0.90	+0.90	+0.72	+0.72	+0.90	+0.72
134	NRA	+0.93	+0.93	+0.72	+0.72	+0.93	+0.72
135	NRA	+0.93	+0.93	+0.72	+0.72	+0.93	+0.72
136	NRA	+0.93	+0.93	+0.72	+0.72	+0.93	+0.72
137	NRA	+0.93	+0.93	+0.72	+0.72	+0.93	+0.72
138	SSALT						
139	NRA	+0.96	+0.96	+0.75	+0.75	+0.96	+0.75
140	NRA	+0.96	+0.96	+0.75	+0.75	+0.96	+0.75
141	NRA	+0.96	+0.96	+0.75	+0.75	+0.96	+0.75
142	NRA	+0.96	+0.96	+0.75	+0.75	+0.96	+0.75
143	NRA	+0.99	+0.99	+0.78	+0.78	+0.99	+0.78
144	NRA	+0.99	+0.99	+0.78	+0.78	+0.99	+0.78
145	NRA	+0.99	+0.99	+0.78	+0.78	+0.99	+0.78
146	NRA	+0.99	+0.99	+0.78	+0.78	+0.99	+0.78
147	NRA	+1.02	+1.02	+0.78	+0.78	+1.02	+0.78
148	NRA	+1.02	+1.02	+0.78	+0.78	+1.02	+0.78
149	NRA	+1.02	+1.02	+0.81	+0.81	+1.02	+0.81

3.3 Sea Surface Height Residuals as Indicators of Global Sea Level Change

Possible mean sea level variations measured from TOPEX/Poseidon altimeter data are reported by Nerem (1995), and this topic is also being actively investigated by several other users of TOPEX/Poseidon data. As a by-product of our performance monitoring, we note that our selective GDR database can be used to explore the performance with respect to mean sea level variations. We report here our observation of an apparent rise in global sea level since the beginning of the on-orbit mission. The term "global," as used here, is in the context that the orbital inclination of TOPEX/Poseidon provides coverage to +66.04 degrees in latitude, that adjacent ascending or

descending groundtracks have a separation of 2.83 degrees of longitude at the equator, and that we use only deep-water measurements in our database.

Our sea level change estimates are obtained by a relatively simple extension of WFF's regular TOPEX altimeter performance assessment procedures.

3.3.1 Computation of Sea Surface Height Residuals

As part of our routine performance assessment processing, we compute an additional one-per-record measurement, the sea surface height residual (SSHres), as:

SSHres (mm) = Sea_Surf_Hght - Ocean_Tide - Solid_Earth_Tide -Pole_Tide - Baro_Corr - Mean_Sea_Surf_Mod

All of the parameters to compute SSHres are directly accessible from each record in the GDR file except for Baro_Corr, the inverse barometer effect. Baro_Corr is based on Dry_Tropo and Latitude (Callahan, 1993) from the GDR file as:

Baro_Corr(mm)= -10.1[Dry_Tropo / (-2.273(1+0.0026*cos(2*Latitude)))-1013.3]

Also, we modify the Mean_Sea_Surf value which is in the GDR file. Latitude- and longitude-dependent corrections (Callahan, 1993) are applied to the GDR mean sea surface values where:

Mean_Sea_Surf_Mod = Mean_Sea_Surf + dR + dX cos(Latitude) cos(Longitude) + dY cos(Latitude) sin (Longitude) + dZ sin(Latitude).

The initial coefficients for this modification, as derived by Richard Rapp (Callahan, 1993) are: dR=+400 mm, dX=0, dY=+240 mm, and dZ=0. Rapp, et al. (1994) have refined these coefficients but, for cycle-to-cycle consistency, we have continued to use the initial values. Because this Mean_Sea_Surf modification is geometry-related and the groundtrack geometry repeats for each cycle, the implementation of the new coefficients would not be expected to change the cycle-to-cycle comparisons.

3.3.2 Trend Analysis

The one-per-cycle SSHres, for cycles 11 through 106, are shown by the rectangles in Figure 3-3 "TOPEX Cycles 17-92 SSHres Fitted by Linear Plus Sinusoidal Annual and Semiannual Terms (AFTER correction for range bias drift)". The applied range drift values are those presented in Section 3.1. Cycles 1 through 10 were not used in this analysis due to non-optimum spacecraft position knowledge and non-uniform data coverage during those cycles. Poseidon altimeter measurements were not used in this analysis.

This range calibration correction, which if not considered would indicate a faster rise in global sea level, has been applied to all the SSHres values in Figure 3-3.

Variations in the global sea surface height residuals can be observed in Figure 3-3, with the maximum SSHres occurring each year during late summer in the northern hemisphere, and with minima occurring in late-winter. Knudsen (1994) and Stammer and Wunsch (1994) indicate that such variations would be expected in that the dynamic heights of northern hemisphere oceans are more affected by heating and cooling cycles than the southern hemisphere oceans.

For our trend analysis, the SSHres for cycles 17 through 92 (2.06 years) were fitted with combined linear and annual sinusoidal terms, as depicted by the solid dots in Figure 3-3. The model has been extrapolated to cycles 11-16 and cycles 93-106, as shown by the open dots. Cycles 11-16 were excluded from the solution because prior to cycle 17 the TOPEX and Poseidon scheduling was such that neither altimeter was on for full cycles. The cycles later than 92 were not included in the solution because the TOPEX ground processing system began to use a different model for its precision orbit determination; such a model change may have a subtle effect on the cycle-to-cycle consistency.

The dashed line in Figure 3-3 depicts the calculated linear trend, with a positive slope of 0.12083 mm / cycle which translates to an apparent sea level rise of +4.5 mm / year. The standard deviation of the sea level rise estimate is +5.8 mm.

3.3.3 Comparison with Narem Results

Our observed level change is in close agreement with that of Nerem (1995) who also used TOPEX altimeter data, despite significant differences in the processing and data editing steps. Nerem's estimate is that sea level is rising at the rate of +3.9 mm / year.

We find it a great compliment to the integrity of the TOPEX standard data products that, using only the GDR products and standard GDR post-processing (Callahan, 1993), our data base yields results consistent with Nerem's.

3.4 Over-Land Losses of Lock: Seasonal Variations

The TOPEX Radar Altimeter's design was optimized for open-ocean tracking. The altimeter's capability of acquiring over-land tracking data is an extra feature.

True to its design, the altimeter rarely loses lock in areas of open ocean. It often loses lock over land, particularly in areas of rugged terrain. Whenever a loss-of-lock occurs, the altimeter automatically switches to Coarse Acquisition Mode to search for pulse returns from the Earth's surface. As part of our continuing altimeter performance assessment activities, we daily record the number of acquisitions the altimeter performs.

Using our database from daily Altimeter Instrument File (AIF) data, the number of times the altimeter switched to Coarse Acquisition Mode per day was extracted and plotted. We have observed a distinct seasonal relationship, with a minimum number of Coarse Acquisitions during the Northern Hemisphere winter and a maximum in the summer. Further study of this relationship, using full-cycle multi-season Sensor Data Records (SDR) with geographical coordinates, leads to the conclusion that the altimeter better maintains lock over the same terrain when there is snow cover.

3.4.1 TOPEX Altimeter Acquisition Cycles

The TOPEX altimeter design provides good ocean data as soon as possible when going from land to water. This design has four modes of operation related to tracking and acquisition that depends on the onboard automatic signal processing. In two modes the pulsewidth is set to 50 ns, and the other two modes use the 3.125 ns pulse-

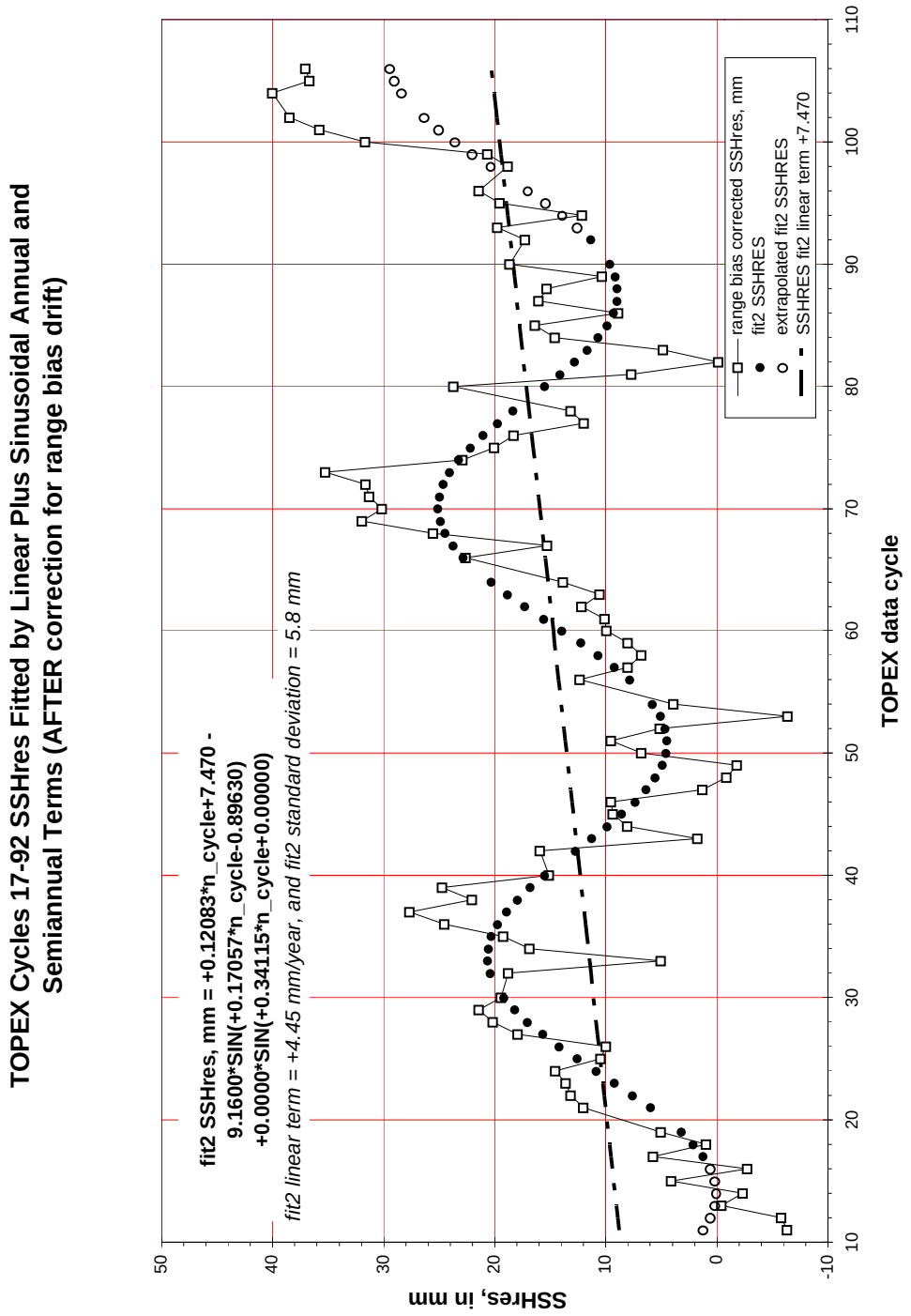

Figure 3-3 TOPEX Cycles 17-92 SSHres Fitted by Linear Plus Sinusoidal Annual and Semiannual Terms (AFTER correction for range bias drift)

width. The normal ocean mode is all fine track (FTRK) where the pulsewidth is 3.125 ns and the return pulse is tracked based on a middle gate power.

When the altimeter logic determines that FTRK does not have an adequate signal, it normally enters coarse track (CTRK) with a pulsewidth of 50 ns and with a threshold value for tracking. On occasion, the altimeter logic senses a total loss of lock on the signal and enters the coarse acquisition mode (CACQ). The CACQ mode scans a minimum-to-maximum range window with a 50 ns pulsewidth, searching for the best signal. Normally, after one sweep of the range window, the altimeter enters CTRK. Once a good signal is detected in CTRK, the mode most often transitions directly to FTRK. However, it may switch to the intermediate fine acquisition (FACQ) mode wherein the altimeter scans a range window width using a 3.125 ns pulsewidth. After selection of the strongest signal in FACQ, the altimeter logic then commands a transition to FTRK. The system design is to have the altimeter either already in FTRK or in CTRK during the transition from land to water, and to enter FTRK quickly.

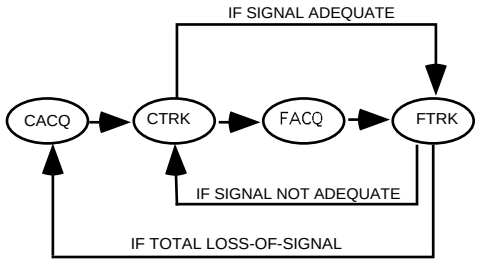

A complete acquisition cycle, CACQ to CTRK to FACQ to FTRK, takes about 4.5 seconds. CTRK to FTRK normally takes about 2 seconds. Loss of lock in this paper refers to losing the entire knowledge of the range where the signal is and starting a full acquisition process from CACQ.

3.4.2 Occurrences of Coarse Acquisition Mode

The number of occurrences per day of Coarse Acquisition Mode, from the AIF data for Cycle 17-92, is shown in Figure 3-4 "Number of Occurrences per Day of Coarse Acquisition Mode, for Cycle 17 through Cycle 92". We began with Cycle 17 because, prior to that, there was frequent switching between the TOPEX and CNES altimeters within each cycle. Since Cycle 17, the respective altimeters have been on for complete cycles. On the days when altimeters are switched, the count of Coarse Acquisition Modes is abnormally low because the altimeter is not in Track Mode for an entire day. During those earlier cycles, there were also a few days with special altimeter testing which would have affected the count.

Subsequent to the beginning of Cycle 17, we have deleted from the dataset the following:

- Cycle boundary days with an altimeter transition (TOPEX/CNES).

- Day 218 of 1993, which had a spacecraft safehold.
- Days when the altimeter had a Single Event Upset (SEU).

The count of Coarse Acquisitions in Figure 3-4 clearly shows an annual cycle, with a minimum of 400-500 acquisition sequences per day during the Northern Hemisphere winter and a maximum of about 1000-1100 per day during summer. The plotted summertime peak is truncated because our database field which contains the count can accommodate values only up to 999; larger counts are set to 999.

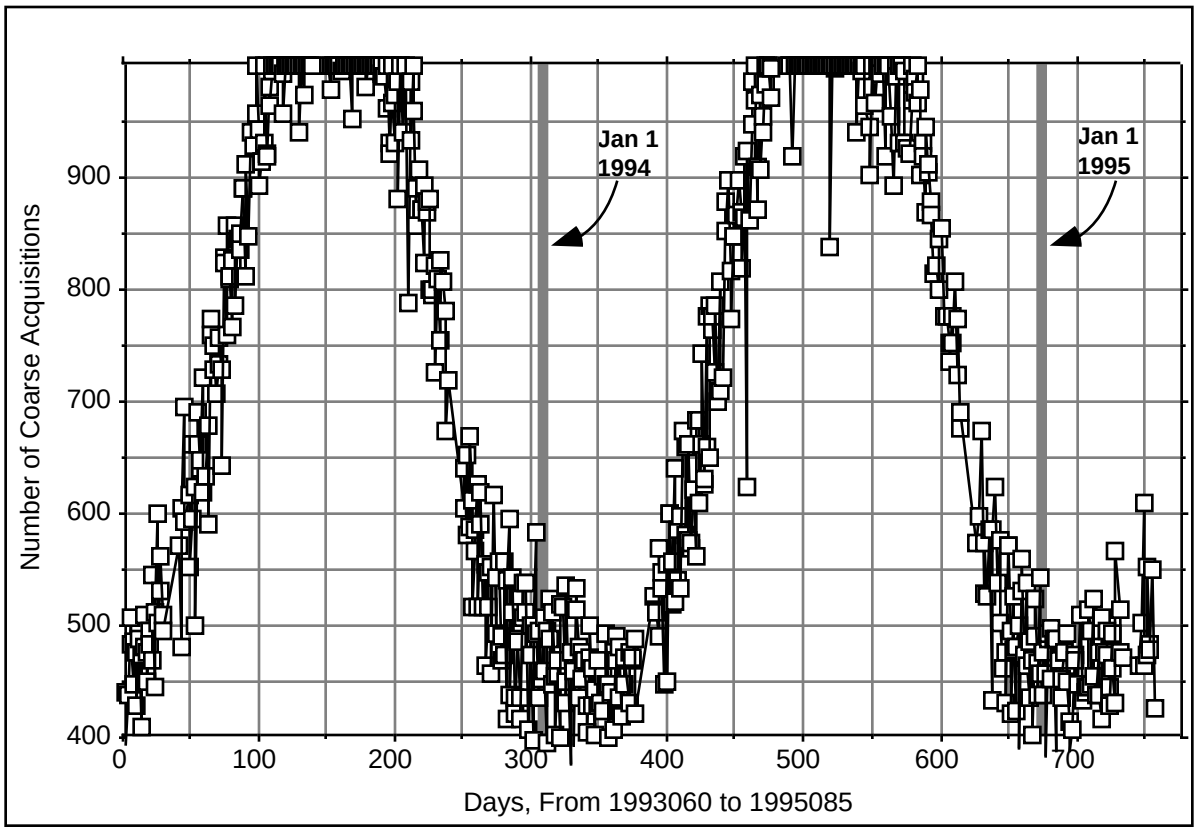

Figure 3-4 Number of Occurrences per Day of Coarse Acquisition Mode, for Cycle 17 through Cycle 92

3.4.3 Latitudinal Relationship

We became interested in whether the larger number of losses-of-lock during Northern Hemisphere summers were uniformly distributed within the Earth's land areas, or if there were particular geographic areas causing the disparity. Since the AIF do not contain geographic coordinates (latitude and longitude), we used SDR files for this aspect of our study.

We selected for analysis four complete cycles, one for each season, as follows:

Fall Cycle 43
(November 13-23, 1993)

Winter	Cycle 52 (February 10-20, 1994)
Spring	Cycle 61 (May 11-21, 1994)
Summer	Cycle 70 (August 8-18, 1994)

For each cycle, a histogram was made of Coarse Acquisition count versus latitude. The four histograms appear in Figure 3-5 "Histograms of Seasonal Occurrences of Coarse Acquisition Mode, per One-Degree Latitude Band, for: Northern Hemisphere Fall (Cycle 43), Winter (Cycle 52), Spring (Cycle 61) and Summer (Cycle 70).".

The four histograms are generally similar from the southernmost latitude to 40˚N. The histograms diverge from latitude 40˚N to the maximum northern latitude reached by the TOPEX/POSEIDON spacecraft, 66.0˚N. The most dramatic increase is north of 60˚N during the summer.

3.4.4 Snow Cover Effects

We attribute the decrease in losses-of-lock in the winter to the high-latitude snow cover in the Northern Hemisphere. We have observed one of the reasons that an altimeter loses lock over terrain is the effect of differing brightness in the footprint. Just as the altimeter maintains lock over the open-ocean very well in part because of the ocean's uniform brightness, it will track snow-covered land areas relatively well because of snow's more uniform brightness.

As seen in Figure 3-5, the best tracking performance (i.e., fewest losses-of-lock) of the four cycles is during mid-February (Cycle 52), when the Northern Hemisphere snow cover reaches its late-winter extent, down to about 45˚N latitude. The next-best performance is mid-November (Cycle 43) when snow cover generally extends southward to 55˚N, covering most of Alaska, Scandinavia, and large portions of northern Eurasia (Gurney et al, 1993). By mid-May (Cycle 61), the snowline has retreated to north of 60˚N latitude. Then, in mid-August (Cycle 70), the over-land losses-of-lock are at a maximum due to the almost total lack of snow in the TOPEX/POSEIDON coverage area. The snow coverage areas described above are extracted from a 15-year snow coverage database (Matson et al, 1986).

There is not a similar summer/winter altimeter tracking scenario for terrain in the Southern Hemisphere. South of 40˚S latitude, there is relatively little land, with land practically non-existent between latitude 58˚S and the farthest reaches of the altimeter, the Antarctic Peninsula.

3.4.5 Conclusion

Our conclusion is that the large disparity between the TOPEX altimeter's losses-of-lock in the Northern Hemisphere summer (maximum) versus the winter (minimum) is due to: 1) high-latitude terrain snow cover in the winter, and 2) a high percentage of terrain in the northern high latitudes, as contrasted with a sparseness in the Southern Hemisphere.

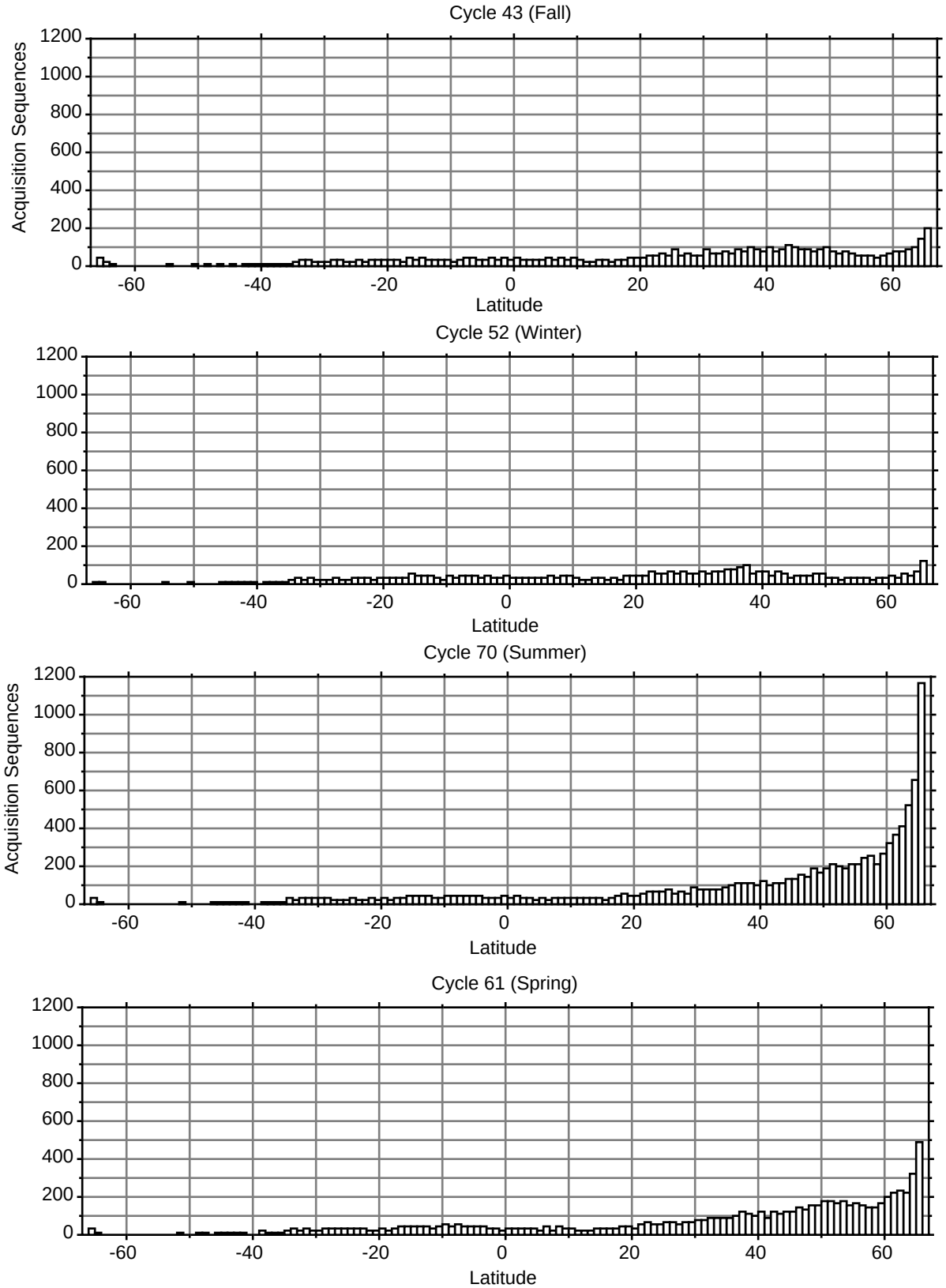

Figure 3-5 Histograms of Seasonal Occurrences of Coarse Acquisition Mode, per One-Degree Latitude Band, for: Northern Hemisphere Fall (Cycle 43), Winter (Cycle 52), Spring (Cycle 61) and Summer (Cycle 70).

This information should be useful to those investigators who are using land data from the TOPEX radar altimeter, and to the designers of future land-coverage altimeter missions. High-latitude Northern Hemisphere altimeter measurements will be more plentiful during the winter months.

3.5 Range Corrections for the Effects of Waveform Leakage

Waveform leakage spikes have been observed in the TOPEX on-orbit waveforms, in both Ku- and C-Band (Hayne et al, 1994). George Hayne has been studying the effects of these leakages on the altimeter's range measurements. A summary of his findings to date is presented in the memorandum, Waveform Leakage Range Correction, which constitutes Attachment A.

Section 4

Engineering Assessment Synopsis

4.1 Performance Overview

After nearly three-and-a-half years of on-orbit operations, the NASA Radar Altimeter on the TOPEX/POSEIDON spacecraft remains healthy and its performance meets or is better than all pre-launch requirements. The performance requirements are listed in Section 4.0 of the February 1994 Engineering Assessment Report.

The primary pre-launch specification for the altimeter is to monitor and maintain range calibration to the +1.5 cm level. We are well aware that TOPEX science investigators are achieving extraordinary results with this altimeter data set, and are seeking unprecedented range measurement accuracy. With our improved analysis techniques, we believe that we are now achieving range calibration (i.e., internal range consistency) at the one-centimeter level, and are making strides towards the sub-centimeter level.

We are continuing our NASA Radar Altimeter performance assessment on a daily basis, and are continuing to develop improved analysis techniques. Our performance assessment techniques are relevant not only for the NASA Radar Altimeter, but should be very applicable to future altimeters, as well.

Section 5

References

5.1 Supporting Documentation

Brooks, Ronald L., Jeffrey E. Lee, Dennis W. Lockwood, and David W. Hancock III, 1995, TOPEX Radar Altimeter Over-Land Losses of Lock: Seasonal Variations. TOPEX/POSEIDON Research News, August 1995, pp. 9-12.

Callahan, P.S., 1993, GDR Users Handbook, JPL Document 633-721.

Gurney, R.J., J.L. Foster and C.L. Parkinson (editors), 1993, "Atlas of Satellite Observations Related to Global Change: Part VII-Cryosphere," Cambridge University Press.

Hancock, David W.,III, Ronald L. Brooks, and Jeffrey E. Lee, 1995, Passive Microwave Radiation Effects on the TOPEX Altimeter Cal-2 Measurements. TOPEX/POSEIDON Research News, August 1995, pp. 4-8.

Hayne, G.S., D.W. Hancock III, C.L. Purdy, and C.S. Callahan, 1994, The Corrections for Significant Wave Height and Attitude Effects in the TOPEX Radar Altimetry. Journal of Geophysical Research, v. 99, no. C12, pp. 24,941-24,955.

Knudsen, Per, 1994, Global Low Harmonic Degree Models of the Seasonal Variability and Residual Ocean Tides from TOPEX/POSEIDON Altimeter Data. Journal of Geophysical Research, v. 99, no. C12, pp. 24,643-24,655.

Matson, M., C.F. Ropelewski, and M.S. Varnadore, 1986, "An Atlas of Satellite-Derived Northern Hemisphere Snow Cover Frequency," NOAA/NESDIS and NOAA/NWS (joint publication).

Nerem, R.S., 1995, Global Mean Sea Level Variations from TOPEX/POSEIDON Altimeter Data. Science, v. 268, pp. 708-710.

Rapp, Richard, Yuchan Yi, and Yan Ming Wang, 1994, Mean Sea Surface and Geoid Gradient Comparisons with TOPEX Altimeter Data. Journal of Geophysical Research, v. 99, no. C12, pp. 24,657-24,667.

Stammer, Detlef, and Carl Wunsch, 1994, Preliminary Assessment of the Accuracy and Precision of TOPEX/POSEIDON Altimeter Data with Respect to the Large-Scale Ocean Circulation. Journal of Geophysical Research, v. 99, no. C12, pp. 24,584-24,604.

Zieger,A.R., D.W. Hancock III, G.S. Hayne, and C.L. Purdy, 1991, NASA Radar for the TOPEX/POSEIDON Project. Proc. IEEE, v. 97, no. 6, pp. 810-826

ATTACHMENT A

DRAFT TOPEX Informal WFF Internal Memorandum

TO: Distribution

FROM: George S. Hayne

SUBJECT: Waveform Leakage Range Correction

Introduction

We reported earlier, in *Hayne et al*.[1994], the existence of waveform leakage spikes observed in TOPEX on-orbit data for both the Ku- and the C-band altimeters. We pointed out that the tracker error arising from the waveform leakages would depend on the sign of the altimeter s range rate, and that the magnitude of the tracker range error would be approximately one centimeter.

We now report a more complete analysis, and present an average range correction for the waveform leakage which can be predicted solely on the basis of quantities available on the TOPEX geophysical data record (GDR).

We will first review the characteristics of the waveform leakages, and describe their relationship to the altimeter s fine-height word. This will require some discussion of the fine-height positioning logic and its relationship to range rate. We will find the leakage-caused range error for the Ku- and the C-band altimeters as a function of fine-height word value. We discuss the average correction as the fine-height word sweeps through its range of operation; the sweep rate is a function of range rate and therefore of TOPEX latitude. The fine-height values for the Ku- and C-band altimeters are different, and we will describe the relationship of the C- and Ku-band fine-height values and particularly their average positions as a function of sign of range rate and also as a function of the C-minus-Ku fine height difference. This difference can be estimated from the ionospheric range correction after adjusting some additional small correction terms. The result will be an additive average combined range correction for the effects of the waveform leakage features, and this correction is a function solely of quantities available from the TOPEX GDR. By *combined* range, we mean the range estimate as corrected for the delay due to ionospheric electron content; this combined range is a weighted sum of the Ku- and C-band ranges after all other range corrections have been applied (*e.g*., troposphere, electromagnetic bias, and Doppler effect). Finally, we present examples of the range corrections for leakage effects for one TOPEX data pass.

Waveform Leakage Characteristics

In *Hayne et al*.[1994], we distinguished between waveform features which were independent of the fine-height word, and those which depended upon the value of the fine-height word. Recall that the TOPEX altimeter range is the sum of a coarse-height and a fine-height word. (These should properly be referred to as coarse-*range* and fine-*range*, but we continue the use of the incorrect term *height* because of its use in all of the TOPEX hardware documentation.) The waveform leakages are in the second category; their position does depend upon the fine-height word. Figure 1 below shows the set of waveform leakages for the fine-height word at the midpoint of its

full range of operation. Notice that in this figure and in the remainder of this report the (on-board) waveform sample set will be numbered 1 through 128. There is an offset leakage, and eight individual numbered leakage spikes, #1 through #8. The amplitude of the numbered set of spikes is independent of receiver gain (*i.e.*, independent of altimeter AGC, or automatic gain control, value). These leakage spikes probably enter the altimeter at or just after the analog-to-digital conversion of the in-phase (I) and quadrature (Q) video output of the receiver. The numbered leakages are symmetric around waveform sample 64 which is the zero-frequency location of the frequency-domain processing within the altimeter. The numbered leakages are probably due to incomplete electromagnetic shielding of harmonics of the low-voltage power supply switching frequencies. Such leakages were not observed in prelaunch test data, and probably a result of some change occurring at launch. One possibility would be a small shift in position of some of the rf absorber material which physically resembles steel wool. Figure 1 also shows a typical Ku-band mean return waveform (scaled down by a factor of 20), and the locations of the Ku tracking EML (early, middle, and late) gates. A gate is the average of a specified range of waveform samples (see *Zieger et al*.[1991] for a more complete discussion of TOPEX gates).

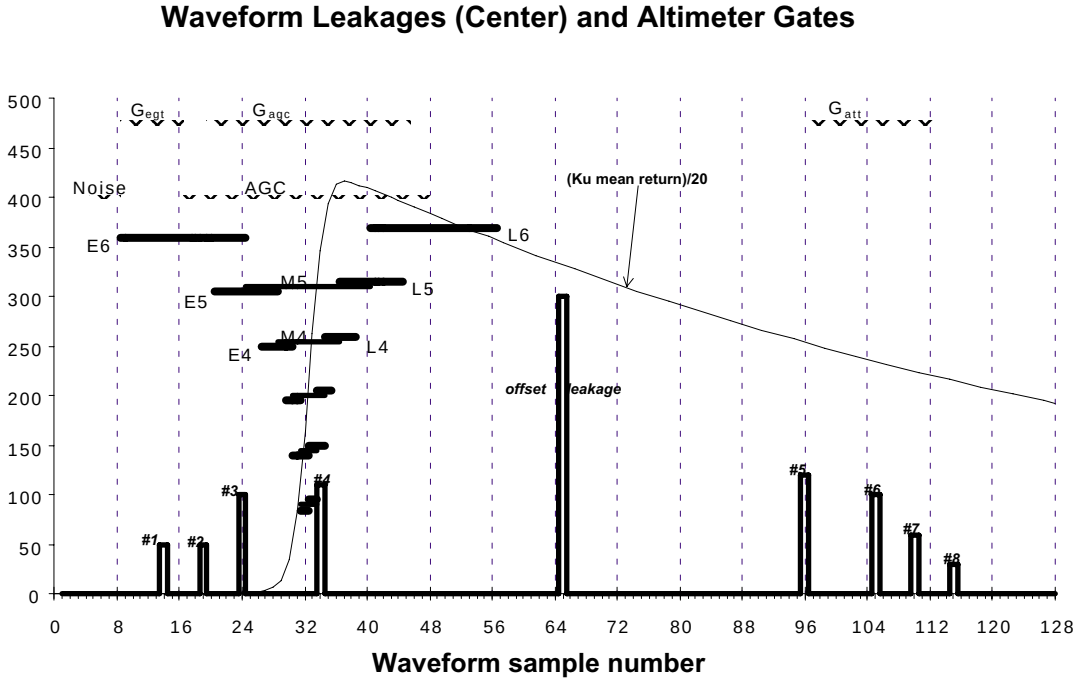

Figure 1. TOPEX waveform leakages at mid-point of fine-height range together with a typical Ku-band mean return waveform and the various Ku early, middle, and late (E, M, and L) gates. The E, M, and L gates are designated by gate index for index 4 and 5, but for index 3, 2, and 1 are unlabeled in this Figure. Also shown are the gates Gegt, Gagc, and Gatt used in producing the attitude-related quantity Vatt in the ground processing.

Notice that all these leakages in Figure 1 are small, of the order of 100-200 counts, compared to the mean Ku waveform peak of the order of 8000 counts and the AGC value of 4096. The waveform leakages sketch for the C-band altimeter is similar to the Ku-band sketch of Figure 1 except that the C-band mean return and all C-band E, M, and L gates are shifted three waveform sample

positions higher (to the right). The C-band mean waveform peak is of the order of 2000 counts, but leakages in the C-band data are also a factor of 4 smaller than the Ku leakages of Figure 1, so the ratio of leakage to peak value is the same for both C- and Ku-band.

Fine-height and coarse-height words, and the waveform leakage positions

The TOPEX altimeter s waveform samples and gates are positioned in range by the sum of a coarse-height and a fine-height word. The on-board tracker adjusts coarse-height and fine-height values until the waveform samples (hence the track gates) are correctly positioned on the radar return waveform, and the altimeter-measured range is the sum of the coarse-height and fine-height words. Both the coarse-height and fine-height values are telemetered to the ground, where they are added early in the ground data processing to produce a total range. Only the total range is carried through the processing, which means that the fine-height value is not available from any of the standard TOPEX data products.

The coarse-height and fine-height words control the gate positioning by a different mechanism. The coarse height controls the equivalent of a series of finite range steps, while the fine height implements a phase rotation in the frequency domain FFT processing within the altimeter s digital filter bank. It will be convenient in this report to use 1 *ws unit* to designate 1 waveform sample separation unit, 3.125 ns in ranging time or about 46.9 cm in range. The full range adjustment by the fine-height word is 8 ws units, or 25 ns in two-way ranging time.

The least significant bit (l.s.b.) in the coarse-height word is 4 ws units, half the full range of the fine-height word, so that a given range value can have two possible combinations of coarse-height and fine-height values: either the fine-height could be somewhere in the upper half of its range for one coarse-height value, or the coarse-height word could be increased by one l.s.b. and the fine-height word decreased by 4 ws units with the same total range but the fine-height now in the lower half of its range. The TOPEX altimeter tries to keep the fine-height word somewhere in its lower half for positive range rate, for range increasing with time. As time increases the fine-height value will be incremented upwards until it reaches 4 ws units, the middle of the fine-height range, at which time the altimeter will increase the coarse-height value by 1 l.s.b and decrease the fine-height value by 4 ws units; the result is that the fine-height word will have a sawtooth appearance, starting at 0 and incrementing up to 4 ws units, with a flyback to 0 and the incrementing process starting over again. For negative range rate, the altimeter will try to keep its fine-height word somewhere in its upper half range, with a resulting negative-going sawtooth pattern from 8 ws units down to 4 ws units and then repeating.

The position of the numbered waveform leakages of Figure 1 is a function of the fine-height word as discussed in *Hayne et al*. [1994]. Figure 1 is specific to the fine-height s being at the center or midpoint of its range, *i.e*., at 4 ws units. As the fine-height is increased from 4 to 8 ws units these leakages will shift leftward, shorter in range, by 4 ws units. If the fine-height decreases, the leakages shift to the right, longer in range. For positive range rate the fine-height word will, as described in the previous paragraph, be executing a sawtooth in its lower half range, moving plus or minus 2 ws units relative to an average fine-height value of 2 ws units. As a result, for positive range rate the leakages will move plus or minus 2 ws units relative to a mean position of 2 ws units to the right of the position shown in Figure 1. Likewise, for negative range rate the leakages will move to a mean position 2 ws units to the left of the position shown in Figure 1.

The leakage designated #4 is the principal cause of the leakage-caused range error because of that leakage s proximity to the middle gate (M). Recall that the E and L gates are used in significant waveheight estimation and in selecting a gate index, but that the range tracking is in effect done by comparing gate M gate to the AGC gate. Negative range rates will move leakage #4 leftward (relative to Figure 1) into the Ku-band M gate, and positive range rates will move #4 to the right and away from the Ku-band M gate. Although the fine-height value is unavailable for data correction (since it disappeared once the coarse-height and fine-height were added early in the ground processing), we can find the average fine-height values for positive and negative range rates. We should be able to derive an average correction once we determine the waveform leakage-caused range error as a function of fine-height value. The next section will show the range error due to leakages.

Leakage-caused range error as function of fine-height value

The TOPEX ground processing corrections for the effects of significant waveheight and attitude were generated using an extensive altimeter simulation program called WALTOPEX, as described by *Hayne et al*.[1994]. We modified WALTOPEX to allow us to simulate the effect of the waveform leakages, and to assess the TOPEX altimeter s range response to these leakages as a function of fine-height value for both the Ku-band and the C-band. The following Figures 2 through Figure 6 show the results. Notice that these figures present the additive range correction for the leakage effects, the value which should be added to the altimeter s range estimate to compensate for the presence of the waveform leakages.

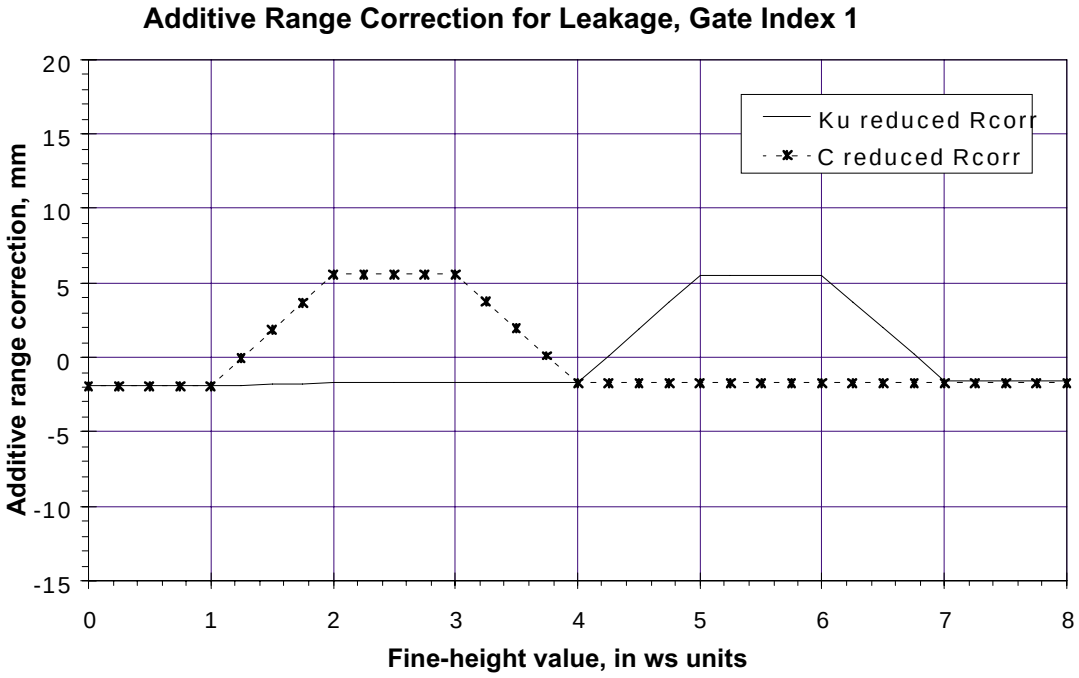

Figure 2. TOPEX additive range correction for waveform leakage effects for gate index 1.

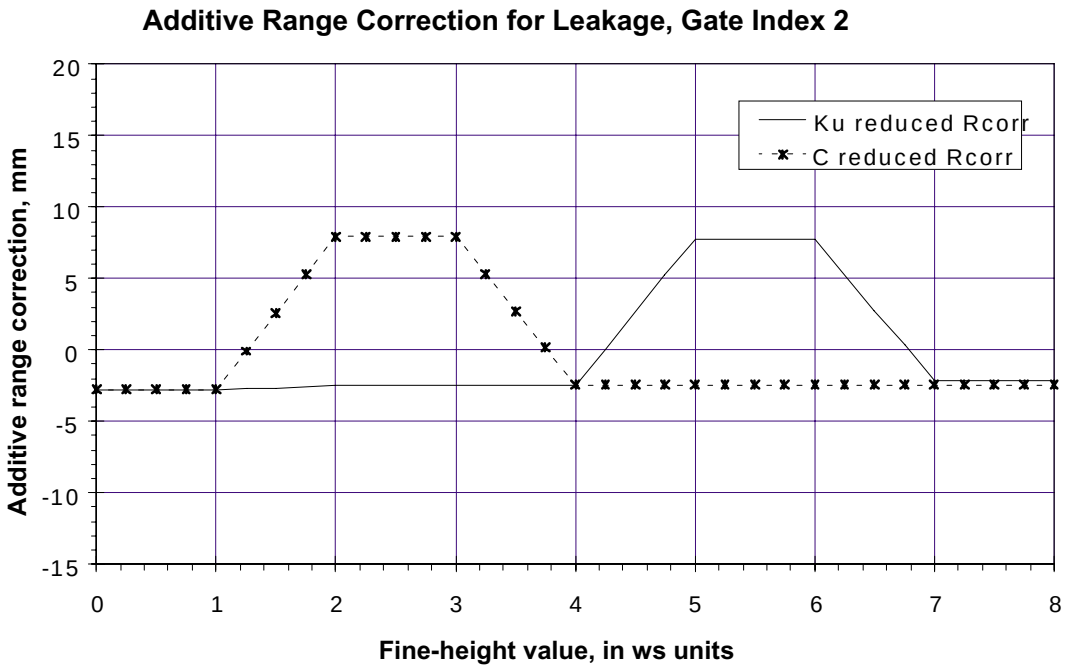

Figure 3. TOPEX additive range correction for waveform leakage effects for gate index 2.

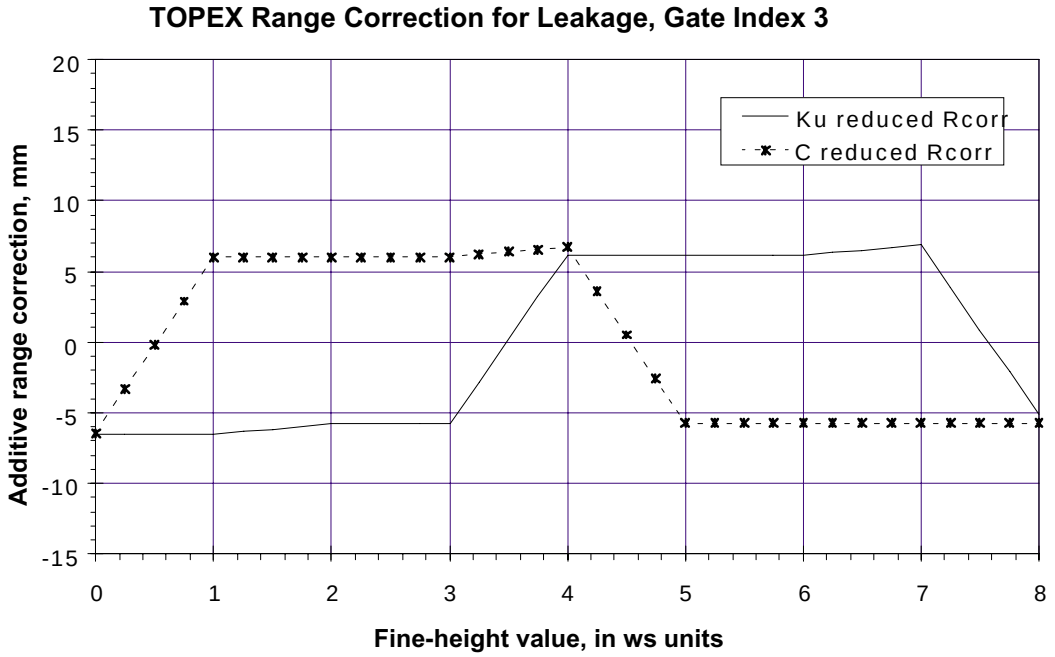

Figure 4. TOPEX additive range correction for waveform leakage effects for gate index 3.

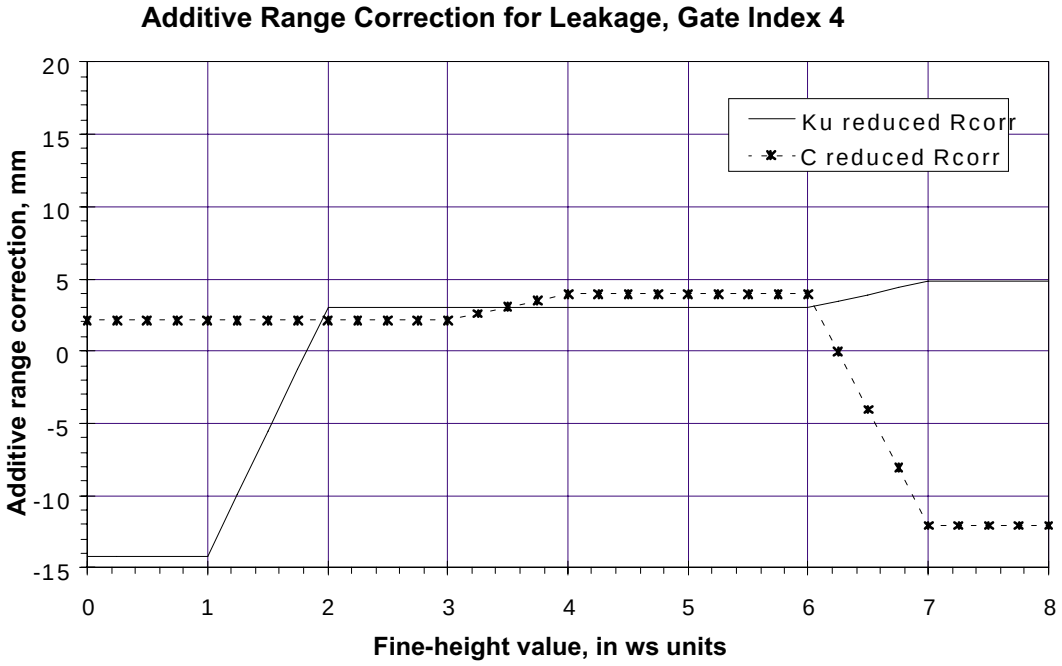

Figure 5. TOPEX additive range correction for waveform leakage effects for gate index 4.

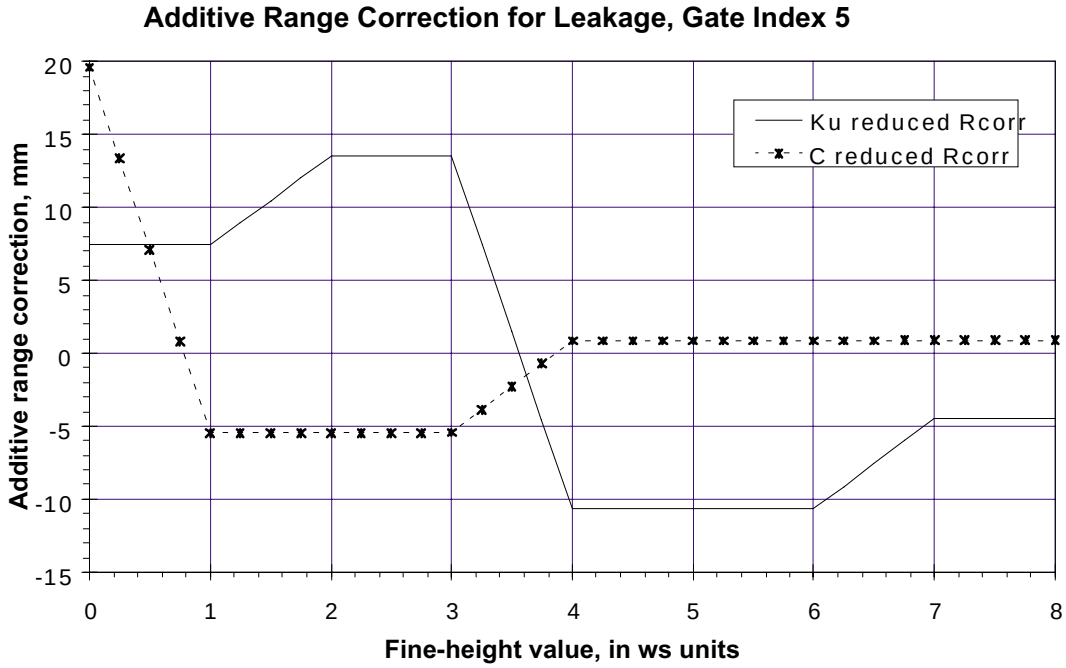

Figure 6. TOPEX additive range correction for waveform leakage effects for gate index 5.

The range corrections have the behavior that simple arguments would predict. Remember that as fine-height increases from the situation of Figure 1, the leakages will move leftward. The primary effect of Ku-band leakages is that at higher Ku-band fine-height values the leakage #4 will contribute excess power to the middle gate M. The Ku-tracker will respond to the excess M power by moving the gates leftward, or lower in range, so that the excess M power causes an underestimate of range. An additive correction for this range would have to be positive. This is what can be seen for Ku-band in Figures 2 and 3, for gate index values 1 and 2. The M gate width is the same for gate index 1 and 2, so Figures 2 and 3 should be very similar. In Figures 2 and 3, if the Ku fine-height value is decreased progressively from 4 ws units (remember that Figure 1 shows the leakages for a fine-height value of 4 ws units) up to 8 ws units, leakage # 4 will move down into the M gate; by the time the Ku-band fine-height reaches 8 ws units, leakage # 4 will have moved out the left side of the M gate. Because the C-band gates are all 3 ws units higher than the Ku-band gates, the C-band range effects will be similar to the Ku-band effects but will appear at C-band fine-height values 3.0 ws units higher than the Ku-band fine-height values.

For larger gate index values, 4 or 5, the picture becomes a bit more confused. The simple argument of the preceding paragraph has considered only the effect of leakage #4 on the M gate. The values plotted in Figures 2 through 6 all come from the WALTOPEX simulation which considers the effects of all leakages on all gates and finds what the TOPEX altimeter will do in the presence of the leakages. It is gratifying, however. that the simple arguments of the preceding paragraph are confirmed by the WALTOPEX low gate index results shown in Figures 2 and 3.

Details of the average range correction produced by the fine-height sweep

If there were only a single Ku-band TOPEX altimeter (*i.e.*, if there were no C-band system to consider), we could immediately say that the average fine-height for negative range rate would be 6.0 ws units and that the fine-height would sweep from 8 down to 4 ws units repeating this sawtooth as time increases. The time-average range correction would then be the average of the Ku range correction values from 4 to 8 ws units in Figures 2 - 6, depending on the gate index value. Similarly, the range correction for positive range rates would be the average Ku correction from 0 to 4 ws units in Figures 2-6.

The maximum range rate magnitude for the TOPEX altimeter is about 15 m/sec (see Figure 16, later in this report), or about 32 ws units per second. At the TOPEX maximum range rate therefore, the altimeter s fine-height word is swept approximately eight times per second over its sweep range of 4 ws units. For full fine-height sweeps at the rate of several times per second, the specific fine-height starting point is unimportant and the fine-height average position adequately determines the leakage range correction for one second range averages. As TOPEX approaches the equator and its range rate approaches zero, the fine-height sweep will also reduce. Within several degrees of the equator the fine-height will be swept over less than 4 ws units in one second, and so the 1-second average correction value will depend in detail on the initial fine-height value and the range rate.

Although the fine-height value is not available in normal TOPEX data products, by a modeling approach we examined the effects of the change of fine-height sweep as a function of latitude by the following method: 1) we used smoothed range rate vs. latitude from the TOPEX ascending pass 027 of cycle 47; 2) starting at the point of zero range rate, we assigned an arbitrary fine-

height value at the starting point; 3) from the starting point, moved forward in time converting range rate vs time into fine-height values vs. time; and 4) then used the fine-height vs. time to produce a series of 1.0 second averages based on the Ku-band gate index 2 range correction curve of Figure 3. The result is a series of 1.0-second averages of the leakage range correction for negative range rate. Similarly, beginning at the same starting point and moving backward in time by 1.0 steps, a series of 1.0 second averages was produced for the leakage range correction for positive range rate.

These 1.0-second modeled average Ku-band average range corrections for gate index 2 are plotted vs. latitude in Figure 7. The same modeled fine-height vs. time data were used with the Ku-band gate index 3 range curve of Figure 4 to produce the Ku-band average range corrections vs. latitude plotted in Figure 8. Figures 7a and 7b show the important aspects of the average range correction for waveform leakage effects. The primary effect is a step-change in the correction at about 1 degree N latitude, when the range rate changes sign. Because TOPEX has a highly circular orbit and because the Earth is fatter at the equator than at the poles, the range rate will be negative as TOPEX moves toward the equator, and positive as TOPEX moves away from the equator. The magnitude of the step-change in Ku-band range correction is about 0.6 cm for gate index 2 and about 1 cm for gate index 3.

Because the range rate vs. time data from an ascending pass were used in producing Figures 7 and 8, the range rate is negative in the left-hand side and positive in the right-hand side of these figures. Similar results are obtained for gate index values 1 or 4. For a descending pass with gate index less than 5, the Ku-band additive range correction has a positive value in the Southern Hemisphere and a negative value in the Northern Hemisphere. It is obvious that carrying out similar modeling for a descending pass s range rate vs. time would produce figures similar to Figure 7 and 8 except that the values would be reflected about the point of zero range rate (approximately 1 degree N latitude). That is, the Ku-band additive range correction for gate index less than 5 would have a negative value in the Southern Hemisphere and positive value in the Northern Hemisphere. For gate index value of 5, the sign of the Ku-band range correction reverses as can be seen in Figure 6.

Notice in Figure 7 and 8 the effect of the smaller number of sweeps of the fine-height as TOPEX approaches the equator. The data in Figures 7 and 8 were generated for a particular value of starting fine-height. A different starting fine-height value would produce a different output set of range corrections vs. latitude, but the envelope of the output would be about the same as that shown in Figures 7and 8. In general the averaging over a second is adequate and the specific fine-height value is not needed for producing 1-per-second range corrections, but somewhere within 5 degrees of the equator the fine-height sweep is too slow and errors greater than a millimeter can occur in the range correction.

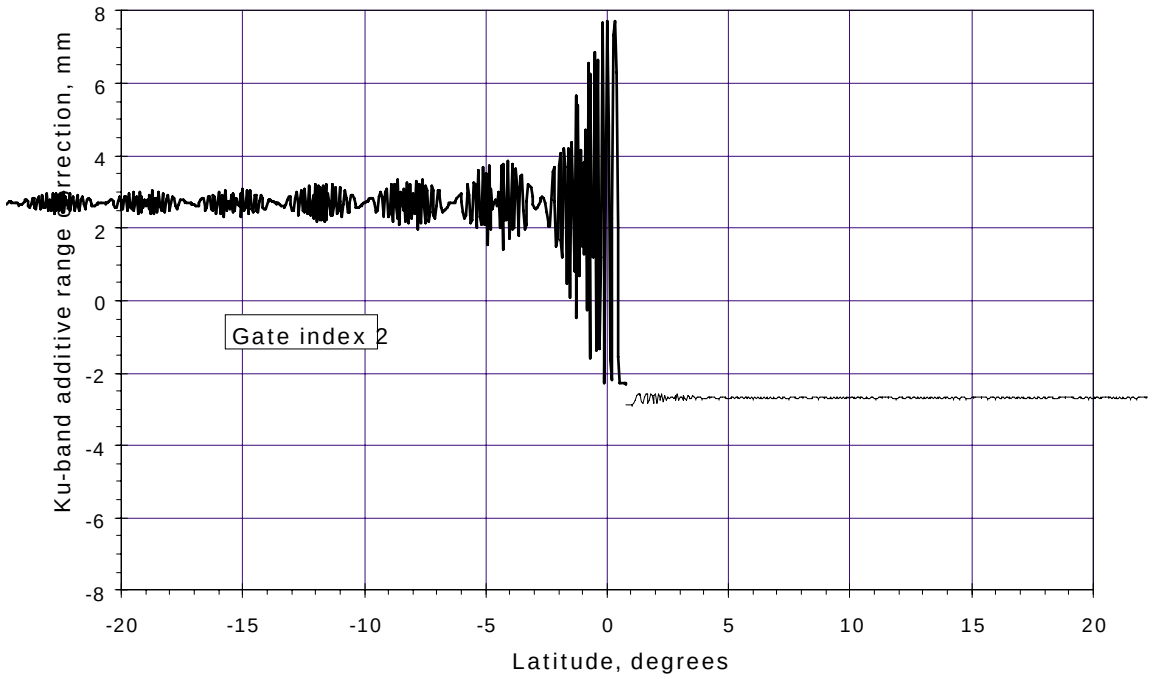

Figure 7. Modeled effect of fine-height sweep on the average additive correction for waveform leakage effects, for a Ku-band altimeter ascending pass with gate index value of 2.

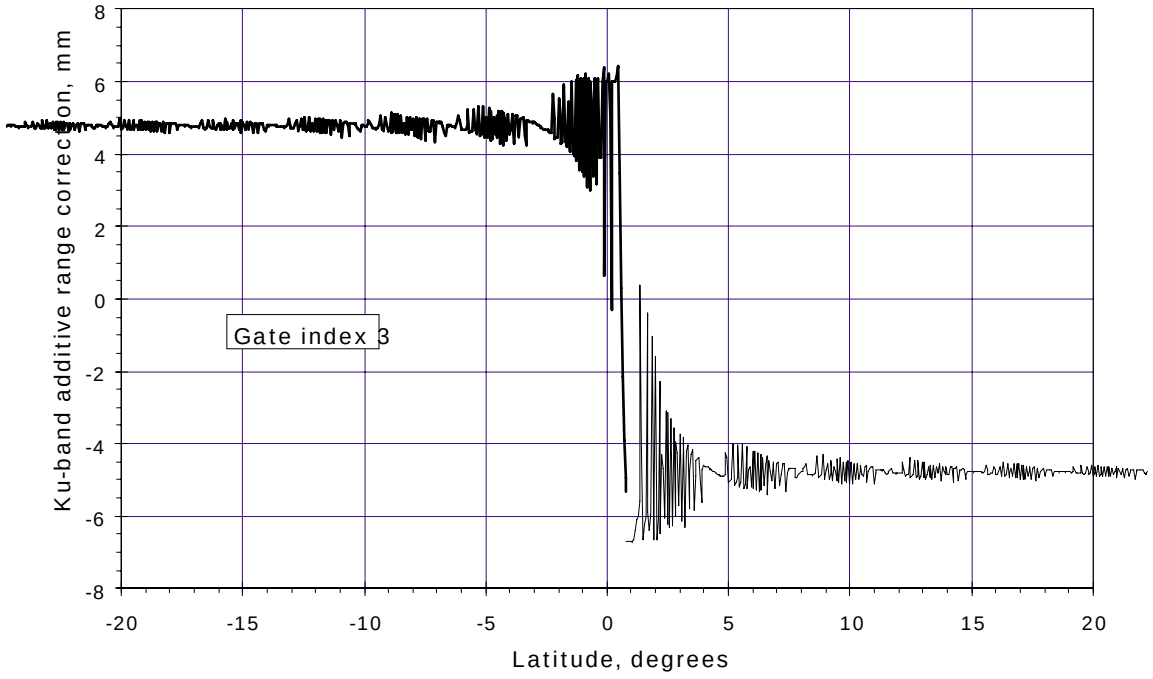

Figure 8. Modeled effect of fine-height sweep on the average additive correction for waveform leakage effects, for a Ku-band altimeter ascending pass with gate index value of 3.

For TOPEX with both C- and Ku-band fine-heights, finding the average fine-height value is a little more complicated, and the details of the Ku- to C-band fine-heights will be addressed in the following section.

Relationship of Ku-band and C-band fine-height values

For TOPEX there is in effect a single coarse-height word and separate fine-height words for the Ku- and the C-band altimeters. The Ku- and C-band fine-height words will be different (the difference is primarily due to ionospheric electron content, the reason that there are both a Ku- and a C-band altimeter for TOPEX) and there are restrictions on the coarse-height so that both the Ku- and C-band altimeters will be kept within the operating range of their fine-height words. Figure 9 is a representation of the fine-height to coarse-height logic for TOPEX, and the result of this logic is that there are conditions in which the Ku-band fine-height will be in a different half of its range than will be the C-band fine-height. Figure 9 is distilled from consultations with and memos from Paul Marth, of the Johns Hopkins Applied Physics Laboratory, whose help we gratefully acknowledge.

The logic in Figure 9 assumes that the C-band and Ku-band fine-height values will never be as much as 4 ws units different from each other. This range difference is sufficient to cover all possible values of ionospheric electron content. In principle, the C-band and Ku-band fine-height values would be the same if there were zero ionospheric electron content However in practice, because of the difficulty in trimming microwave circuitry and system delay factors, the C-band and Ku-band fine-heights will have some arbitrary but constant offset at zero ionospheric electron content. After the altimeter was built, it was decided to move the C-band gates higher in range relative to the Ku-band gates by 3 ws units. The C-minus-Ku fine-height *difference* is actually negative for low ionospheric electron content, increases to a positive value for higher ionospheric electron content. Most TOPEX altimeter data, for range of day and night conditions, will have values of C-minus-Ku fine-height difference ranging from -1.5 to +1.0 ws units.

.

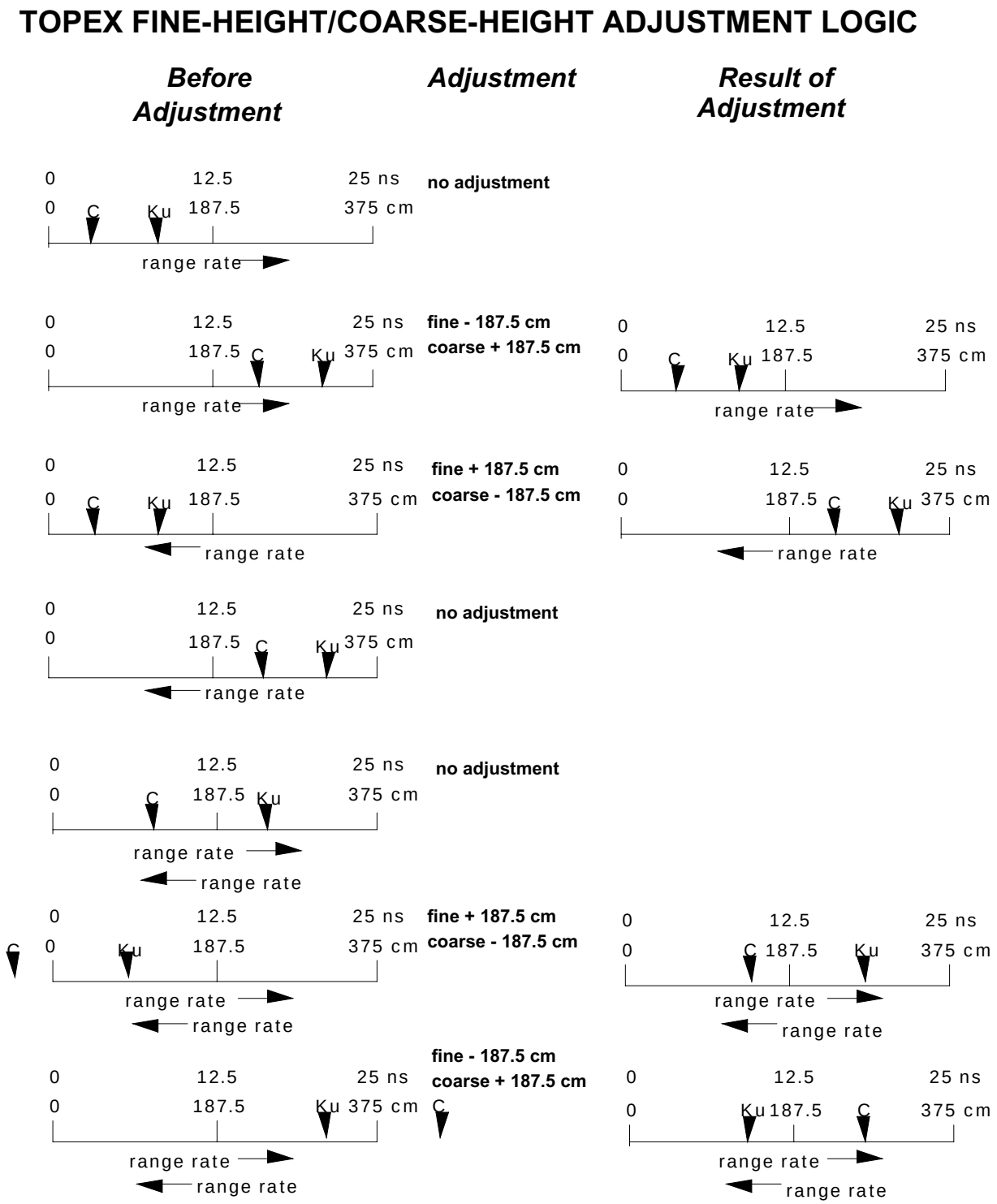

Figure 9. Sketch of fine-height/coarse-height adjustment logic. The top five sketches show the case in which Ku range is greater than the C range, and the labels Ku and C in these five sketches can be reversed to show cases in which the C range is greater than the Ku range.

The consequences of the Figure 9 logic for average fine-height values can be summarized by Figure 10 showing average positions and sweep ranges for the Ku- and C-band altimeters for both positive and negative range rates for cases when the C-band fine-height is greater than the Ku-band fine-height. As indicated in the Figure 10 caption, a similar figure can be obtained for cases when the C-band fine-height is less than the Ku-band fine-height.

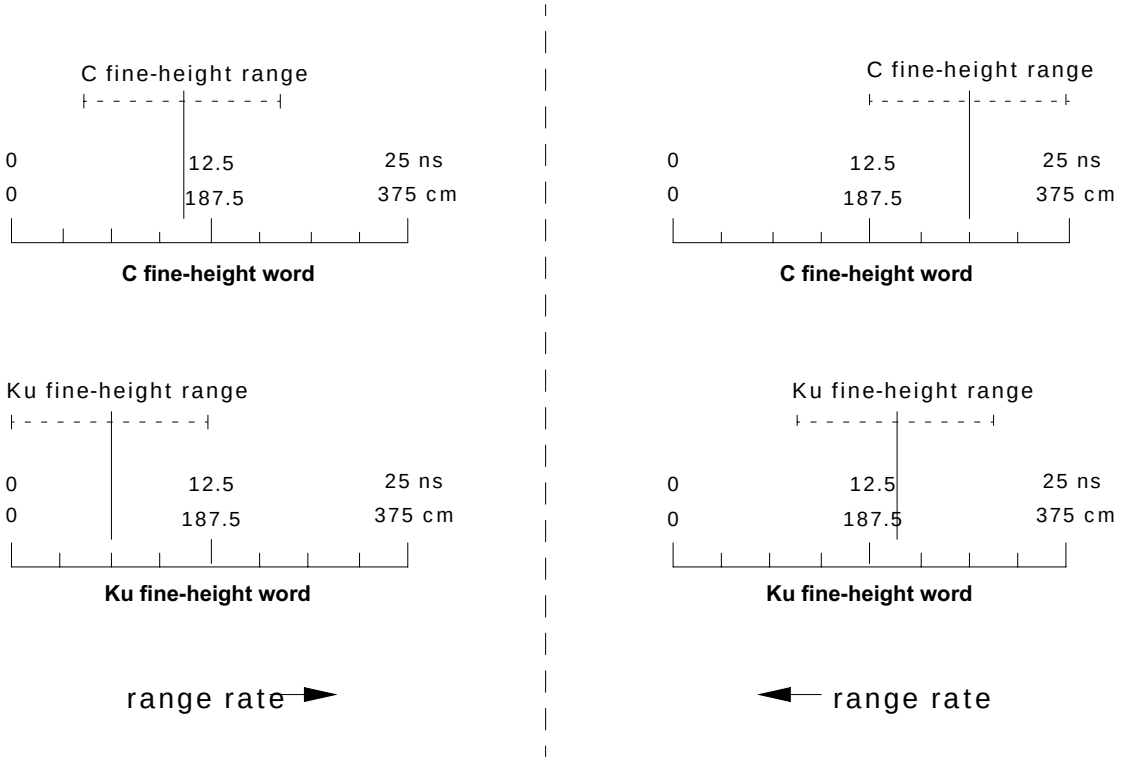

Figure 10. Sketch showing average fine-height values and fine-height sweep ranges for cases in which the C-band fine-height is greater than the Ku-band fine-height, by about 1.5 ws units. The sketch for C-band fine-height less than Ku-band height would look the same except that the labels Ku would be replace by C and vice versa.

A summary of the information in Figure 10 is as follows. For negative range rate, the altimeter whose fine-height word is higher will have its fine height word sweeping from 8 to 4 ws units and repeating in a sawtooth pattern, and its average position will be 6.0 ws units. The altimeter whose fine-height word is lower will execute the same sweep but displaced downward by the fine-height difference. Similarly for positive range rate the lower fine-height altimeter will have a sawtooth sweeping up from 0 to 4 ws units and repeating with an average position of 2.0 ws units, and the higher fine-height altimeter will have the same sweep but displaced upward by the fine-height difference.

Although neither the C- nor the Ku-band fine-height values are available, the C-minus-Ku fine height *difference* is related to the ionospheric correction and therefore can be estimated from quantities on the GDR as will be described later. The C-minus-Ku fine-height difference together with the information sketched in Figure 10 will give us enough information to find fine-height average positions and sweep ranges.

Ku- and C-band average corrections for leakage effects

The average corrections for leakage effects have been calculated, averaging the data of Figures 2 - 6 using the information sketched in Figure 10 and its discussion. These results are presented in the following Figures 11a and 11b through 15 and 15b which show the average Ku-band and C-band range corrections as a function of gate index, range rate sign, and C-minus-Ku fine-height difference. The smooth curves plotted on these figures are simple polynomial fits to the data. The polynomials were fitted only for C-minus-Ku fine-height differences ranging between -1.75 and +3.25 ws units, but this range encompasses the full set values of ionospheric electron content that TOPEX will encounter. The polynomial errors are generally 1 millimeter or less. The polynomial fit coefficients are also printed on these figures, and the quantity delta in the fit expression is the C-minus-Ku fine-height difference in ws units.Values for the Ku-band and C-band polynomial fit coefficients are also given in Tables 1a and 1b.

The gate index 1 Ku-band correction for negative range rates in Figure 11a is almost identical to the C-band correction for positive range rates in Figure 11b. Likewise the Figure 11a C-band negative range rate correction is almost identical to the Figure 11b Ku-band positive range rate correction. There is similar agreement between Figures 12a and 12b for gate index 2, and between Figures 13a and 13b for gate index 3. But between Figures 14a and 14b for gate index 4, and Figures 15a and 15b for gate index 5, the similarities of the curves become less.

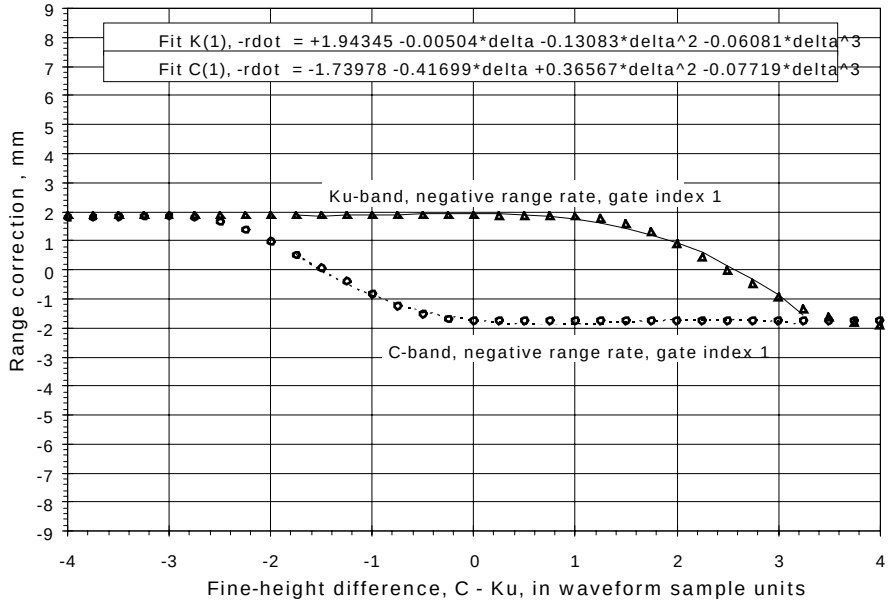

Figure 11a. TOPEX Ku-band and C-band additive range corrections, mm, for waveform leakage effects for gate index 1 and negative range rate.

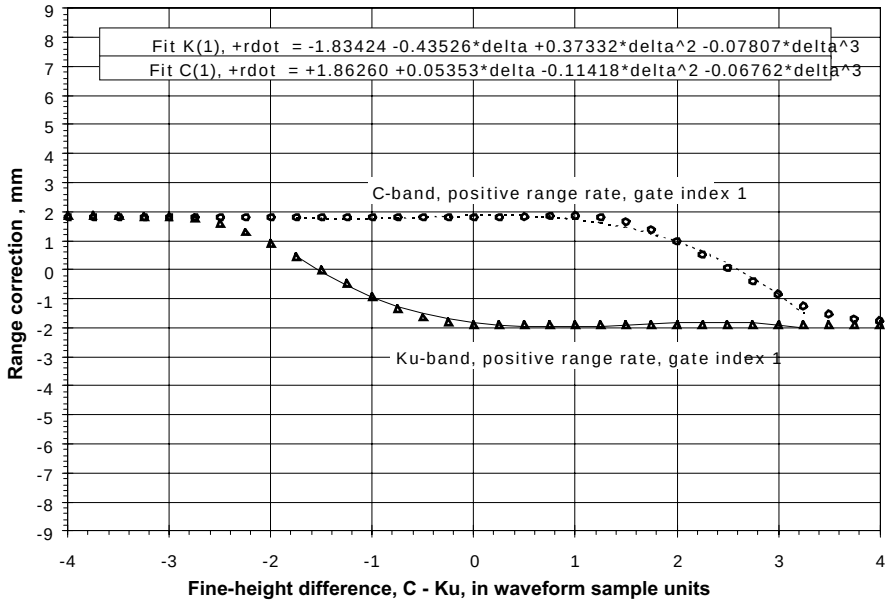

Figure 11b. TOPEX Ku-band and C-band additive range corrections, mm, for waveform leakage effects for gate index 1 and positive range rate.

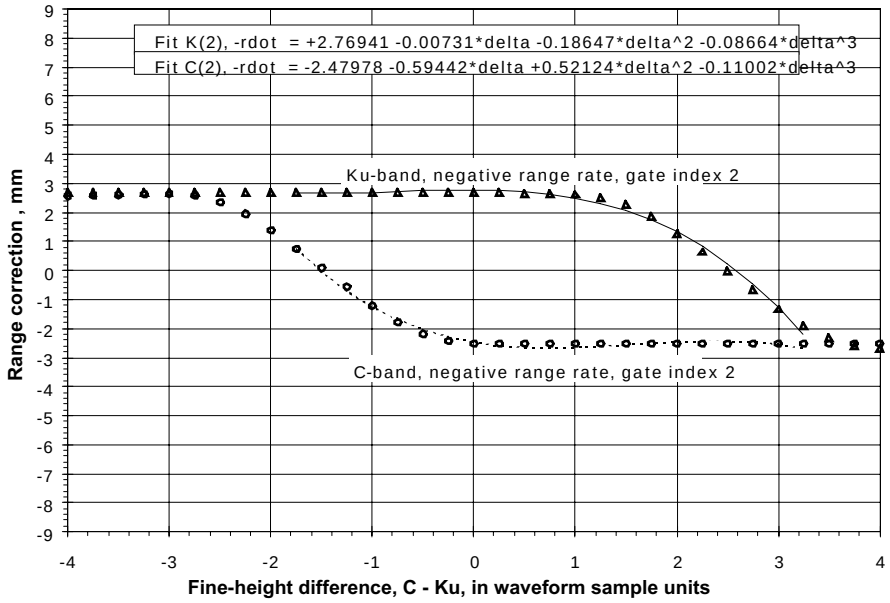

Figure 12a. TOPEX Ku-band and C-band additive range corrections, mm, for waveform leakage effects for gate index 2 and negative range rate.

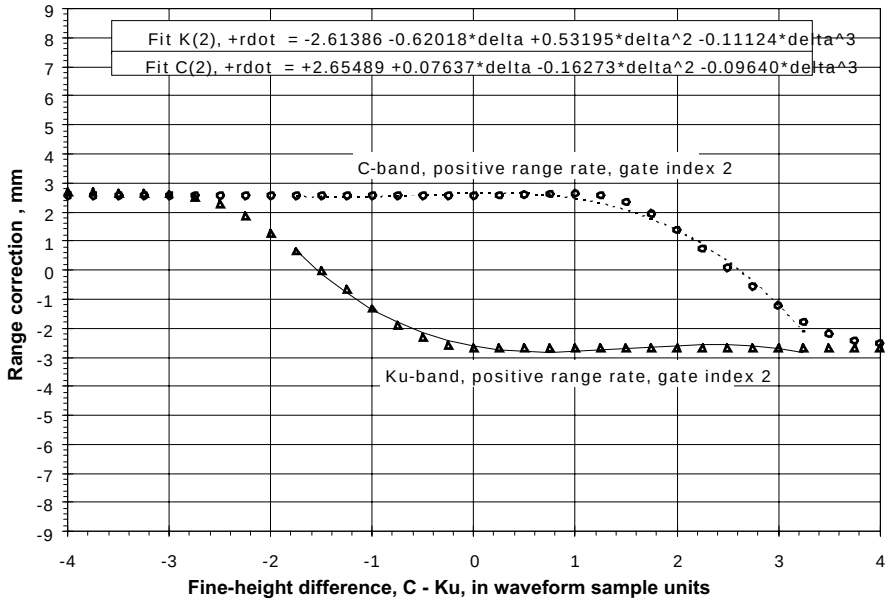

Figure 12b. TOPEX Ku-band and C-band additive range corrections, mm, for waveform leakage effects for gate index 2 and positive range rate.

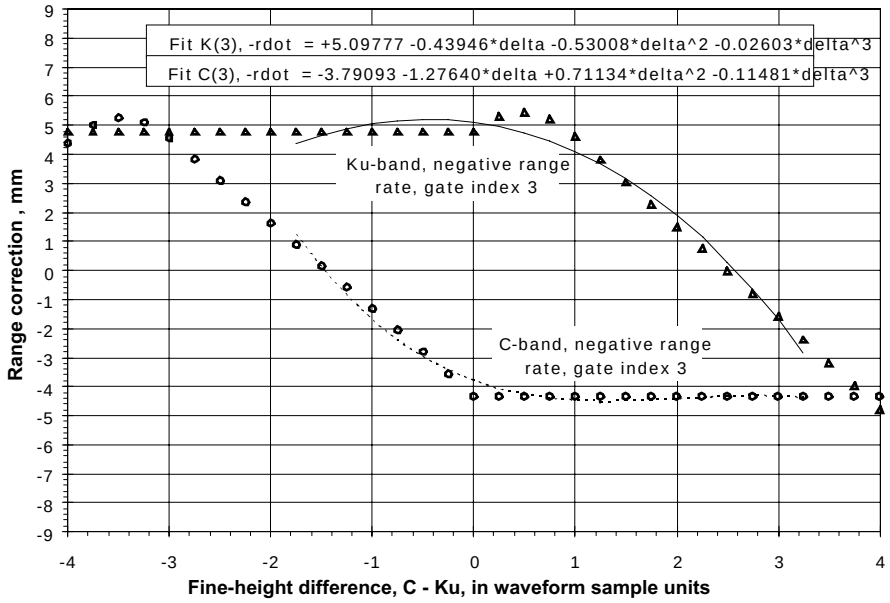

Figure 13a. TOPEX Ku-band and C-band additive range corrections, mm, for waveform leakage effects for gate index 3 and negative range rate.

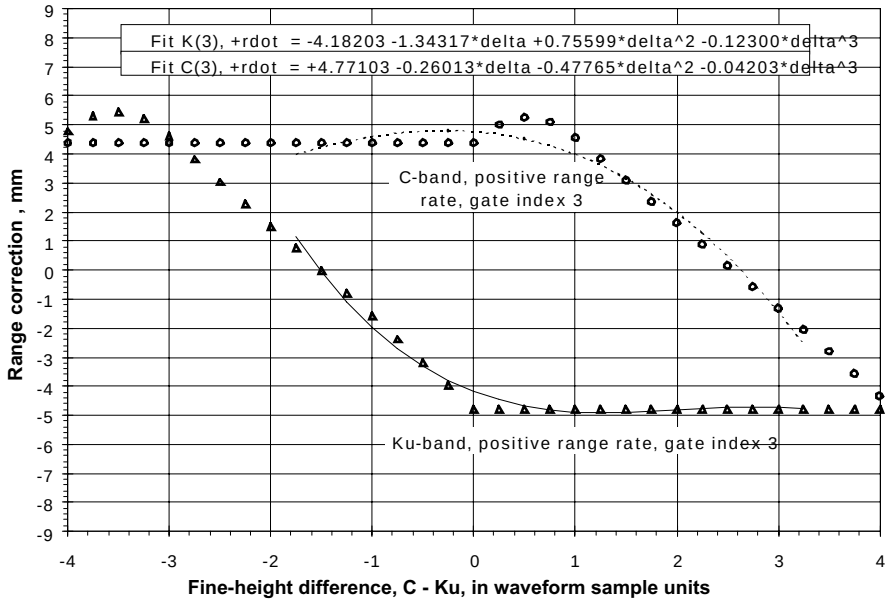

Figure 13b. TOPEX Ku-band and C-band additive range corrections, mm, for waveform leakage effects for gate index 3 and positive range rate.

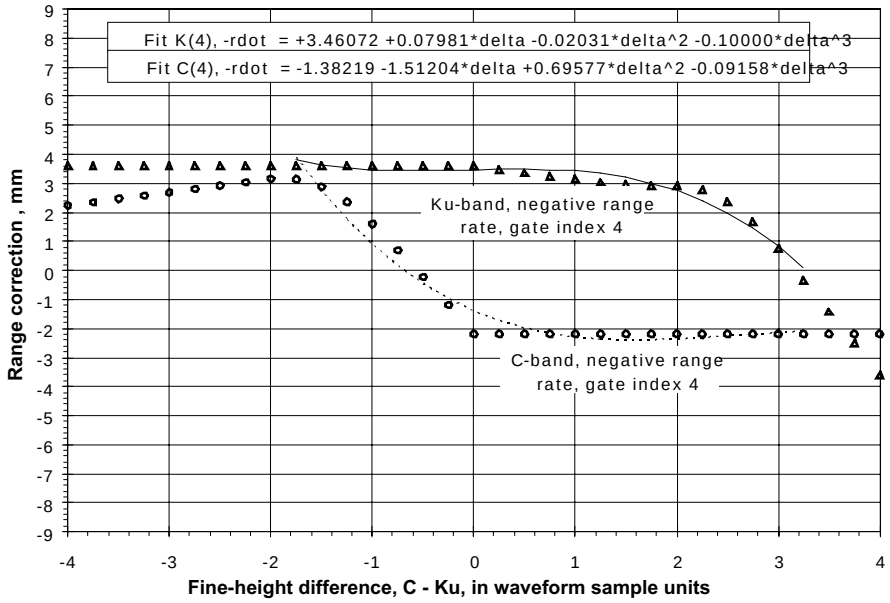

Figure 14a. TOPEX Ku-band and C-band additive range corrections, mm, for waveform leakage effects for gate index 4 and negative range rate.

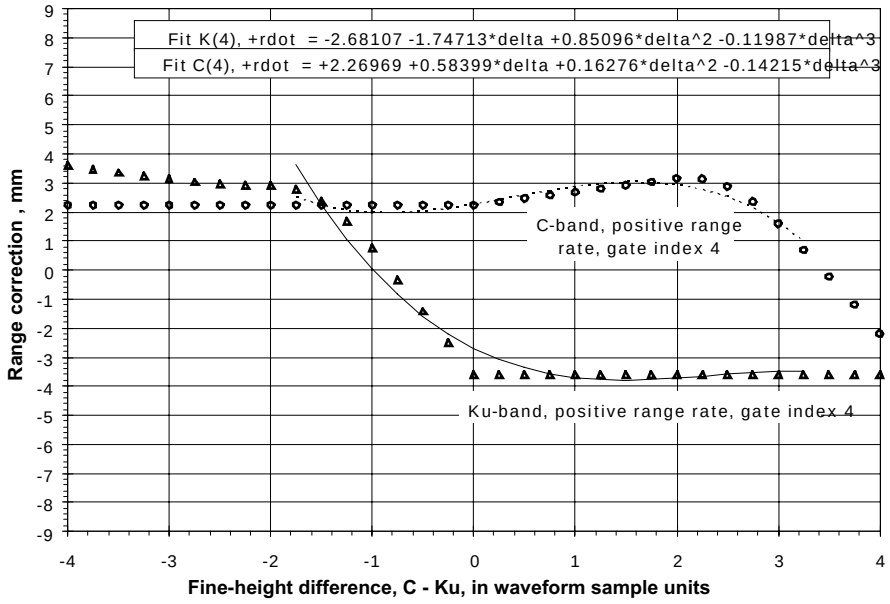

Figure 14b. TOPEX Ku-band and C-band additive range corrections, mm, for waveform leakage effects for gate index 4 and positive range rate.

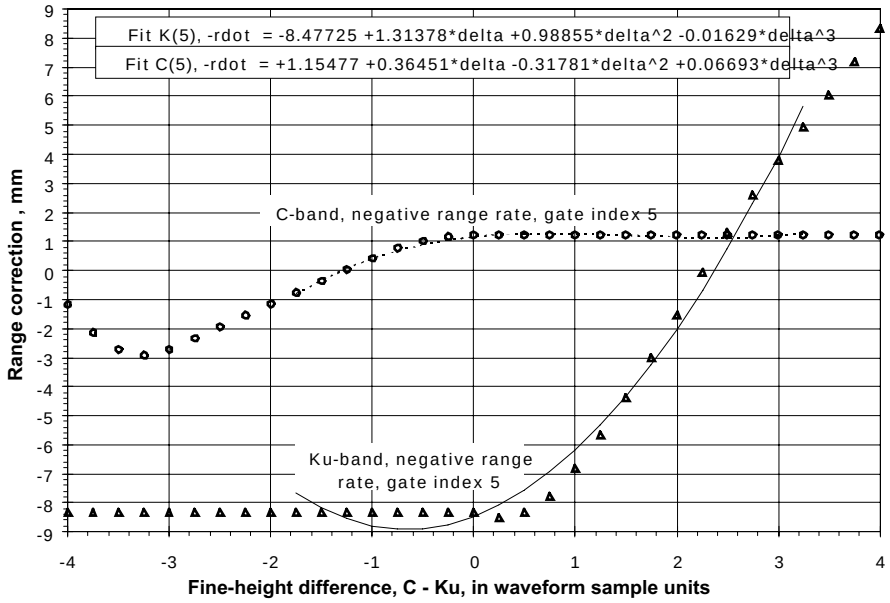

Figure 15a. TOPEX Ku-band and C-band additive range corrections, mm, for waveform leakage effects for gate index 5 and negative range rate.

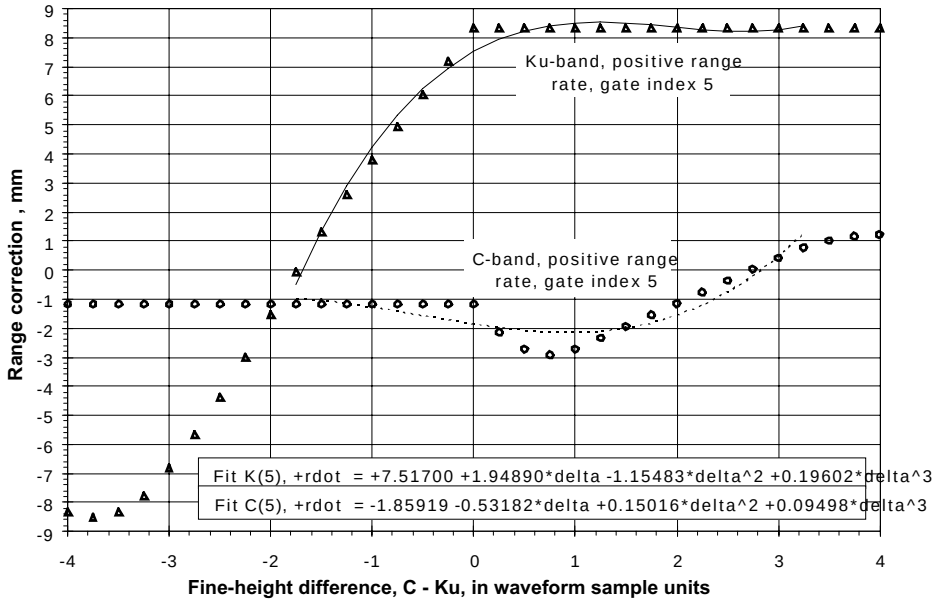

Figure 15b. TOPEX Ku-band and C-band additive range corrections, mm, for waveform leakage effects for gate index 5 and positive range rate.

Table 1a. TOPEX Ku-band additive range correction coefficients. The Ku range correction, in mm, is given by coeff1 + delta*(coeff2 + delta*(coeff3 + delta*coeff4)), where delta is the C-minus-Ku fine-height in ws units.

Ku-band coeff1

	gate index 1	*gate index 2*	*gate index 3*	*gate index 4*	*gate index 5*
negative range rate	+1.94345	+2.76941	+5.09777	+3.46072	-8.47725
positive range rate	-1.83424	-2.61386	-4.18203	-2.68107	+7.51700

Ku-band coeff2

	gate index 1	*gate index 2*	*gate index 3*	*gate index 4*	*gate index 5*
negative range rate	-0.00504	-0.00731	-0.43946	+0.07981	+1.31378
positive range rate	-0.43526	-0.62018	-1.34317	-1.74713	+1.94890

Ku-band coeff3

	gate index 1	*gate index 2*	*gate index 3*	*gate index 4*	*gate index 5*
negative range rate	-0.13083	-0.18647	-0.53008	-0.02031	+0.98855
positive range rate	+0.37332	+0.53195	+0.75599	+0.85096	-1.15483

Ku-band coeff4

	gate index 1	*gate index 2*	*gate index 3*	*gate index 4*	*gate index 5*
negative range rate	-0.06081	-0.08664	-0.02603	-0.10000	-0.01629
positive range rate	-0.07807	-0.11124	-0.12300	-0.11987	+0.19602

Table 1b. TOPEX C-band additive range correction coefficients. The C range correction, in mm, is given by coeff1 + delta*(coeff2 + delta*(coeff3 + delta*coeff4)), where delta is the C-minus-Ku fine-height in ws units.

C-band coeff1

	gate index 1	*gate index 2*	*gate index 3*	*gate index 4*	*gate index 5*
negative range rate	-1.73978	-2.47978	-3.79093	-1.38219	+1.15477
positive range rate	+1.86260	+2.65489	+4.77103	+2.26969	-1.85919

C-band coeff2

	gate index 1	*gate index 2*	*gate index 3*	*gate index 4*	*gate index 5*
negative range rate	-0.41699	-0.59442	-1.27640	-1.51204	+0.36451
positive range rate	+0.05353	+0.07637	-0.26013	+0.58399	-0.53182

C-band coeff3

	gate index 1	*gate index 2*	*gate index 3*	*gate index 4*	*gate index 5*
negative range rate	+0.36567	+0.52124	+0.71134	+0.69577	-0.31781
positive range rate	-0.11418	-0.16273	-0.47765	+0.16276	+0.15016

C-band coeff4

	gate index 1	*gate index 2*	*gate index 3*	*gate index 4*	*gate index 5*
negative range rate	-0.07719	-0.11002	-0.11481	-0.09158	+0.06693
positive range rate	-0.06762	-0.09640	-0.04203	-0.14215	+0.09498

Determining the C-minus-Ku fine-height difference

Let s use D_{CK} to denote the C-minus-Ku fine-height difference in ws units. The ionospheric range correction which is available on the GDR is related to this D_{CK}. Designate the TOPEX Ku-band range as H_K and the C-band range as H_C, and assume that H_K and H_C have been corrected for all effects except for the ionospheric propagation delay. Then the true range after correction for ionospheric delay, designated H_T, is given by

$$H_T = [R/(R-1)]*H_K - [1/(R-1)]*H_C,$$

where R is the square of the ratio of the Ku-band to the C-band frequency. If H_T is expressed as the sum of the H_K and an ionospheric correction term IonoCorr, this additive correction term is

$$\text{IonoCorr} = [1/(R-1)]*(H_K - H_C).$$

The IonoCorr is a negative quantity, since ionospheric electronic content delays the radar propagation causing too large a range estimate by the altimeter. The IonoCorr in meters is available directly from the TOPEX GDR. Inverting the above expression, the difference C-band minus Ku-band range difference in meters is

$$H_C - H_K = -(R-1)*\text{IonoCorr}.$$

But for D_{CK} we need the actual range values within the altimeter, whereas H_K and H_C have already been corrected for Doppler effect, electromagnetic(EM) bias, and attitude/seastate (ANGSS) effects before forming IonoCorr. So we have to remove these corrections before estimating D_{CK}. The Ku-band corrections EM_K and $ANGSS_K$, and the corresponding C-band corrections EM_C and $ANGSS_C$, are all available in meters from the TOPEX GDR, and the expression for C-minus-Ku fine-height difference in ws units becomes

$$D_{CK} = \text{CAL\_D} + (-5.5845*\text{IonoCorr} + EMB_K - EMB_C + ANGSS_K - ANGSS_C + \text{dopp}*\text{Rdot}) / 0.4683,$$

where -5.5845 is the quantity -(R-1) for the TOPEX frequencies, dopp = +0.002656 is a constant related to the difference between the Ku- and C-band Doppler corrections, Rdot is an estimate of the range rate in meters per second, and the constant 0.4683 is the conversion from meters to ws units. The CAL_D is a bias constant related to the internal C-to-Ku offset and its value is -1.6811 ws units. We determined this value CAL_D by making comparisons between the GDR-based C-minus-Ku fine-height difference estimates and the instrument-file-based C-minus-Ku fine-height differences.

The range rate Rdot can be estimated from the satellite altitude SA, the sea surface height SSH, and the time T. The quantities SA, SSH, and T are all on the TOPEX GDR. Suppose that the GDR contains records 1 through N. At any GDR point i, for 1<i<N, the data from records i-1 and i+1 can be used to form the record i Rdot by

$$\text{Rdot}_i = [(SA_{i+1} - SSH_{i+1}) - (SA_{i-1} - SSH_{i-1})]/(T_{i+1} - T_{i-1}).$$

For Rdot_1 for the first record use the next estimate Rdot_2, and for Rdot_N at the last record use the preceding Rdot_{N-1}. Although the SSH has some correction terms already included we can ignore these for purposes of range rate estimation; the correction terms will vary relatively slowly compared to the one-second rate of the GDR.

Data comparisons of the GDR-derived D_{CK} values with the actual fine-height differences from

the TOPEX instrument files show that the D_{CK} estimates of the C-minus-Ku fine-height differences have standard deviations of about 0.1 ws unit. This accuracy will be entirely adequate for purposes of the average range correction for leakage effects, based on the results already shown in Figures 11 through 15.

Final result for range correction

Using the D_{CK} and the polynomials whose coefficients are given in Table 1, values can be found for the additive corrections to the TOPEX ranges to correct for the waveform leakages. Calling the Ku-band range correction dR_K and the C-band correction dR_C, the final additive correction to the combined (ionosphere-corrected) range is dR_{comb} given by

$$dR_{comb} = +1.179*dR_K - 0.179*dR_C.$$

The dR will be in millimeters. The additive correction to sea surface height would be the negative of the range correction dR_{comb}.

Example of leakage correction for an entire TOPEX pass

We will use TOPEX pass 017_132 (*i.e.*, pass 132 of TOPEX cycle 17) to illustrate the range correction procedure described above. This is a descending pass, and the ionospheric electron content is at a maximum near the midpoint of the pass. Figure 16 shows the Ku-band significant waveheight (SWH) value *vs*. latitude; also shown in Figure 16 are the Ku gate index values. Similarly, Figure 17 shows Ku sigma-0 (ocean radar backscatter cross-section) *vs*. latitude, together with the attitude angle *vs*. latitude. There is an attitude bias calibration maneuver (ABCAL) performed for one TOPEX pass every few months, and pass 017_132 happens to include an ABCAL. The attitude excursions, in the latitude range of +40 to -10 degrees in Figure 17, are the result of the ABCAL.

Figure 18 shows the range rate *vs*. latitude, estimated as described earlier and Figure 19 plots, as a function of latitude, the C-minus-Ku fine-height difference estimated from the GDR quantities. To illustrate the quality of the GDR-based estimate of C-minus-Ku fine-height, Figure 20 plots the GDR-estimated C-minus-Ku *vs*. the actual C-minus-Ku fine-height recovered from special processing of the instrument files for pass 017_132. Finally, Figure 21 plots the additive combined range correction *vs*. latitude. This range correction is produced by using the gate index values of Figure 18, the C-minus-Ku fine-height values of Figure 16, and the polynomial coefficients of Table 1a and 1b. The most striking feature of Figure 21 is the step change of approximately 8 mm occurring at the point at which the range rate changes its sign. The smaller steps in Figure 21 are correlated with the changes in gate index shown in Figure 16.

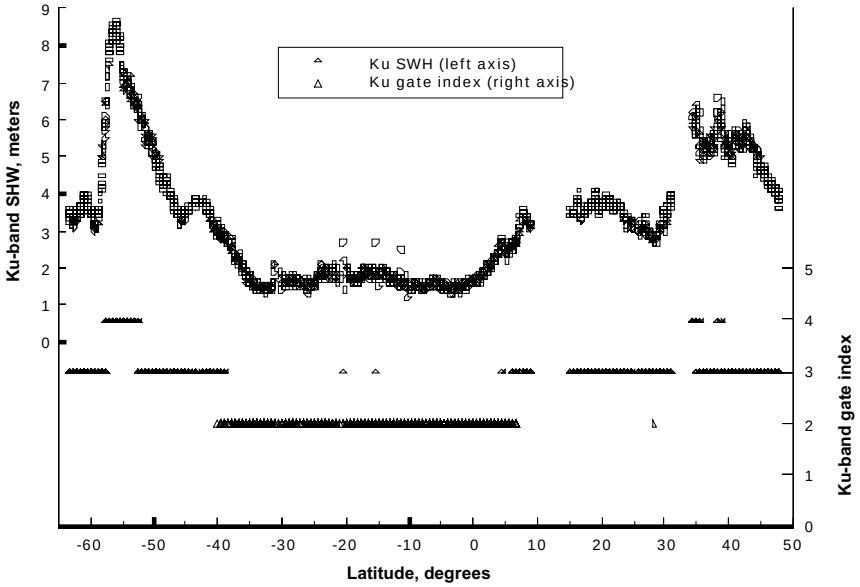

Figure 16. Ku-band significant waveheight and gate index values *vs*. latitude for TOPEX descending pass 017_132.

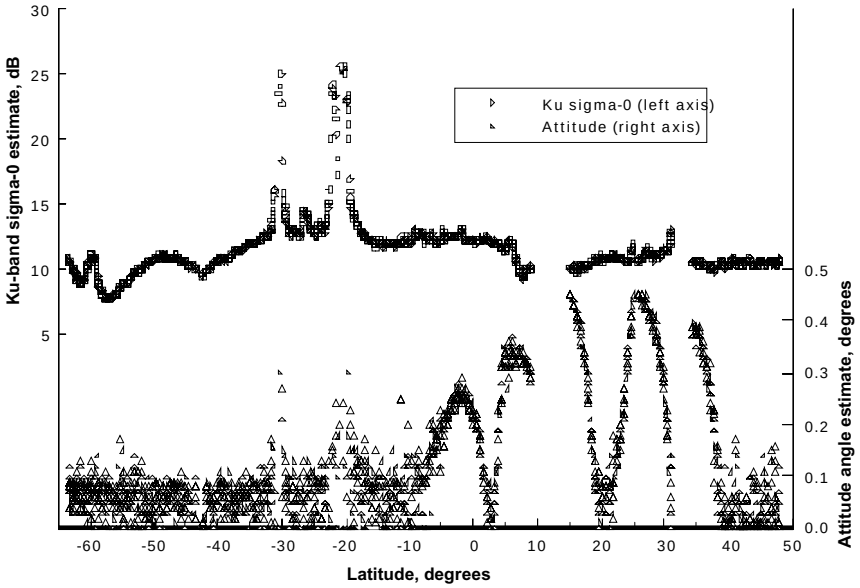

Figure 17. Ku-band sigma-0 estimate and attitude angle estimate *vs*. latitude for TOPEX descending pass 017_132.

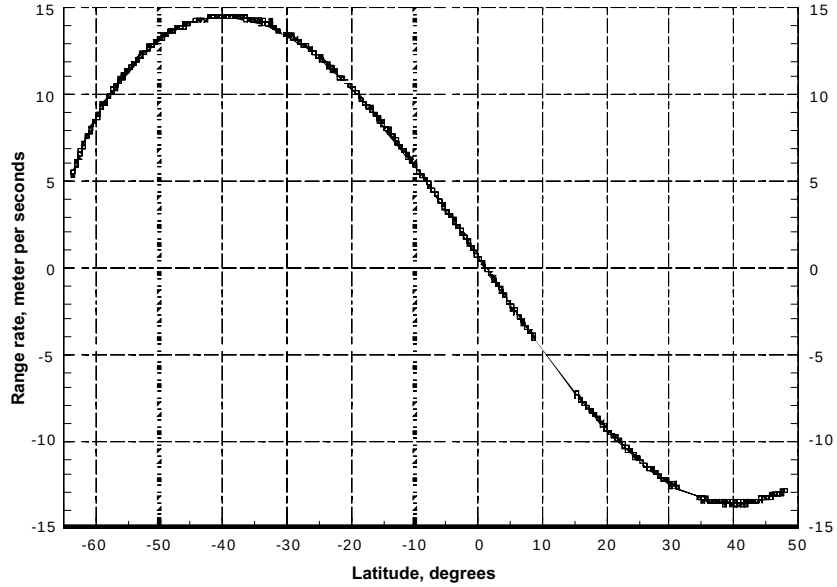

Figure 18. GDR-estimated range rate as a function of latitude for TOPEX descending pass 017_132.

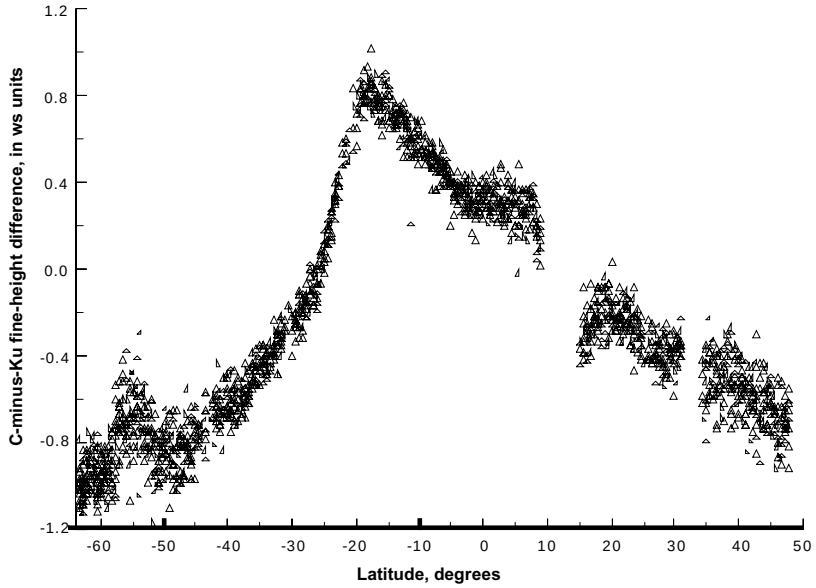

Figure 19. GDR-based estimate of C-minus-Ku fine-height difference, for TOPEX descending pass 017_132, plotted as a function of latitude.

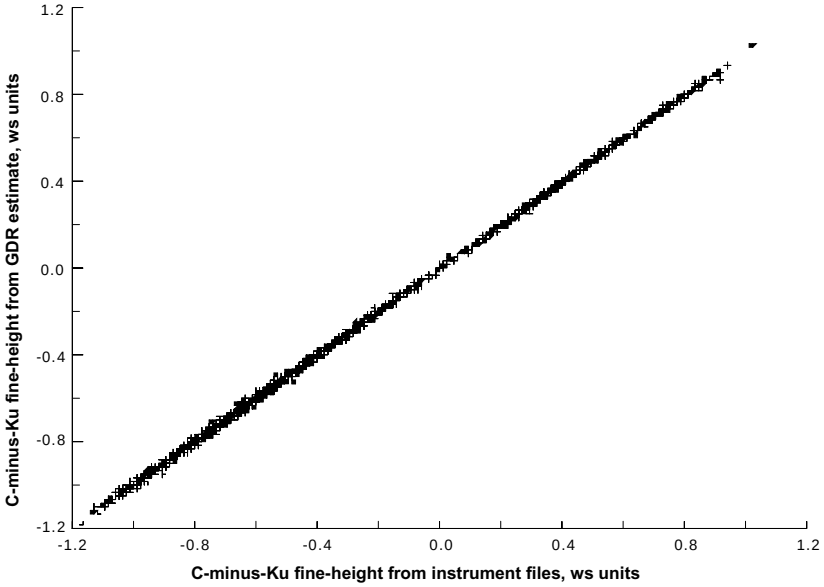

Figure 20. C-minus-Ku fine-height from GDR estimate vs. C-minus-Ku fine-height from instrument file processing, both in waveform sampler units, for TOPEX pass 017_132.

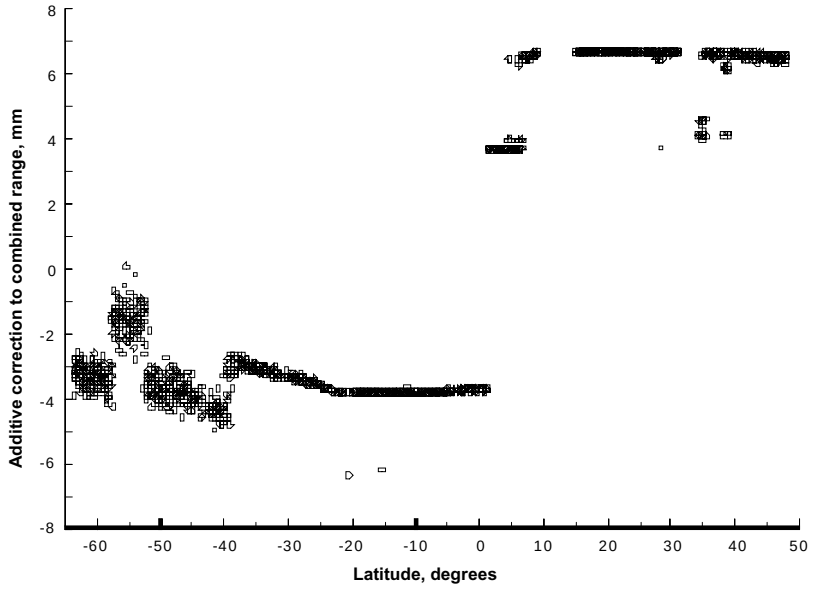

Figure 21. Additive correction to combined range (Ku- and C-band weighted range sum, for ionosphere compensation), for TOPEX descending pass 017_132. Note that for an ascending pass the correction would be reversed: *i.e.*, the Northern Hemisphere additive corrections would be negative and the Southern Hemisphere additive corrections would be positive.

References

Hayne, G.S., D.W. Hancock III, C.L. Purdy, and P.S. Callahan, The corrections for significant wave height and attitude effects in the TOPEX radar altimeter, *J. Geophys. Res., 99(C12)*, 24941-24955, 1994.

Zieger, A.R., D.W. Hancock, G.S. Hayne, and C.L. Purdy, NASA radar for the TOPEX/POSEIDON project, *Proc. IEEE, 97(6)*, 810-826, 1991.